Stony Brook University

Dynamics of Human Origin Recognition Complex During the Cell Division Cycle

A Dissertation Presented

by

Nihan Kara

to

The Graduate School

in Partial Fulfillment of the

Requirements

for the Degree of

Doctor of Philosophy

in

Molecular and Cellular Biology Program

Stony Brook University

May 2014

Stony Brook University

The Graduate School

Nihan Kara

We, the dissertation committee for the above candidate for the

Doctor of Philosophy degree, hereby recommend

acceptance of this dissertation.

Dr. Bruce W. Stillman – Dissertation Advisor
Professor and President, Cold Spring Harbor Laboratory, MCB

Dr. Arne Stenlund - Chairperson of Defense
Associate Professor, Cold Spring Harbor Laboratory, MCB

Dr. David L. Spector - Member
Professor and Director of Research, Cold Spring Harbor Laboratory, MCB

Dr. Janet Leatherwood -Member
Associate Professor, Department of Molecular Genetics and Microbiology
Stony Brook University, MCB

Dr. Darryl Pappin – Outside Member
Associate Professor, Cold Spring Harbor Laboratory

This dissertation is accepted by the Graduate School

Charles Taber
Dean of the Graduate School

Abstract of the Dissertation

Dynamics of Human Origin Recognition Complex During the Cell Division Cycle

by

Nihan Kara

Doctor of Philosophy

in

Molecular and Cellular Biology Program

Stony Brook University

2014

DNA replication occurs once every cell cycle in normal cells and it is a tightly controlled process that ensures complete duplication of the genome. Perturbations in DNA replication may cause catastrophic consequences for the cell including compromised cell proliferation, genomic instability, or cancer susceptibility. The origin recognition complex (ORC) plays a key role during the initiation of DNA replication. I have studied the dynamics of ORC in human cells throughout the cell division cycle to better understand its function in replication initiation. In human cells, the largest subunit of ORC, Orc1 is regulated during the cell cycle. During early S phase it is ubiquitinated and targeted for destruction. New synthesized Orc1 localizes to chromatin during M phase and during late G1 phase is sequentially lost from chromatin, remaining longest on chromatin that is normally late replicating. Orc1 also shows distinctly tight chromatin binding dynamics compared to other ORC subunits. Depletion of Orc1 causes concomitant loss of Mcm3 on chromatin. Together these results suggest that Orc1 acts as pioneer factor by localizing to chromatin during M phase, showing dynamic localization during G1 and recruiting other pre-RC components to chromatin as cell progress through G1. The data suggest that gradual removal of Orc1 from chromatin in late G1 phase may reflect the temporal pattern of DNA replication in S phase.

Table of Contents

List of Figures

List of Tables

List of Illustrations

List of Abbreviations

ATP	Adenosine triphosphate
ATPase	Adenosine triphosphatase
BrdU	5-Bromodeoxyuridine
Bp	Base pair
BSA	Bovine serum albumin
CDK	Cyclin dependent kinase
ChIP	Chromatin immunoprecipitation
CS	Calf serum
DAPI	4'-6-diamidino-2-phenylindole
DDK	Dbf4 dependent kinase
DMEM	Dulbecco's modified Eagle's medium
DNA	Deoxyribonucleic acid
DNase	Deoxyribonuclease
DTT	Dithiothreitol
EDTA	Ethylenediaminetetraacetate
FBS	Fetal bovine serum
FRAP	Fluorescence recovery after photobleaching
H3K4me3	Trimethylated Lys4 of histone H3
H3K27me3	Trimethylated Lys27 of histone H3
H3K9me3	Trimethylated Lys9 of histone H3

HAT	Histone acetyltransferase
kDA or Da	Kilodalton, Dalton
MCM	Minichromosome maintenance complex
MNase	Micrococcal nuclease
ORC	Origin recognition complex
PBS	Phosphate-buffered saline
Pre-IC	Pre-initiation complex
Pre-RC	Pre-replication complex
RNA	Ribonucleic acid
RNase	Ribonuclease
SDS-PAGE	SDS-polyacrylamide gel electrophoresis
Tris	Tris(hydroxymethyl)aminomethane

Acknowledgements

I would like to thank many people whose guidance, support, help and encouragement have supported and inspired me through these years. Firstly, I would like to express my sincere gratitude and deepest appreciation to my thesis advisor, Dr. Bruce Stillman, for his continuous guidance, support and encouragement. His knowledge and enthusiasm inspired me throughout the years. This thesis would not have been possible without his guidance.

I would also like to express my sincere thankfulness and appreciation to my committee chair Dr. Arne Stenlund, and my committee members Dr. Darryl Pappin, Dr. David Spector, and Dr. Janet Leatherwood for their continuous supervision, invaluable advice, feedback and support, which was a very crucial part for me for the progress and improvement of this research.

I am also very thankful to current Stillman Laboratory members: Manzar Hossain, Patricia Wendel, Shuang Ni, Yi-jun Sheu, Saikat Nandi, Justin Kinney as well as former members Anthony Mazurek, Jaclyn Jansen, Marlies Rossmann, Hironori Kawakami and Sylvain Mitelhesier for their invaluable help, discussion and support. I would also like to thank Margaret Falkowski and Carmelita Bautista for their invaluable help in cell culture and antibody generation. I would also like to thank Supriya Prasanth, a former postdoctoral fellow in the Stillman Laboratory for providing some data that integrates into this thesis, as indicated.

Many appreciations go to my classmates Fauzia Chaudhary, An-Yun Chang, Hyejin Cho, Assaf Vestin, Bin Xue, Marcin Stawowzck and Deepika Vasudevan whose friendship were an important part of the greatest memories during my PhD years.

Lastly, I would like to express my deepest gratefulness to my parents, my sister and my brother for their constant support, encouragement and inspiration.

Publications

Organized Orc1 patterning during G1 anticipates spatiotemporal dynamics of DNA replication in S phase. Kara N., Hossain M., Prasanth S. and Stillman B. (in preparation)

Partial MCM4 deficiency in patients with growth retardation, adrenal insufficiency, and natural killer cell deficiency. (2012) *J. Clin. Invest.* **122**, 821–832 Gineau, L., Cognet, C., Kara, N., Lach, F. P., Dunne, J., Veturi, U., Picard, C., Trouillet, C., Eidenschenk, C., Aoufouchi, S., Alcaïs, A., Smith, O., Geissmann, F., Feighery, C., Abel, L., Smogorzewska, A., Stillman, B., Vivier, E., Casanova, J.-L., and Jouanguy, E.

Chapter 1

Introduction

1.1 Initiation of DNA Replication

In eukaryotic cells, the genome is duplicated once during S-phase of each cell division cycle and is highly regulated. DNA replication initiation begins with the assembly of pre-replication complexes (pre-RC) at each origin on chromatin (reviewed in [6-9]). The process begins with binding of the six-subunit origin recognition complex (ORC) to chromatin at hundreds of sites in yeast and thousands of sites in metazoan cells **(Illustration 1)**. The paradigm for initiation of DNA replication derives from studies in the yeast *S. cerevisiae*. In yeast, ORC is bound to the origins of DNA replication throughout the cell division cycle [10] and Cdc6 is recruited to these sites during early G1 followed by binding of Cdt1 that is complexed with the six mini-chromosome maintenance (Mcm2-7) proteins [11, 12]. The Mcm2-7 hetero-hexamer is destined to become part of the active helicase following initiation of DNA replication at each origin. Recruitment of Mcm2-7 helicase complex to ORC-Cdc6 complexes completes the formation of the pre-RC. Loading of Mcm2-7 onto chromatin is called replication licensing because only those origins that have loaded Mcm2-7 can initiate DNA replication. Following Mcm2-7 loading, ORC becomes dispensable [13-15]. Formation of pre-RCs occurs during the

G1 phase of the cell cycle corresponding to the time when cyclin-dependent kinase (CDK) activity is low [16].

DNA replication begins only when the Mcm2-7 complex is activated by recruitment of additional proteins, including the S-phase cyclin-dependent kinase (CDK) and the Dbf4-dependent Cdc7 protein kinase (called DDK) [17-19]. This second step in DNA replication initiation involves recruitment of many other factors, including Cdc45 and the four-subunit GINS protein complex that then forms a larger complex known as the pre-initiation complex (pre-IC). The Cdc45, Mcm2-7 and GINS form a particular complex that has DNA helicase activity and is called the CMG [20, 21]. Activation of licensed origins involves loading of Cdc45 and GINS, which is crucial for activation of the CMG helicase. Loading of Cdc45 is regulated by two kinases Cdc7 (in DDK) and Cdk2 (in S-phase CDK) [22, 23]. Cdc7 phosphorylates multiple Mcm2-7 subunits, particularly a region of the Mcm4 N-terminus that functions in its unphosphorylated form as an intrinsic inhibitor of the initiation of DNA replication [24, 25]. In metazoans, however, the crucial target of DDK is unknown. In yeast, the S-phase CDK (Clb5-Cdc28) phosphorylates Sld2 and Sld3, promoting their binding to Dbp11, which in turn facilitates loading of the GINS complex in a Cdc45 dependent manner [26-28].

A final step in DNA replication is elongation and involves synthesis of nascent strands. Formation of the pre-IC is followed by origin unwinding. Single-stranded DNA binding protein RPA binds to unwound DNA [29-31]. Then, DNA polymerase alpha/primase is loaded and synthesizes an RNA primer that is extended by DNA polymerase alpha DNA polymerase activity [32-34]. Replication factor C (RFC), a multi-subunit protein complex, recognizes and

binds primer-template DNA and allows loading of PCNA (Proliferating cell nuclear antigen) to form processive DNA polymerase delta or epsilon complexes [35, 36]. Cdc45 may act as a bridge between the pre-RC and the proteins involved in elongation step since it has been shown that Cdc45 interacts with components of pre-RC such as Orc2 [37], Mcm2-7 [23, 38, 39], and proteins required for elongation like RPA [23], DNA polymerase alpha [29, 39] and epsilon [23].

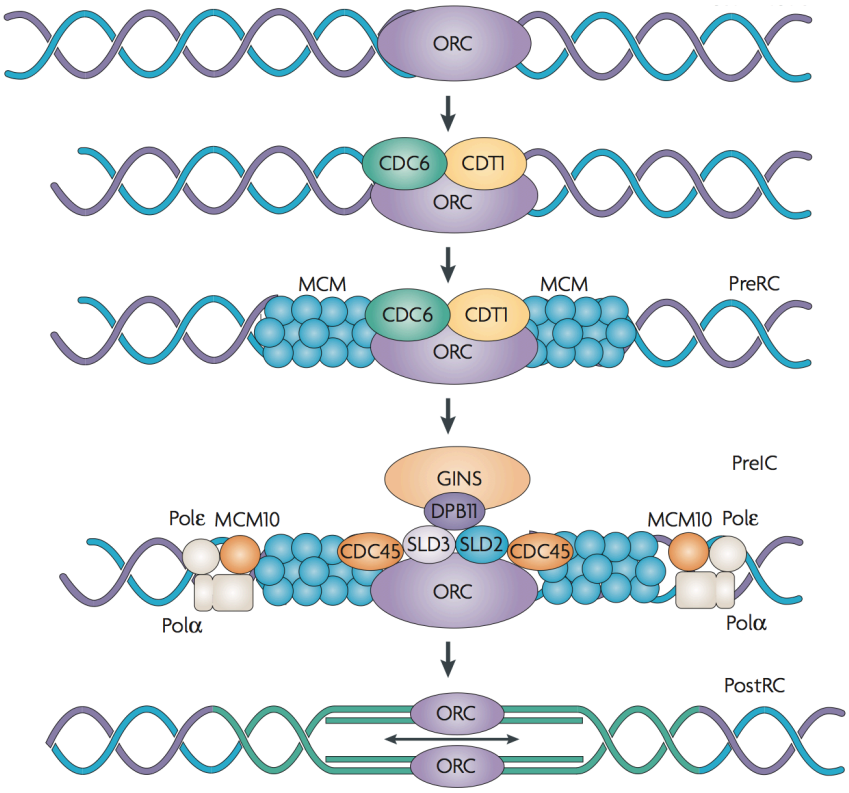

Illustration 1. Overview of DNA replication initiation. In metazoans, binding of ORC is cell cycle regulated (unlike yeast where ORC is bound to chromatin throughout the cell cycle). Orc1 binds to chromatin during mitosis to G1 transition, and ORC complex recruits Cdc6 and Cdt1, which in turn facilitate binding of Mcm2-7 complex. The resulting pre-replication complex (Pre-RC) is activated to form pre-initiation complex (Pre-IC) by the recruitment of additional factors. These include Cdc45, Sld2, Sld3, Dbp11, GINS complex and Mcm10. The initiation of DNA replication requires phosphorylation of pre-RC by CDK and DDK and recruitment of DNA polymerases. After replication all the components of pre-IC leave the chromatin except for some ORC subunits (Post-RC). Re-initiation of DNA replication cannot take place until G1 in next cell cycle when pre-RC is formed. (Adapted from Aladjem, M. I. (2007). "Replication in context: dynamic regulation of DNA replication patterns in metazoans." Nat Rev Genet 8(8): 588-600.)

1.2 Spatio-temporal dynamics of DNA Replication

In metazoans, DNA replication initiates from thousands of sites called replication initiation regions or origins. In budding yeast, there are about 400 origins in each genome that consist of partially conserved sequence elements called ARS (autonomously replicating sequence), whereas in fission yeast the sequence requirements are less defined and distributed over large DNA segments that are rich in A and T bases. In metazoans the nature of these initiation sites are even less well defined. In contrast to yeast, attempts to find efficient ARS sequences in metazoans have failed. Instead, it has been shown that any DNA fragment of sufficient length can act as a replication initiation site in human cells [40-42].

Although the G1-S transition is a cell cycle regulated event, not all origins fire at the beginning of S phase. In yeast, a very well defined temporal program of origin activation occurs during S phase, with each origin being activated at a characteristic time [43]. Origin timing is determined in part by rate limiting DNA replication factors such as Cdc45, Sld2, Sld3 and Dbf4 [44] and chromatin context [45]. Likewise, in metazoan cells not all origins are utilized at the same efficiency each cell division cycle and throughout the course of cell type differentiation during development the origin activity varies. Selection of new replication initiation sites occur at each cell cycle during a distinct time point during G1 which is called as origin decision point [46]. In addition to that, each selected origin starts firing in a temporal order which is determined later in G1 phase and this is known as timing decision point [47, 48].

DNA replication follows a global level of spatio-temporal patterning throughout S phase in which patterns of DNA replication change during early, mid and late S phase **(Figure 1)** [49]. Replication foci form these 120 nM structures, which are stable throughout S phase and over many cell generations [50, 51]. In early S phase there are numerous small foci throughout the nucleus, excluding the nucleoli and the nuclear periphery. In mid S phase, these foci become larger and better defined at the nuclear periphery and around nucleoli. Finally, during late S phase even larger but fewer replication foci are seen in electron dense interior regions of heterochromatin as well as smaller and fewer foci at the nuclear periphery. The presence of these foci suggests that certain clusters of replication origins are activated at the same time and that the timing is regulated, with some clusters activated early in S phase and others activated late. Another important aspect of DNA replication is the observation that the spatio-temporal pattern of DNA replication within the nucleus of each cell is inherited from mother to daughter cells [52-54]. It has been shown that the replication sites in G1/S border overlap in two consecutive cell generations. Interestingly, maps of chromatin interactions determined by chromosome conformation capture technologies reveal the most definitive correlation with DNA replication timing profiles, indicating that clusters of replicons form a domain of the chromosome which is replicated at a characteristic time in S phase and are spatially compartmentalized into the visible replication foci in cells [55-58].

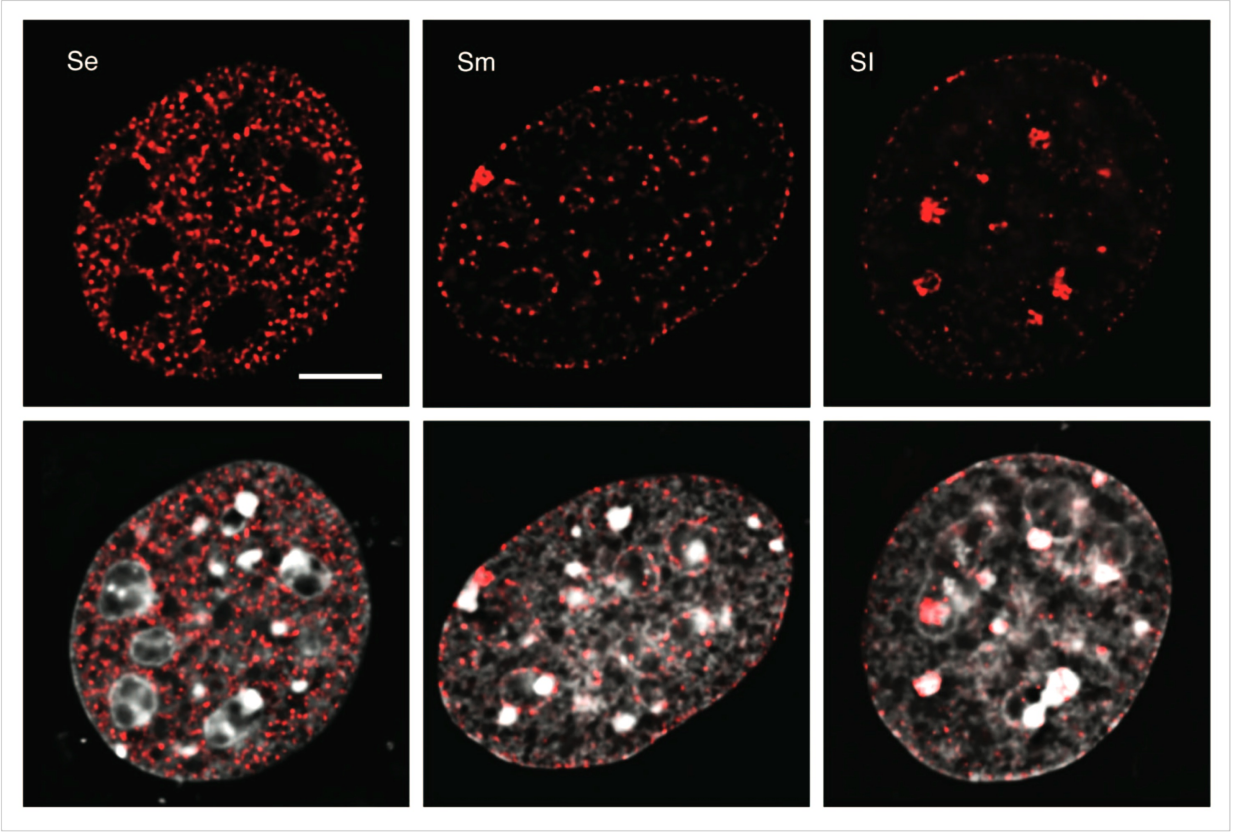

Figure 1. DNA replication follows a global spatio-temporal dynamics over S phase. Super resolution light microscopy images represent three characteristic replication patterns: Se (early S phase), Sm (middle S phase) and Sl (late S phase). Nascent DNA is detected by short pulse labeling of nucleotide analog (red), DNA is detected with DAPI (grey). (Adapted from Casas-Delucchi, C. S. and M. C. Cardoso (2011). Epigenetic control of DNA replication dynamics in mammals. Nucleus. 2: 370-382.)

It is known that chromatin structure largely influences replication timing, for example it has been shown that there is a strong correlation between histone acetylation levels and replication timing in several organisms including, budding yeast, Drosophila, Xenopus and human cells (Reviewed in [59, 60]).

In budding yeast, Sir3, which interacts with the Sir2 histone deacetylase to silence sub-telomeric heterochromatin and silent mating type loci, delays initiation of sub-telomeric origins [61]. Deletion of histone deacetylase Rpd3 causes some of the late non-telomeric and sub-telomeric origins to fire earlier, concomitant with earlier Cdc45 loading onto those origins along and higher acetylation levels of histones around those origins. In addition, recruitment of histone acetyltransferase Gcn5 to the vicinity of a late replication origin causes early firing from this origin [45]. This suggests a role for histone acetylation in DNA replication timing. It is important to note that Rpd3 also plays a role in transcriptional repression. There are two functionally distinct Rpd3 complexes involved in this process, Rpd3L and Rpd3S. Rpd3L is recruited to promoters by sequence-specific proteins like Ume6 [62]. On the other hand Rpd3S is non-specifically recruited to actively transcribed regions to deacetylate the chromatin and suppresses transcription from the cryptic start sites [63]. It has been shown that Rpd3's effect on replication timing is independent of its role in transcriptional silencing [64]. According to a genome-wide analysis of replication timing done in *rpd3Δ* cells using a BrdU-IP-Chip method, Rpd3 deletion causes an increase in histone acetylation surrounding Rpd3 regulated origins and advances initiation of more than 100 non-telomeric origins and Rpd3L plays the dominant role. Rpd3S plays a minor role, only affecting 6 origins [65]. Histone acetylation has also been shown to be

required for efficient origin activation in yeast since histone acetylation mutants have delayed origin activation [66].

In human cells, a strong correlation between histone acetylation and origin activity was observed by a microarray study [67]. In another study, the histone deacetylase inhibitor trichostatin A advanced the timing of replication initiation in human cells [68]. Also, it has been shown that histone acetylation brings transcriptional independent control of replication timing in the human beta-globin locus [69]. Similarly, in mouse cells, DNA replication timing is correlated with chromatin status and late replication is followed by a reduction in H3K9 and H4 acetylation [70]. These observations illustrate the importance of histone modifications in the spatio-temporal program of DNA replication.

Interestingly, the largest subunit of the origin recognition complex, Orc1 interacts with the MYST histone acetyl transferase Hbo1 in human cells [71]. Therefore the link between Hbo1 HAT and Orc1 might indicate an important role in establishment of spatio-temporal regulation of DNA replication. It is also known that Hbo1 interacts with Mcm2 in addition to ORC. When Hbo1 protein was depleted by siRNA in human cells, Mcm2-7 failed to associate with chromatin even though ORC and Cdc6 loading was normal [72].

In cells, controlling the number and efficiency of the replication initiation sites is important to maintain genomic stability. In human cells, which accommodate around six billion base pairs in the DNA in their nucleus, control of replication initiation is crucial to prevent un-

replicated regions from entering into mitosis and also to prevent re-replication during a single S phase.

In eukaryotes replication initiation sites have different efficiencies with some origins firing in only a subset of S-phases in a population of cells. If the selection of replication initiation sites were totally stochastic then it would be highly likely that some regions of the genome remain unreplicated since those regions lack any initiation regions. This phenomenon has been addressed as the random completion problem [73, 74]. Therefore it is more likely that origin selection and efficacy is a non-random process to ensure that the entire genome is replicated.

The dynamics of DNA replication is flexible over the course of development and differentiation. During early embryogenesis in *Xenopus* embryos, DNA replication starts at the same time randomly in all over the chromatin and with start sites for DNA replication located close together [75, 76]. During the mid-blastula transition, concomitant with onset of transcription and global changes in chromatin structure, DNA replication dynamics change, with the inter-origin distance increasing and a temporal pattern of replication timing being introduced [75, 76]. In mammalian cells, reprogramming of mouse somatic cells into embryonic stem cells is accompanied by a reduction in size of replication domains [77]. Other genome-wide studies also showed that upon differentiation, the replication-timing program changes in about half of the genome and involves 400-800kb units [56, 78-80].

In fission yeast, it has been shown that ORC dynamics during the M/G1 period of the cell cycle pre-determine DNA replication origin usage and efficiency in S phase, and is also related

to the timing of pre-RC assembly in G1 [81]. Timing of ORC binding to an origin is correlated to the time of firing of the origin in S phase. Delaying Orp1 binding, the *S. pombe* Orc1 homolog, to an early origin by mutating it resulted in a delay in Mcm4 recruitment and Cdc45 binding and this was also reflected as a delay in DNA replication timing. Lengthening the M phase using a microtubule-depolymerizing agent caused redistribution of Orp1 at origins such that a more homogenous loading of Orp1 occurred at origins and the consequent DNA replication pattern of these origins changed, with efficient and early origins firing later while inefficient and late origins firing earlier in S phase. Furthermore, over-expression of Cdc45, Hsk1 (Cdc7 homolog) and Dfp1 (Hsk1 activator) caused increased firing in efficient and inefficient origins [81].

In *Drosophila*, high density ORC binding to chromosomal sites is a determinant of early replication of those sites and ORC is found to be associated with H3.3 enriched open chromatin sites [82]. Again, another study shows that ORC is enriched on sites with open chromatin features where there is dynamic nucleosome turnover [83]. Early replicating origins are correlated with different clusters of chromatin features. Two of these clusters are enriched in sites with activating histone marks, the presence of chromatin remodelers like ISWI, and DNA binding proteins such as RNA Polymerase II. These two clusters have the strongest correlation with early origin activation strength. Another cluster consists of repressive chromatin marks, heterochromatin binding proteins and another cluster contains insulator elements [84]. Recently, it has been reported that human Orc1 is associated with transcriptional start sites (TSSs), and transcription rate from those sites is correlated with replication timing [2], although this conclusion was based on Orc1 ChIP sequence data that was not very convincing.

1.3 Assembly of the Origin Recognition Complex (ORC)

The origin recognition complex is composed of six subunits; Orc1-6 [85]. Human ORC is a dynamic complex in contrast to its budding yeast counterpart **(Illustration 2)** [85, 86]. Orc1, Orc4 and Orc5 are defined as typical AAA+ ATPase-like proteins with Orc1, Orc4 and Orc5 containing functional ATP binding sites based on their primary sequence motifs. Mutations in ATP binding sites of Orc4 and Orc5 have been shown to impair complex assembly in vitro while Orc1 ATP binding is not required [3]. ORC complex assembles on chromatin in an ATP dependent manner during mitotic exit. Assembly of ORC is an Orc1 dependent process. Following ORC assembly during mitotic exit or during G1 phase, entry into S phase results in ubiquitin mediated proteolysis of Orc1 and subsequent dissociation of ORC complex from chromatin [3, 87-89]. Levels of Orc2, Orc3, Orc4 and Orc5 are constant throughout the cell division cycle [3] however the chromatin bound level of Orc2 decreases as the Orc1 level on chromatin also decreases as cells progress through S phase [89]. Moreover co-immunoprecipitated levels of Orc2, Orc3 and Orc4 also decrease when Orc1 is immunoprecipitated from synchronized cells [89]. Orc6 interacts with ORC complex, however it only represents a small fraction of total Orc6 in cells [3].

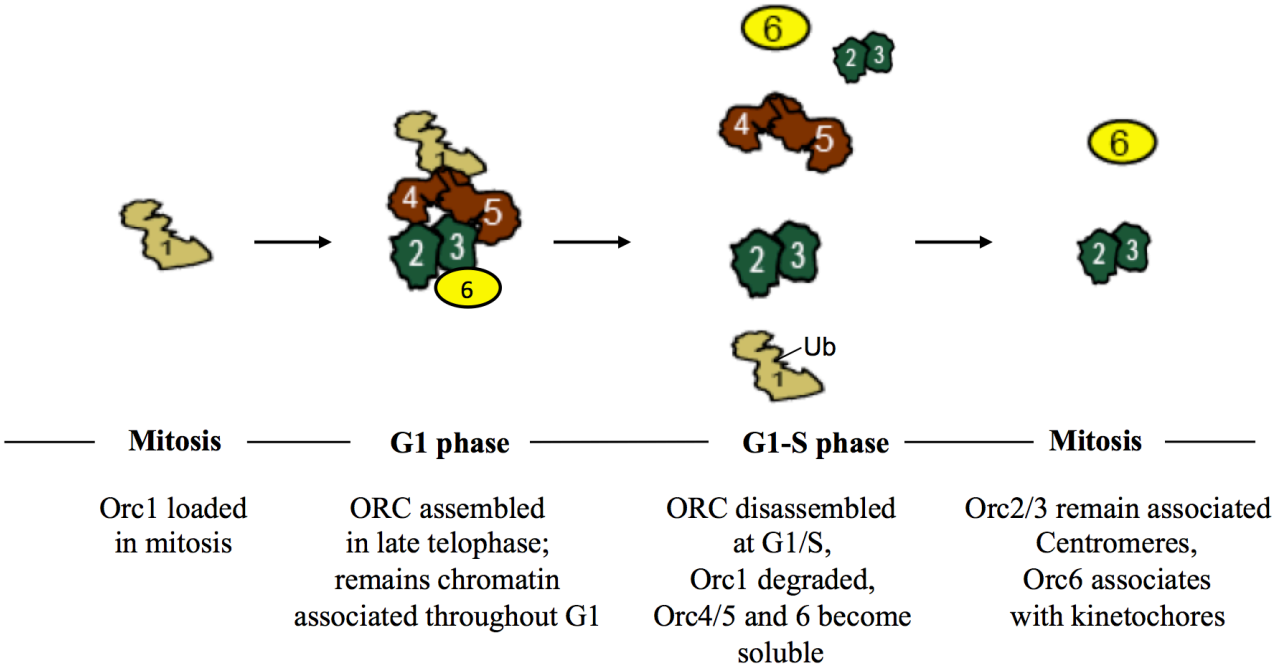

Illustration 2. Assembly of Origin Recognition Complex. Orc1 is loaded onto chromatin during mitosis and ORC assembles during G1 phase. At the G1/S boundary Orc1 is degraded and Orc4/5 and Orc6 dissociates. Orc2/3 remain associated with centromeres and ORc6 associates with kinetochores during mitosis. (Adapted from Siddiqui, K. and Stillman, B., (2007). ATP-dependent assembly of the human origin recognition complex. The Journal of Biological Chemistry, 282(44), pp.32370–32383.)

1.4 Diverse functions of the Origin Recognition Complex subunits

In addition to its roles in DNA replication, ORC is known to be involved in other cellular processes including chromosome segregation, cytokinesis, and heterochromatin maintenance and centrosome duplication.

During mitosis Orc2 and Orc3 subunits are required for stable spindle attachment and their absence causes aberrant mitosis with multipolar spindles [5](Ni and Stillman, unpublished). Another subunit of ORC, Orc6, which is the smallest subunit of ORC, has a role in cytokinesis. Orc6 is essential for cytokinesis in both *Drosophila* [90] and human cells [91]. Depletion of Orc6 from cells by RNA interference results in cytokinesis defects in human cells. In *Drosophila*, Orc6 co-localizes and interacts with the Septin protein Pnut and stimulates its GTPase activity of the Septin complex [92].

ORC also has a role in heterochromatin maintenance. Multiple ORC subunits localize to heterochromatin and co-localize with HP1 foci. It has been recently shown that Orc1 and Orc3 interact with HP1alpha and knockdown of Orc2 or Orc3 disrupts HP1 localization to heterochromatin [93]. In other studies ORC has been found to associate with H3K9me3, H3K27me3 and H4K20me3 marks, again suggesting a role in heterochromatin maintenance [94, 95].

ORC also plays a role in centrosome biology. ORC subunits localize to centrosomes and Orc1, the largest subunit of ORC, controls centrosome copy number. Cyclin A promotes Orc1 to localize to centrosomes and in the centrosome Orc1 inhibits Cyclin E dependent centrosome re-duplication in a single cell division cycle [96]. All these different functions of ORC indicate a diverse array of ORC associated proteins facilitating ORC in these functions.

Recently, mutations in different ORC subunits have been implicated in Meier-Gorlin syndrome, which manifests itself with intra-uterine growth retardation, post-natal short stature and microcephaly [50, 97-99]. Meier Gorlin mutations in a region of Orc1 that is responsible for cyclin E/CDK inhibition cause centrosome re-duplication in a single cell division cycle [100]. It has been also recently shown that mutations in the BAH domain of Orc1, which is found in MGS, disrupt Orc1 association with histone H4 that is modified by di-methylation on lysine 20, H4K20me2, and also disrupts Orc1 binding at an origin region [101].

Besides general understanding of ORC assembly dynamics, I proposed to study ORC chromatin dynamics as well as complex assembly in vivo to better understand its role in replication initiation and possible role in spatio-temporal regulation of DNA replication. Here, we propose that Orc1 acts a pioneer factor by binding to condensed mitotic chromosomes, and later recruiting other ORC subunits to those sites to facilitate assembly of pre-RC on origins during G1. Orc1 shows dynamic organized patterning in G1 nuclei that anticipates spatio-temporal dynamics of replication in S phase indicating possible role of Orc1 in spatio-temporal regulation of DNA replication.

Chapter 2

Generation and characterization of monoclonal antibodies against human Orc1 protein

2.1 Purification of human Orc1 protein

In order to better understand ORC complex dynamics in vivo, I wanted to perform ORC immunoprecipitations in synchronized cells. At the time, Orc1 antibodies that could immunoprecipitate Orc1 were unavailable. Therefore I raised monoclonal antibodies capable of immunoprecipitating Orc1. For this purpose I have expressed recombinant human Orc1 protein as a glutathione S-transferase (GST) fusion protein in *E.coli* cells and purified the hybrid protein using a glutathione affinity column. The conditions for purification were optimized to get the highest protein yield with lowest levels of contaminant proteins.

I used the recombinant Orc1 protein as an antigen for antibody generation and therefore purified a truncated version of Orc1 protein: GST-Orc1ΔN400 (expressing the GST-Orc1-401-861 protein) for immunization of mice. pGEX-6P1 GST-Orc1 ΔN400 vector was transformed into E.coli BL21 DE3 Codon plus cells and cells were grown in appropriate medium. Then, cultured cells were induced with synthetic lactose analog IPTG (isopropyl-beta-D-

thiogalactopyranoside) overnight and harvested the next day. To optimize yield and purity of the purified protein, different lysis buffer conditions and gluthathione resin were tested **(summarized in Table 1)**. The effect of different buffer systems (HEPES, Tris, Phosphate buffer), detergent, ATP, DTT and different resin material (Sigma glutathione agarose beads [Buffer 3] or GE healthcare glutathione sepharose beads [all other buffers]) were investigated. Buffer system 1 and 8 were based on a previous study that used purified ORC recombinant proteins [3], buffer system 5 was based on a previous study that utilized purified human Orc1-5 using a similar pGEX system [102]. Triton X-100 was tested since it may reduce non-specific hydrophobic interactions being a non-ionic detergent, which in turn may facilitate efficient solubilization and elution of the protein of interest. DTT (dithiothreitol) was tested since it is a reducing agent and may promote solubilization of proteins with cysteine residues. To purify the recombinant Orc1 protein, cells were lysed in indicated lysis buffer and then the extract was bound to glutathione column, washed several times and elution was done using reduced glutathione in corresponding elution buffer **(Figure 2)**. The results indicated that the most efficient solubilization of Orc1 was when using buffer system 6 and 8. These two buffer systems also enabled the highest efficiency for the amount of eluted proteins. The presence of Triton in buffer 6 helped solubilize the protein compared to buffer 1. The other modifications including, DTT, or Tris in buffer systems did not significantly increase the yield or solubilization. ATP had a positive effect in solubilization and yield. Based on these findings I therefore used the buffer system 6 and 8 for purification of recombinant Orc1.

In the recombinant GST-Orc1 ΔN400 protein, there is a prescission protease site between the GST tag and Orc1 protein to enable cleavage of the GST tag from the recombinant Orc1

(Figure 3). GST-Orc1-ΔN400 is 88kDa protein; while the prescission protease cleaved Orc1-ΔN400 fragment is 62kDa. Results indicated that buffer system 6 gave higher yield after elution with prescission protease, however there was another band right above the Orc1 fragment visible in the Coomassie Brilliant Blue dye stain. In contrast, when buffer system 8 was used, the prescission protease eluate was cleaner. For this reason I used the prescission protease cleaved recombinant Orc1 fragment from buffer system 8 for the immunizations of mice.

2.2 Screening monoclonal hybridoma cell lines

Three mice were immunized with two boosts of purified recombinant Orc1 protein. Next, bleeds from these mice were tested in whole cell extracts for the ability to detect Orc1 in immunoblots and the ability to immunoprecipitate recombinant Orc1 from the same extracts **(Figure 4)**. It was evident that all three bleeds reacted against Orc1 in whole cell extracts, with other cross-reacting proteins as seen from the western blot **(Figure 4A)**. The results also showed that all three bleeds were able to immunoprecipitate full length MBP-Orc1 (arrow) as well as its degradation products (lower bands) **(Figure 4B)**. All three bleeds also successfully immunoprecipitated purified GST-Orc1-ΔN400 protein (result not shown).

Mice 2 and 3 were sacrificed and spleen cells were harvested. Afterwards, the spleen cells were used for fusion with NS1 mouse myeloma cell line to generate hybridoma cell lines for production of monoclonal antibody. The hybridomas were grown as monoclonal cultures and supernatants from these cultures were used for screening. Initially the hybridomas were screened

by enzyme-linked immunosorbent assay (ELISA) using the antigen and positive clones were screened further. A total of 92 supernatants were screened for ability to immunoprecipitate purified MBP-Orc1 ΔN100, and among them a total of 27 supernatants were able to immunoprecipitate MBP-Orc1 ΔN100 (results not shown). Those 27 supernatants were further tested for their ability to immunoprecipitate Orc1 from HeLa whole cell extracts **(Figure 5)**. Few of the supernatants were able to immunoprecipitate Orc1 and co-immunoprecipitate Orc4. Interestingly none of these supernatants that tested positive could detect Orc1 in western blots **(Figure 6)** suggesting that the supernatants were not able not detect the denatured form of Orc1 in western blots. Therefore, these supernatants can only detect the native, un-denatured form of Orc1 protein.

Based on these results, I selected three clones: 45-1-139, 78-1-188 and 81-1-172 (marked with asterisk) that immunoprecipitated Orc1 and co-immunoprecipitated Orc4 from whole cell extracts **(Figure 5)**. Those monoclonal hybridoma cell lines were further used for production of ascites to obtain higher antibody titer. Ascites production is an excellent method to obtain high titers of the antibody [103, 104].

Monoclonal hybridoma cell line supernatants (a total of 44) were also screened for their ability to detect Orc1 in western blots **(Figure 6)**. Our result showed that, clone 46-1-144 detected a band corresponding to the size of Orc1 protein (arrow). This particular clone was selected for ascites production and further characterization.

Supernatants from monoclonal hybridoma cell lines were also tested for the ability to detect Orc1 protein in fixed cells by immunofluorescence. Two different fixation methods involving either methanol or paraformaldehyde were utilized for immunofluorescence detection of Orc1 with supernatants. Human osteosarcoma U2OS cells grown on coverslips were used for the assay. Alexa-fluor 488-conjugated goat anti mouse secondary antibody was used for fluorescence. However none of the supernatants tested positive for detecting Orc1 (results not shown).

2.3 Characterization of antibodies

Ascites containing high titer antibodies from clones 45-1-139, 78-1-188 and 81-1-172 were tested again using HeLa nuclear extracts for ability to immunoprecipitate Orc1 **(Figure 7)**. Orc2 and Orc3 immunoprecipitations were also performed as a control. The results showed that, all three of the anti-Orc1 monoclonal antibodies immunoprecipitated Orc1, which could be seen as the same molecular weight band protein that was immunoprecipitated by anti-Orc2 and anti-Orc3 antibodies. Among those anti-Orc1 antibodies, antibody 78-1-188 was selected for further characterization.

First, anti-Orc1 monoclonal antibody 78-1-188 was tested for its ability to specifically immunoprecipitate Orc1 **(Figure 8)**. It can be seen that the antibody immunoprecipitated endogenous Orc1 (lower arrow) along with an over-expressed GFP-Orc1 fusion protein (upper arrow) **(Figure 8A)** from U2OS cell extracts indicating that the antibody was indeed

immunoprecipitating Orc1 protein. The antibody also co-immunoprecipitated other ORC subunits including Orc3 and Orc4 **(Figure 8B),** again indicating that the antibody recognized Orc1 specifically and co-precipitated other proteins that interact with Orc1. The fact that this antibody co-immunoprecipitated other ORC subunits was very useful since I was able to use this antibody to study ORC complex dynamics during cell division cycle.

I wanted to determine the binding site of the anti-Orc1 monoclonal antibody 78-1-188 on its target antigen Orc1 protein. For this purpose, I performed epitope mapping of the antigen **(Figure 9)**. I used N-terminal truncation mutants of MBP-Orc1 for immunoprecipitation with Orc1 antibody **(Figure 9A)**. The results show that the antibody immunoprecipitated full length MBP-Orc1 and MBP-Orc1-ΔN400, however it failed to immunoprecipitate MBP-Orc1-ΔN500 and other successive N-terminal truncation mutants. This suggested that the epitope was in the region between 400 and 500 amino acid of Orc1 protein. The antibody also failed to immunoprecipitate MBP-Orc1 1-400 and this was expected since the antigen used for immunization of mice also lacked this region of Orc1 protein (longer exposure blot also shows absence of this interaction, data not shown).

The ascites for clone 46-1-144 that detected Orc1 in western blots was also tested for specificity **(Figure 10)**. The antibody has been shown to detect Orc1 from HeLa and U2OS whole cell extracts **(Figure 10A)**. To test for specificity, HeLa cells were transfected with an siRNA oligonucleotide directed against Orc1 that is known to deplete Orc1 from human cells [89], or a non-targeting siRNA oligonucleotides against the Epstein Barr virus nuclear antigen 1 (EBNA) or luciferase (GL3), and harvested 72 hours post-transfection. Extracts from these cells

were used to test the antibody's ability to specifically detect Orc1 protein **(Figure 10B)**. The results showed that the band detected by the antibody 46-1-144 was depleted from extracts that had the Orc1 siRNA treatment. This result showed that anti-Orc1 mouse monoclonal antibody 46-1-144 detects Orc1 specifically.

To summarize, I was able to generate anti-Orc1 monoclonal antibodies that could immunoprecipitate Orc1 and co-immunoprecipitate Orc1 interacting proteins such as Orc3 and Orc4. I also raised a monoclonal antibody that could be used for detecting Orc1 in western blots. These antibodies can be utilized for many purposes such as studying Orc1 interacting proteins by immunoprecipitation, mass spectrometry analysis, determining Orc1 binding sites on chromatin by chromatin immunoprecipitation (ChIP), and studying of ORC complex dynamics in vivo by immunoprecipitation.

1	2	3	4	5	6	7	8
HN/300	**HN/300 no ATP**	**HN/300 Sigma Beads**	**HN/300 + 2mM DTT**	**TrN/50**	**HN/300 + 0.1% Tx100**	**TN/300**	**PN/300**
20mM HEPES-NaOH pH 7.5 300mM NaCl 0.02% Np-40 5mM MgOAc 10% Glycerol 5mM beta-mercaptoethanol 2mM ATP	20mM HEPES-NaOH pH 7.5 300mM NaCl 0.02% Np-40 5mM MgOAc 10% Glycerol 5mM beta-mercaptoethanol	20mM HEPES-NaOH pH 7.5 300mM NaCl 0.02% Np-40 5mM MgOAc 10% Glycerol 5mM beta-mercaptoethanol 2mM ATP	20mM HEPES-NaOH pH 7.5 300mM NaCl 0.02% Np-40 5mM MgOAc 10% Glycerol 5mM beta-mercaptoethanol 2mM ATP 2mM DTT	20 mM Tris pH 7.5 50 mM NaCl 2 mM MgCl2 1 mM DTT 0.5% NP-40 2mM ATP	20mM HEPES-NaOH pH 7.5 300mM NaCl 0.02% Np-40 0.1% TritonX-100 5mM MgOAc 10% Glycerol 5mM beta-mercaptoethanol 2mM ATP	20mM Tris-HCl pH 7.5 300mM NaCl 0.02% Np-40 0.1% TritonX-100 5mM MgOAc 10% Glycerol 5mM beta-mercaptoethanol 2mM ATP	20 mM KH2PO4, pH 7.5 300 mM KCl 0.02% NP-40 10% glycerol 5 mM MgOAc 5 mM beta-mercaptoethanol 2mM ATP

Table 1. Buffer systems used for purification of GST-Orc1 ΔN400. Buffer systems numbered form 1 to 8 were used to purify recombinant Orc1 protein. The effect of different buffer systems (HEPES, Tris, Phosphate buffer), detergent, ATP, DTT and different resin material (Sigma glutathione agarose [Buffer 3] or GE healthcare glutathione sepharose [all other buffers]) were tested. Elution was done using the same buffer composition for buffer system 5 and 6. For other buffer systems, elutions were done in the presence of 150 mM corresponding salt.

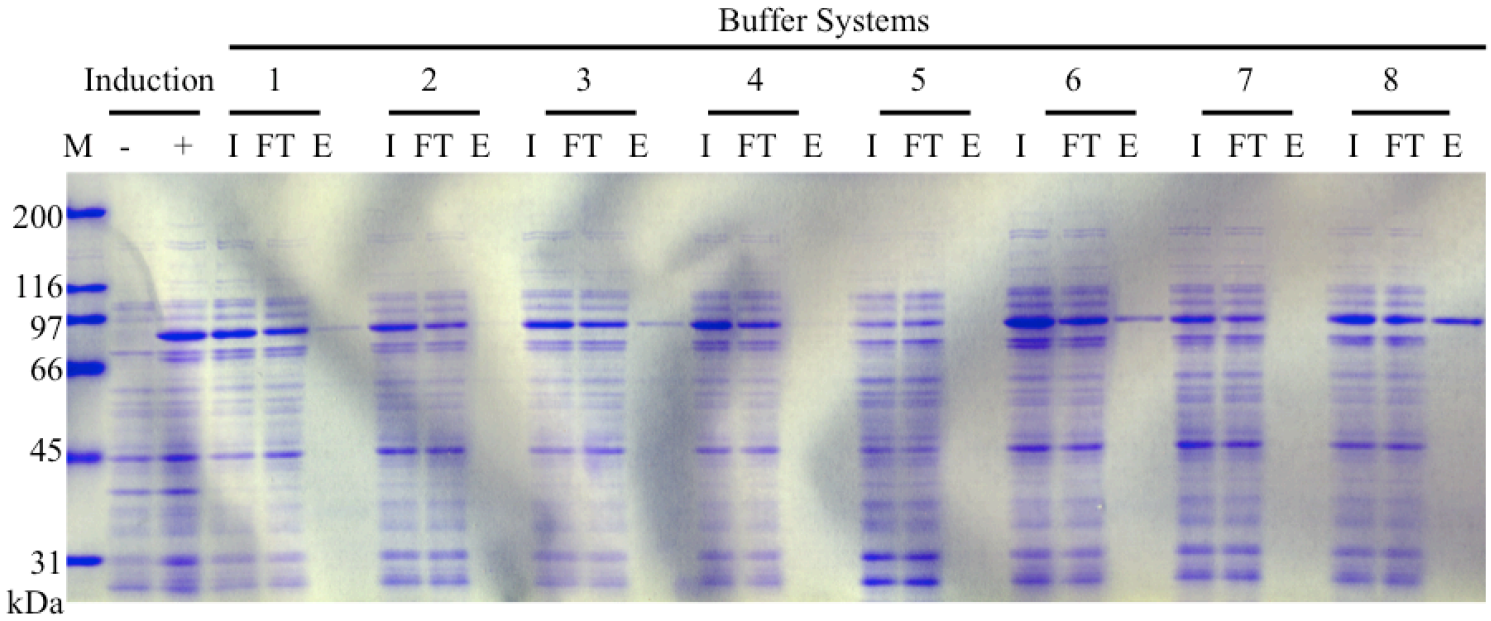

Figure 2. Testing different buffer systems for efficient extraction and purification of GST-Orc1 DN400. M: marker, the corresponding molecular weights are indicated in kDa (kilodaltons). I: input lysate. FT: flow through (unbound material). E: eluted fraction using reduced glutathione.

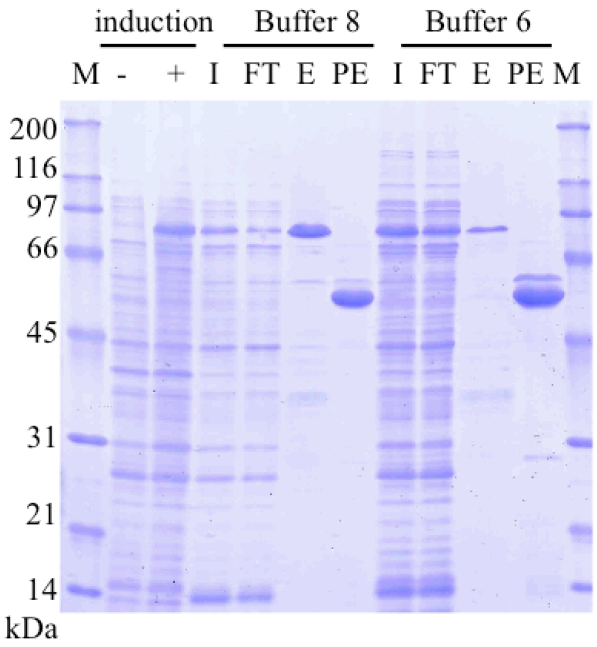

Figure 3. GST tag in recombinant Orc1 is cleaved by preScission protease. M: marker, the corresponding molecular weights are indicated in kDa (kilodaltons). I: input lysate. FT: flow through (unbound material). E: eluted fraction using reduced glutathione. PE: eluted fraction after prescission protease treatment. Buffer system used is indicated on the top. GST-Orc1-ΔN400 is 88kDa protein; while the prescission protease cleaved Orc1-ΔN400 is 62kDa.

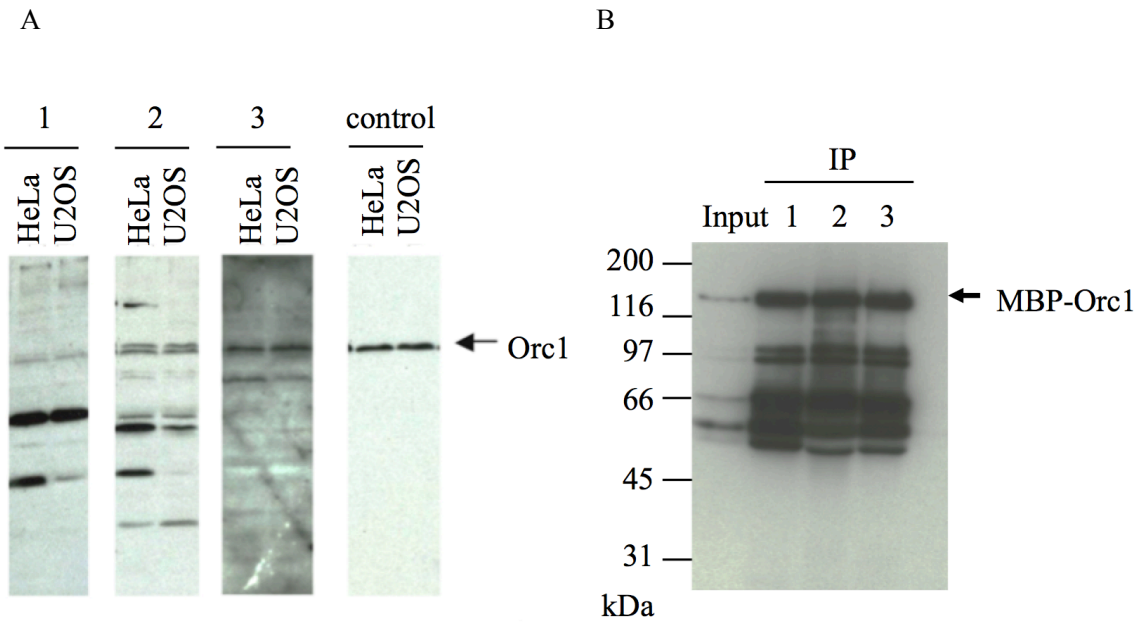

Figure 4. Three mice were injected with purified Orc1-ΔN400 and bleeds were tested on whole cell lysates by western blots and immunoprecipitations. Hela and U2OS whole cell lysates were tested. A. Bleeds 1, 2 and 3 were diluted 1:1000 and blots were incubated overnight with the antibody. For positive control anti-Orc1 antibody PKS1-40 was used. Arrow corresponds to Orc1 protein. B. Bleeds 1-3 were used to immunoprecipitate purified MBP-Orc1 protein. Arrow corresponds to full length MBP-Orc1.

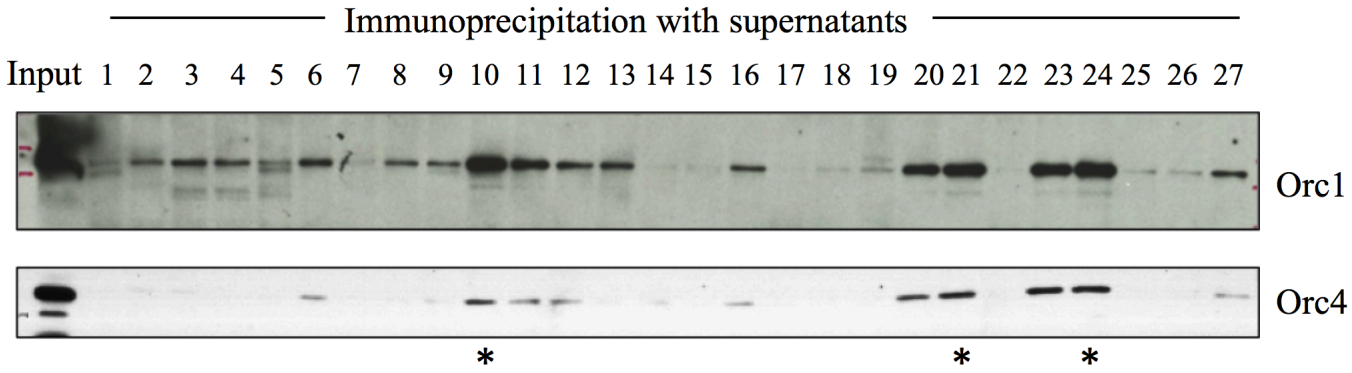

Figure 5. Supernatants from monoclonal hybridoma cell lines screened for ability to immunoprecipitate Orc1. HeLa whole cell extract was used for immunoprecipitations. Supernatants numbered from 1 to 27 were used at 1:2 dilution. Immunoprecipitated Orc1 and co-immunoprecipitated Orc4 blots are shown. Asterisks denote the selected hybridoma cell lines for ascites production. Supernatant 10: clone 45-1-139, supernatant 21: clone 78-1-188, supernatant 24: clone 81-1-172.

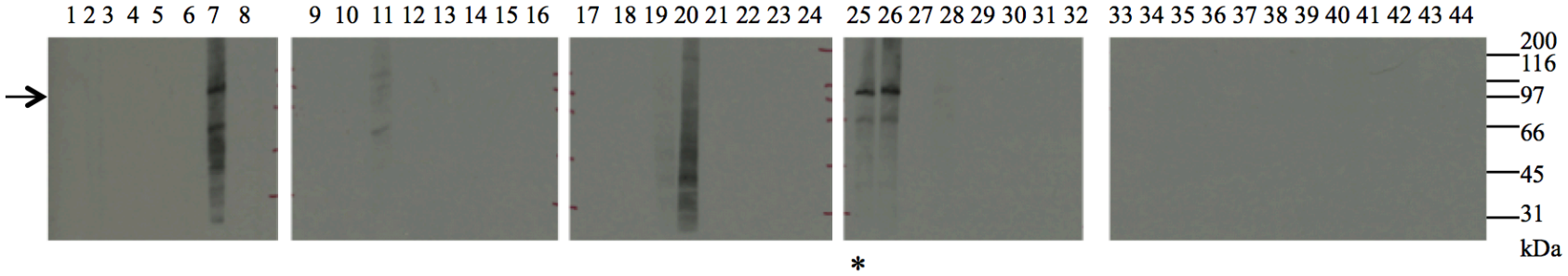

Figure 6. Screening monoclonal supernatants for ability to detect Orc1 in western blots. HeLa whole cell extract was used. Transferred membranes cut as individual strips were incubated with the indicated supernatant (1-44) separately, and HRP-conjugated anti-mouse secondary antibody was used for detection. Appropriate size for Orc1 is indicated with an arrow. Asterisk shows the supernatant #25 corresponding to clone 46-1-144 that was selected for ascites production. Supernatants numbered 23, 40 and 43 correspond to clones 45-1-139, 78-1-188, 81-1-172, respectively, that were shown to immunoprecipitate Orc1 in Figure 5.

Kk;

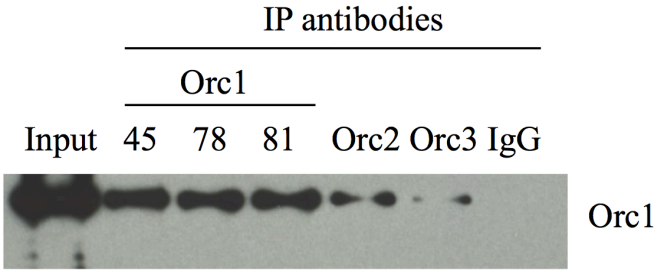

Figure 7. Monoclonal antibodies immunoprecipitate Orc1 from nuclear extracts. Hela nuclear extracts were used for immunoprecipitation. Anti-Orc1 antibodies 45, 78 and 81 denotes ascites from clones 45-1-139, 78-1-188, 81-1-172 respectively.

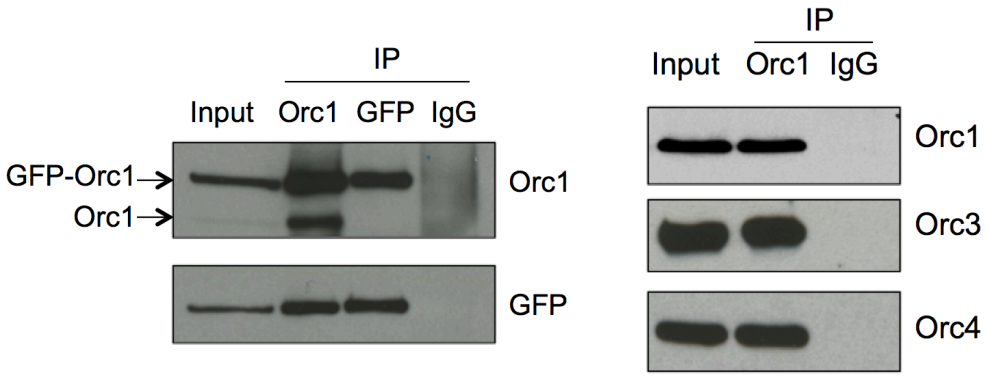

Figure 8. Monoclonal antibody immunoprecipitates GFP-tagged-Orc1 and endogenous Orc1, co-immunoprecipitates ORC subunits. A, Monoclonal antibody 78-1-188 can immunoprecipitate endogenous Orc1 protein as well as over-expressed GFP-Orc1 fusion protein from U2OS whole cell extracts, corresponding proteins are indicated with an arrow. B, Monoclonal antibody can co-immunoprecipitate other subunits of ORC including Orc3 and Orc4.

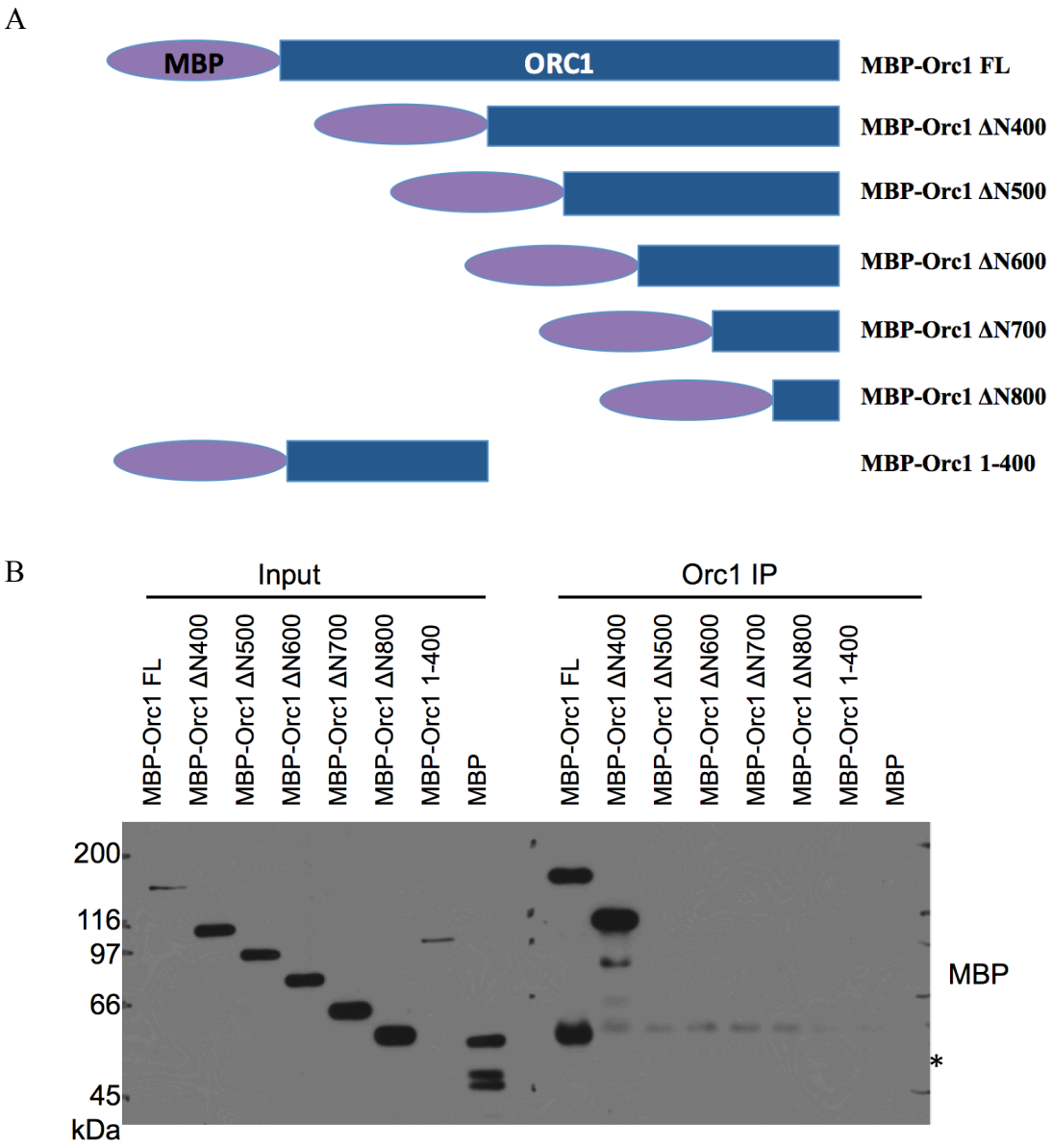

Figure 9. Epitope mapping for monoclonal Orc1 antibody. A, Antibody is used to immunoprecipitate purified MBP-Orc1 full length (FL) and truncation mutants. B, Epitope mapping for the Orc1 antigen reveals that the antibody recognizes MBP-Orc1 FL and MBP-Orc1-ΔN400 versions but not other N-terminal truncated mutants. Anti-MBP antibody was used for the blot. The corresponding sizes for the molecular weight marker are shown in kDa (kilo Daltons). Asterisk indicates cross-reacting antibody heavy chain in IP section of the blot.

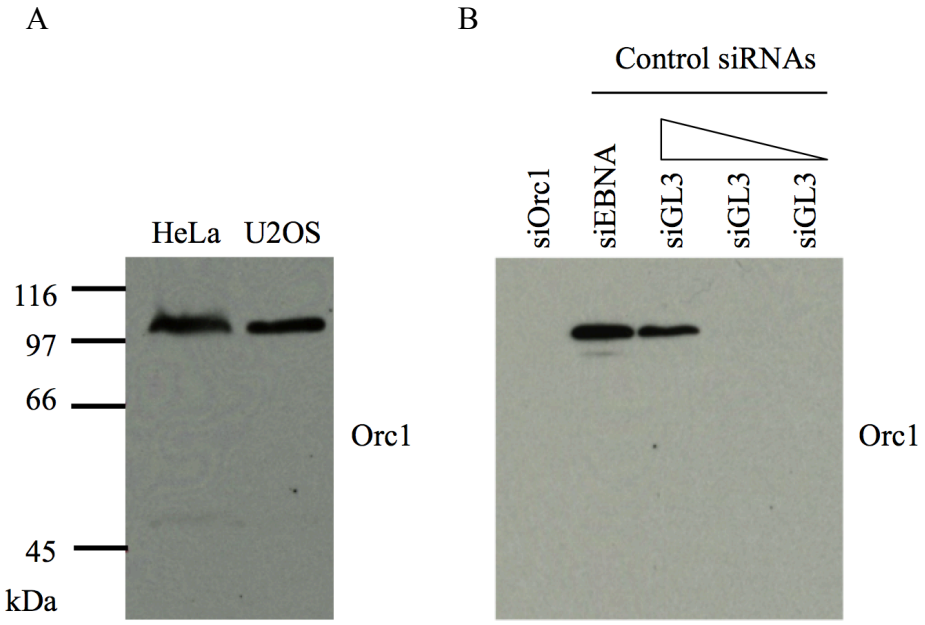

Figure 10. Orc1 antibody specifically recognizes Orc1 in cell extracts. A, Anti-Orc1 antibody 46-1-144 detects Orc1 in HeLa and U2OS whole cell extracts. B, Antibody detects Orc1 specifically in western blot. HeLa cells were treated with siRNA oligos against Orc1, or non-targeting siRNA oligos EBNA and GL3. The Orc1 band is lost in siOrc1 treated extract. GL3 treated extract had been loaded as 100%, 50% and 10% (gradient). The corresponding sizes for the molecular weight marker are shown in kDa (kilo Daltons).

Chapter 3

Chromatin dynamics of the Origin Recognition Complex

3.1 Successive salt extraction of chromatin reveals distinct protein and DNA profiles

Recent advances in genome wide tools including microarray platforms and next generation sequencing have led to advances in genome-wide profiling of chromatin binding proteins. The coverage, hence the depth of information has increased several fold with these advancements. Despite the advances in genome wide tools, the experimental protocols that are used to study chromatin interacting proteins such as chromatin immunoprecipitation have not significantly changed. One particular concern in chromatin preparation methods is that the preparation might not result in quantitative recovery of starting material. Successive salt extraction method provides a powerful tool to study protein chromatin dynamics, recovery and genome-wide profiling of physical properties of chromatin [105, 106].

My original goal was to identify a method to solubilize ORC subunits and perform chromatin immuno-precipitation to identify DNA sequences to which ORC bound throughout the cell division cycle. Therefore, to better understand the dynamics of ORC on chromatin I tested successive salt-extracted chromatin fractions of HeLa cells. First, nuclei were briefly treated with micrococcal nuclease (MNase) and then intact nuclei were subjected to successive

salt extractions with increasing salt concentration buffers **(Figure 11A)** [106]. It has been shown that successive salt-extraction of intact nuclei treated with MNase results in fractions with dramatically different genome-wide profiles; with the low salt soluble fraction enriched in highly accessible chromatin containing transcriptionally active genes and higher salt soluble chromatin representing the bulk of the chromatin. Interestingly, the profile of the insoluble fraction resembles that of low salt soluble fraction. The insoluble fraction is also enriched in transcribed regions albeit the peaks are wider, and there are additional regions in the insoluble fraction that are not present in the low salt soluble chromatin possibly representing other regions with chromatin bound complexes [105]. It is possible that large molecular weight complexes bound to these regions make it inaccessible to nucleases, rendering these regions insoluble. Treating the nuclei with successive salt extractions causes solubilization of nucleosomes **(Figure 11B)**. Initial 80 mM salt extraction solubilizes a small fraction of mono-nucleosome sized chromatin fragments. At 150 mM salt extraction those mono-nucleosome sized chromatin fragments are solubilized more effectively and as the salt concentration was increased to 300 mM di-nucleosome sized and larger chromatin fragments were solubilized in addition to mono-nucleosome sized fragments. 600 mM salt extraction solubilized tri-nucleosome sized fragments and almost no mono-nucleosome sized chromatin fragments were left beyond this point. After 600mM salt treatment the insoluble pellet consisted largely of multi-nucleosome sized larger chromatin fragments.

The protein profile at each successive extraction showed extensive differences **(Figure 11C)**. Successive salt extracted fractions were run on a SDS-PAGE gel and proteins were visualized by Coomassie Brilliant Blue staining, showing that successive salt fractions have

different protein profiles. The majority of histones were solubilized at 300 mM salt extraction and they were almost completely solubilized after 600mM salt extraction, while some proteins, especially high molecular weight proteins, were still insoluble even after high salt treatment. A histone H4 immuno-blot also showed that by 600 mM salt concentration almost all histone H4 was solubilized **(Figure 12)**.

3.2 Analysis of pre-RC components in different fractions

Chromatin association of key pre-replication complex (pre-RC) proteins was studied in successive salt extracted fractions from HeLa cells **(Figure 12)**. The results indicate that, Mcm2 and Mcm4 subunits of Mcm2-7 complex were readily solubilized at 80 and 150 mM low salt concentrations. This suggests that Mcm2-7 subunits were not tightly associated with chromatin. This result is not surprising since it has been shown that Mcm2-7 proteins alternate between soluble and chromatin bound forms during the cell division cycle [1]. The results indicate that the soluble Mcm2-7 fraction was readily solubilized at low salt extractions while the chromatin bound form was solubilized at higher salt concentrations.

Analysis of ORC subunits revealed that among the other ORC subunits Orc6 was the one that was most readily solubilized at low salt. However a small fraction of the protein remained insoluble. Orc6 is known to interact with ORC weakly and the association is likely transient [3]. This might explain why Orc6 is most readily solubilized. Orc2, Orc3 and Orc4 were also

solubilized albeit at higher concentrations and again a small portion of the proteins remained insoluble.

Interestingly, Orc1 and Cdc6 proteins were salt resistant and remained insoluble up to 300mM salt, and were solubilized only at high salt fractions. A fraction of these proteins also remained insoluble in the pellet fraction. These findings are consistent with earlier findings that Orc1 is fairly salt resistant in mammalian cells [87, 89, 107] and Cdc6 being associated with nuclease resistant structures on chromatin [108]. Fluorescence recovery after photobleaching (FRAP) analysis with YFP tagged proteins in human cells also showed a distinct profile for Orc1 [93]. Orc1 did not recover after photobleaching, while Orc2, Orc3 and HP1 were readily recovered. This indicates that Orc2 and Orc3 assemble and dissemble from chromatin more readily while Orc1 is more tightly bound to chromatin and less dynamic.

The relative resistance of ORC, especially Orc1, to salt extraction indicates a tight association between the ORC and chromatin. We have investigated the extent of MNase digestion and found no significant difference in solubility of pre-RC components. Moreover increasing the incubation time for extractions did not improve the results as the majority of the proteins were extracted within a five minutes time frame. Presence or absence of detergent in extraction buffers did not affect the results as well (results not shown). These findings suggest that the insolubility of ORC is a true phenomenon rather than an experimental artifact. General insolubility of ORC complex subunits is likely due to Orc1, which associates with chromatin tightly and facilitates the assembly of ORC on chromatin.

3.3 Different cellular fractionation methods reveal similar ORC chromatin dynamics

The finding that ORC components are resistant to extraction and a fraction of them remain insoluble led us to investigate whether this is a general phenomenon. For this reason I performed two different cellular fractionation protocols in HeLa cells **(Figure 13)**. In the first method, which was developed to study pre-RC chromatin association, cells were lysed in Triton based sucrose rich buffer [1], then nuclei were collected and resuspended in a no salt buffer and optionally treated with micrococcal nuclease. Proteins that remained in the pellet fraction were enriched in chromatin bound proteins and proteins bound to nuclear matrix **(Figure 13A)**. The second method was developed to purify chromatin bound proteins under native conditions [4]. In this method, cells were lysed in Nonidet P-40 based sucrose rich buffer. Next, nuclei were collected and resuspended in buffer B' and homogenized with a Dounce B pestle to facilitate efficient lysis of nuclei. Then, the nucleoplasmic fraction was collected. The chromatin enriched pellet was treated with the nuclease benzonase to digest both DNA and RNA. After centrifugation the supernatant containing solubilized native chromatin proteins was collected **(Figure 13B)**.

I investigated ORC chromatin association using the above-mentioned methods **(Figure 14)**. Employing the first method, the results indicated that histones were associated with chromatin as expected (found in P3 fraction on MNase untreated extract) and MNase treatment solubilizes a significant fraction of histones **(Figure 14A)**. An anti-tubulin blot showed that it

was only present in the S2 fraction indicating that the extraction of cytosolic proteins was complete. A small fraction of Mcm2 was associated with chromatin while the majority of Mcm2 was readily solubilized with or without MNase treatment. ORC subunits including Orc1, Orc2, Orc3 and Orc4 were mainly associated with chromatin and MNase treatment partially solubilized these proteins. These results suggested that ORC was bound to chromatin tightly in these cells. Orc6, on the other hand, was also found in the nucleoplasmic fraction in MNase untreated cells (S3). The finding that ORC was not completely solubilized after MNase treatment suggests ORC might be associated with nuclear matrix structures.

Native cellular fractionation method revealed that benzonase treatment solubilized histones and a significant fraction remained tightly bound to chromatin and insoluble. Mcm2 was found in the soluble nuclear fraction (N: nucleoplasm) and also in the chromatin bound fraction. A small fraction of Mcm2 was resistant to benzonase treatment, suggesting tighter chromatin association (**Figure 14B**). Interestingly, the Mcm2 that remained chromatin bound ran slower than the soluble Mcm2 protein, suggesting that it might be phosphorylated. A fraction of Orc2, Orc3, Orc4 and Orc6 was found in soluble nucleoplasmic fraction, while another fraction was chromatin bound and another fraction remained resistant to nuclease digestion. The results suggested that these proteins exist in nuclei as both soluble or chromatin bound forms. It is possible that certain combinations of these ORC subunits might exist as a sub-complex in the soluble fraction and recruited to chromatin as a sub-complex once Orc1 is bound to chromatin. Unlike other ORC subunits, Orc1 was only found in chromatin bound fraction. Interestingly, a much larger portion of Orc1 was nuclease resistant compared to other ORC subunits, again suggesting Orc1 chromatin association was stronger and tighter in comparison to the other ORC

subunits. For example, Orc2 and Orc3 was also more readily solubilized in lower salt conditions than Orc1 (**Figure 14B**). Among all ORC subunits studied Orc6 was the most readily solubilized subunit. Overall, these results again recapitulated the findings obtained by studying successive salt fractionation of MNase treated nuclei **(Figure 12)**.

3.4 Optimization of cellular fractionation method

The finding that ORC, and particularly the complex containing the Orc1 subunit, was salt and nuclease resistant raised the question whether it would be efficient to study ORC complex assembly and disassembly dynamics in vivo using cellular extracts which might not effectively solubilize ORC subunits. In order to circumvent this issue I sought to find a cellular extraction method that effectively solubilized ORC and other chromatin associated proteins.

For this purpose I investigated the effect of several buffer conditions in the cellular extraction method developed earlier [3], including buffering agent, pH, type of salt, salt concentration, presence and type of nuclease. In the end, I optimized a protocol to effectively solubilize ORC and other chromatin binding proteins **(Figure 15)**. Nuclear extracts were prepared by resuspending the cells in hypotonic buffer and the suspension was homogenized with a Dounce B pestle to facilitate complete cell lysis. The intact nuclei were treated with DNase I and Benzonase nuclease cocktail in low salt. After the digestion, salt concentration was adjusted to 400mM NaCl to enable solubilization of chromatin-associated proteins efficiently **(Figure 15A)**.

Analysis of ORC and MCM from these extracts revealed that Mcm3 was completely solubilized with nuclease and high salt treatment **(Figure 15A)**. Orc2, Orc4 and Orc6 subunits were almost completely extracted and little or no protein is left in the insoluble pellet fraction. Orc1 and Orc3 were efficiently solubilized and a small fraction of these proteins still remained in the insoluble pellet fraction **(Figure 15B)**. Interestingly, these two ORC subunits bind the heterochromatin protein HP1 [93]. An anti-tubulin blot showed that cytoplasmic fractionation was complete prior to nuclear extraction. These results encouraged us to pursue the study of ORC assembly dynamics in vivo now that I had an efficient extraction protocol for ORC constituents.

In summary the results indicated that ORC was associated with chromatin tightly and among other ORC subunits Orc1 had the highest degree of salt and nuclease resistance indicating its tighter and less dynamic association with chromatin, as was shown by FRAP analysis earlier [93]. The distinct Orc1 chromatin dynamics might also indicate possible Orc1 and nuclear matrix interaction and is further discussed in Chapter 6.

3.5 Chromatin immunoprecipitation of ORC subunits

As mentioned earlier in Chapter I, there is evidence in fission yeast that ORC dynamics during the M/G1 period of the cell cycle pre-determine DNA replication origin usage and efficiency in S phase, and is also related to the timing of pre-RC assembly in G1. Timing of ORC binding to an origin is correlated to the time of firing of the origin in S phase [81]. In the fruitfly *Drosophila*, the density of ORC on chromatin is reflected by the temporal dynamics of DNA replication since sites with higher ORC content tend to replicate earlier in S phase [82].

By studying ORC chromatin localization by ChIP-Seq at different stages during cell cycle, I might be able to determine if there is correlation with temporal profile of DNA replication. Moreover I would be able to compare ORC binding sites with other chromatin features such as active or repressed chromatin marks, DNase hypersensitivity, and correlation with binding sites of other chromatin binding proteins.

At the time, there were only few studies involving ORC ChIP followed by semi-quantitative or real time quantitative-PCR (RT-qPCR) analysis [109-116]. However, these studies often used only a few handpicked sites to show binding of ORC and a few sites to show absence of binding at the same regions on chromatin (MCM4/PRKDC, TOP1, LMNB2 and beta-globin loci). In addition, these studies did not show the primers they used were actually working,

and lacked characterization of the antibodies used, and did not include data showing antibodies immunoprecipitate ORC from cross-linked extracts except for one study [112].

A recent paper on Orc1 ChIP-seq that utilizes low-density chromatin that is enriched in protein-DNA complexes shows enrichment of human Orc1 at 13,000 peaks over the genome with approximately 8000 peaks reproduced in replicate experiments [2]. When I investigated their published data the peak intensity looked low (around 20 reads per peak for Orc1 compared to RNA Pol IIa which has about 200 reads at some of the same loci), also some of the earlier loci (LMNB2 and CSF2) that were shown to be bound by Orc1 using the same antibody [109, 117, 118] were not bound by Orc1 in this recent study or the peak intensity was too low, or the regions nearby also had peaks. In addition, the polyclonal antibody used in these studies was never characterized properly [109].

Therefore, I proposed to take an unbiased approach to look at all ORC binding sites genome-wide by next-generation sequencing and I first proposed to confirm that the conditions I am using are suitable for immunoprecipitating ORC.

Conventional chromatin immunoprecipitation techniques rely on denaturing conditions, which usually contain SDS in nuclear lysis buffer [119]. Briefly, Hela suspension cells were fixed with formaldehyde and quenched by glycine. Cells were lysed in a hypotonic buffer and then nuclei were lysed in 1x volume of buffer A (50 mM Tris-Cl pH 7.5, 1%SDS,). Next, 1x volume IP dilution buffer (20mM Tris pH7.5, 150mM NaCl, 1%Tx100, 0.01%SDS) was added to lysed nuclear extracts and the mixture was sonicated. After removal of insoluble debris by a

high-speed spin, the lysates were further diluted by addition of 3x volume IP dilution buffer. I have performed Orc1 and Orc3 chromatin immunoprecipitations using these extracts and antibody crosslinked to magnetic beads. I tested the amount of solubilized ORC proteins after sonication, about 90% of Orc1 and Orc3 were solubilized **(Figure 16A)** and only a small fraction was left in the insoluble pellet after 16 cycles of sonication, which sheared the chromatin to an average size of 500bp **(Figure 16B)**. However when I performed Orc1 immunoprecipitation using this chromatin extract, I failed to detect any Orc1 by western blot. Also the Orc3 immunoprecipitation was inefficient **(Figure 16C)**.

One possibility why I failed to immunoprecipitates Orc1 is that the conditions used for the ChIP is denaturing and therefore unsuitable to bring down native Orc1. Since I earlier found that the Orc1 antibodies that immunoprecipitates Orc1 failed to detect denatured Orc1 in western blots, denaturing conditions in ChIP also seemed to prevent antibody-antigen recognition. Thus I proposed to use a ChIP method using non-denaturing conditions. For this purpose, I optimized a non-denaturing ChIP method to immunoprecipitate ORC **(Figure 17A)**.

It is possible to shear DNA by sonication or micrococcal nuclease digestion. The conditions for sonication and micrococcal nuclease (Mnase) digestion have been optimized (results not shown). Extensive cycles of sonication (up to 20 cycles) were required to fragment the DNA to about 300bp length which might be very harsh for proteins and might dissociate the DNA bound proteins as well as protein complexes. On the other hand, Mnase treatment resulted in fragments of mono-nucleosome sized DNA at 5000u/mL enzyme concentration. I also compared Mnase and sonication methods for solubilization and chromatin immunoprecipitation

efficiency. Orc1 and Orc3 were more readily solubilized with micrococcal nuclease treatment than sonication **(Figure 17B)**. Both methods yielded very efficient immunoprecipitations of Orc2 and Orc3 (**Figure 17C)**. For Orc1, I tested all three monoclonal antibodies that were generated (45-1-139, 78-1-188, 81-1-172). However, among those antibodies only clone 78-1-188 immunoprecipitated Orc1 effectively **(Figure 17D)**, which is the same monoclonal antibody that was further characterized in Chapter II. Since I was interested in ORC dynamics throughout the cell cycle and would like to investigate the dynamics of ORC chromatin binding and whether there is correlation with temporal ORC binding and temporal regulation of DNA replication, I used synchronized HeLa suspension cells to perform non-denaturing ChIP with Mnase treatment.

Asynchronously growing HeLa suspension cells were blocked with addition of thymidine in two consecutive rounds to the culture medium, which creates an imbalance in nucleotide pools causing feedback inhibition of nucleotide synthesis and inhibition of DNA synthesis [120]. The cells were monitored by flow cytometry for DNA content and inspected under bright field microscopy for the presence of condensed mitotic chromosomes. The majority of the cells progressed through mitosis at 9-10 hours after release (results not shown), and we know that by this time point Orc1 starts to localize to chromatin (live cell imaging observation, Chapter V), and Orc2 and Orc3 are known to be present at centromeres during mitosis [5]. Flow cytometry profile showed that cells were in G1/S right before release, then cells progressed through S phase by 6 hours, were in G2/M at 9 hours and started entering G1 by 12 hours after release. At 17h cells reached late G1 **(Figure 18A)**.

Since the goal was to perform ChIP-Seq, I wanted to have biological replicates for each experiment. There are 4 time points that I want to investigate, asynchronous cells, 9 hour mitotic cells, 12 hour early G1 and 17 hour late G1 cells. The extracts for ChIP were prepared as described earlier, the cells were fixed, lysed, and then extracts were treated with Mnase to fragment the DNA. The extracts were then tested for the presence of Orc1 and Orc2 **(Figure 18B)**. The Orc2 levels were constant at each time point while the Orc1 levels were lower at M phase cells since Orc1 levels start to increase during M after it gets degraded at S phase.

The ChIP extracts were subjected to immunoprecipitation by anti- Orc1, Orc2 and Orc3 antibodies and the IP efficiency was assessed after reverse crosslinking by western blot **(Figure 19)**. Under these conditions I was able to chromatin immunoprecipitate Orc2 and Orc3 from these extracts at each time point studied during cell cycle and from asynchronous extracts **(Figure 19 A, B)**. For Orc1, it was hard to conclude that the immunoprecipitations worked due to the high background in the western blots **(Figure 19 C)**. The background was due to the crosslinking performed for ChIP extract preparation, and even tough the extracts were reverse crosslinked overnight, the background did not improve. Since our earlier results indicated that Orc1 associates with chromatin strongly and was nuclease and salt resistant, the crosslinking that is performed prior to extract preparation might not be necessary and this is generally known as native ChIP and used extensively for histone proteins [121]. The advantages of using the native ChIP protocol include antibody epitope recognition might be more efficient and higher immunoprecipitation yield can be obtained. Disadvantages of this technique are: it might not generally be applicable to non-histone proteins, and protein can rearrange on chromatin during preparation. We still wanted to see white this method could be utilized for Orc1 ChIP. Thus I

have performed the exact protocol without crosslinking as well and immunoprecipitated Orc1 from this extract **(Figure 20)**. Orc1 was immunoprecipitated efficiently using non-crosslinked (native) extracts. Orc1 was also immunoprecipitated from crosslinked extract as well, appearing as a darker band over the high background. I also tested whether Orc1 that was immunoprecipitated from non-crosslinked extracts has DNA by phenol-chloroform purification and found that it was the case (result not shown).

At the end, I performed Orc1, Orc2 and Orc3 immunoprecipitations using crosslinked non-denaturing extracts from asynchronous, mitotic, early G1 and late G1 cells. I also performed Orc1 immunoprecipitations using non-crosslinked non-denaturing extracts from asynchronous, mitotic, early G1 and late G1 cells. After phenol-chloroform purification, DNA was used to prepare sequencing libraries. I have used Illumina TruSeq barcoded kit for this purpose, which enabled me to pool up to 12 samples at a time. Samples were then sequenced using HiSeq2000 instrument. The resulting data was analyzed using Galaxy web tool offered by the CSHL Bioinformatics Facility, which enables users to upload data and analyze using powerful servers (http://bioinfo.cshl.edu/index.html).

The data for Orc1, Orc2, Orc3 ChIP-Seq showed extensive background all over the genome lacking any specific peaks for all the time points studied **(Figure 21)**. PRKDC locus is one of the loci where Orc1 has been shown to be bound by Orc1 ChIP-seq [2]. Earlier studies also indicated this locus was bound by Orc1 and Orc2 by ChIP-qPCR [112, 122, 123]. However as mentioned earlier, these studies did not use characterized antibodies, nor did they include extensive analysis of the locus. Only few amplicons were investigated in the locus. Our results

indicate extensive reads all over the PRKDC locus by Orc1, Orc2 and Orc3, however the intensity of this reads is low **(Figure 21)**. One reason why I might have obtained these low abundance sequences throughout the genome might be that, ORC in human cells is a low abundance complex and lacks sequence specificity for DNA binding thus it is hard to enrich enough to obtain meaningful data. Another possibility is ORC binds all over the genome and the enrichment at particular sites is really low. Another possible reason why I did not observe any specific peaks might be due to size selection of 150-200 base pairs fragments during library preparation. A final possibility for the lack of peaks in the genomic data is that the PCR amplification of the post immuno-precipitated and size-selected DNA might be saturated, causing apparent uniform enrichment across all regions of the genome. It is possible that ORC binds to smaller sized DNA fragments and size selection during library preparation causes loss of these fragments. Therefore I have prepared ChIP-seq libraries with smaller size DNA inserts and the libraries will be sequenced.

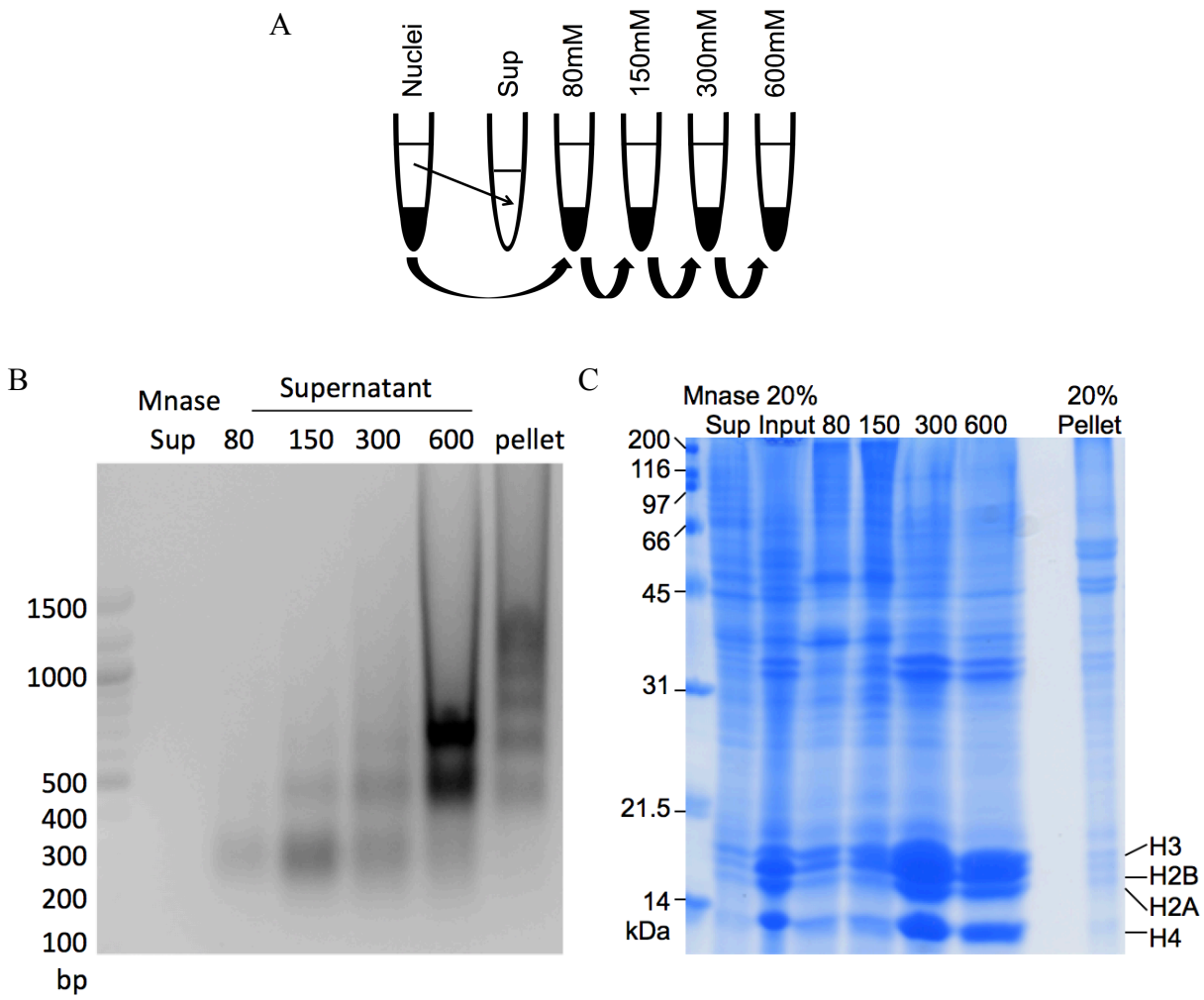

Figure 11. Profiling of successive salt-extracted fractions of chromatin in human cells. A, Illustration depicting the experimental outline: cells are first lysed in hypotonic buffer. Intact nuclei treated with MNase, supernatant is saved (MNase sup). Nuclei then subjected to successive salt-extraction with increasing salt concentration. The insoluble pellet after the last salt extraction (600mM) is also saved. B, DNA profile of successive fractions on agarose gel shows that increasing salt concentration solubilizes larger chromatin fragments. C, Protein profile of successive fractions revealed by Coomassie stain, histones are almost completely solubilized after 600mM salt extraction.

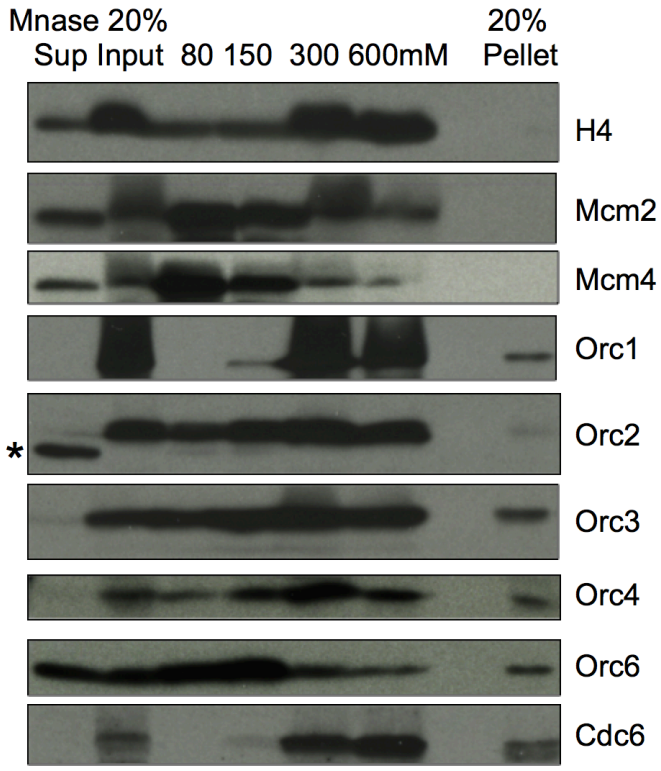

Figure 12. Chromatin dynamics of key pre-RC components. Profile of pre-Replication Complex (pre-RC) components in successive salt-fractions are studied by western blots. H4: Histone H4. Asterisk (*) in Orc2 blot represents a non-specific band [3].

A

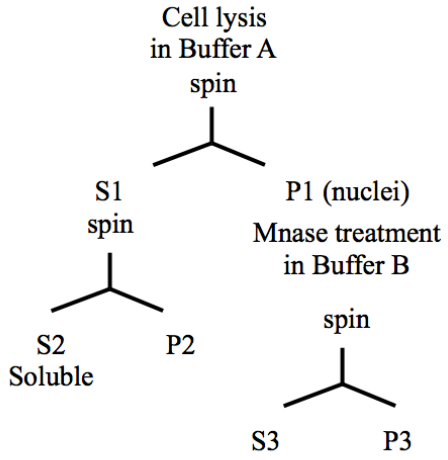

Buffer A:
10 mM HEPES pH 7.9
10 mM KCl
0.1% Triton X-100
1.5 mM MgCl2
0.34 M sucrose
10% glycerol
1 mM DTT

Buffer B:
3 mM EDTA
0.2 mM EGTA
1 mM DTT

B

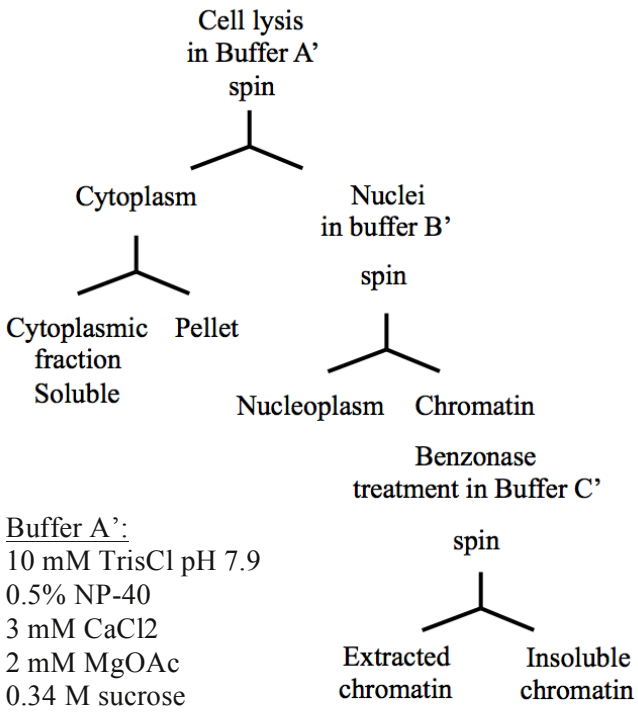

Buffer A':
10 mM TrisCl pH 7.9
0.5% NP-40
3 mM CaCl2
2 mM MgOAc
0.34 M sucrose
1 mM DTT

Buffer B':
20 mM HEPES pH 7.9
150 mM KOAc
0.1% NP-40
1.5 mM MgCl2
3mM EDTA
10% Glycerol
1 mM DTT

Buffer C':
20 mM HEPES pH 7.9
150 mM KOAc
1.5 mM MgCl2
10% Glycerol

Figure 13. Comparison of cellular fractionation methods. A, Cellular fractionation method. Cells are lysed in hypotonic buffer, nuclei is treated with Mnase to release proteins from chromatin. Compositions of buffers are listed. Adapted from [1]. B, Native cellular fractionation method. Cells are lysed in hypotonic buffer, nuclei is treated with nuclear lysis buffer. Chromatin is treated with Benzonase to release chromatin bound proteins. Compositions of buffers are listed. Adapted from [4].

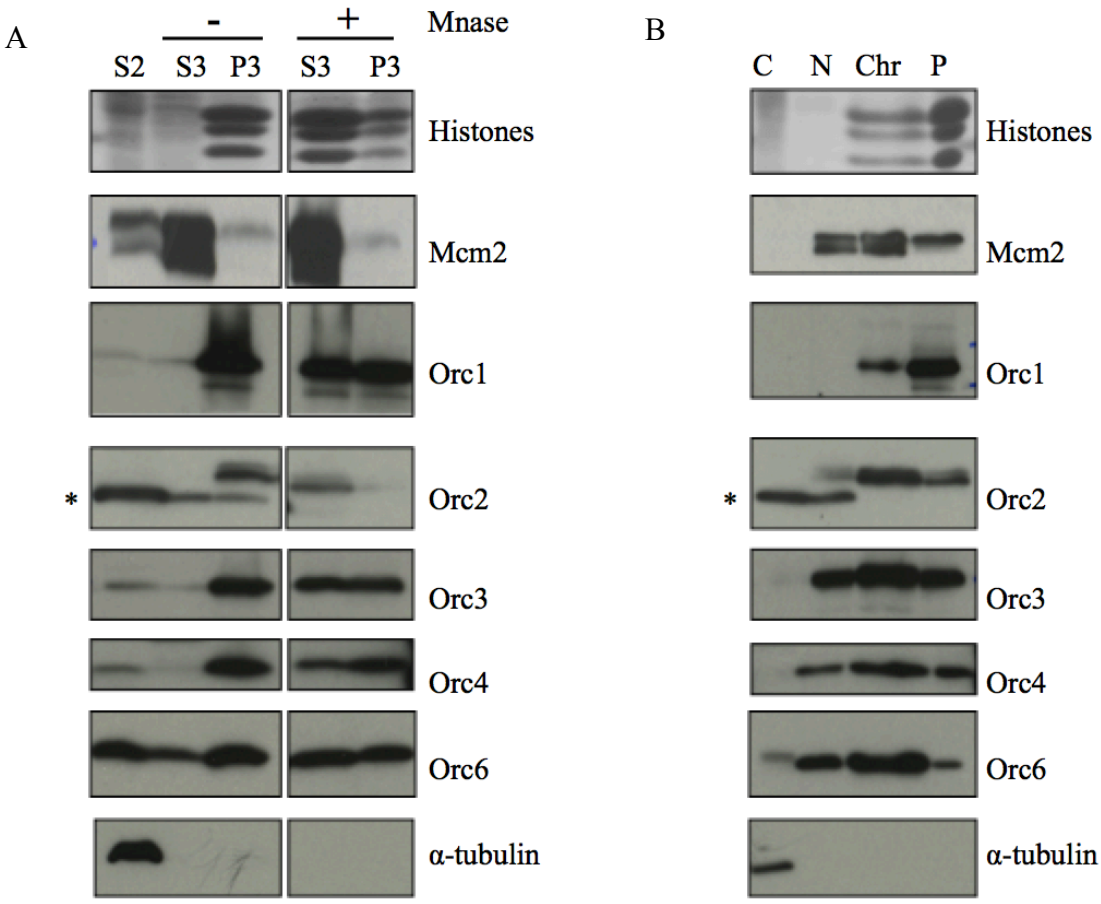

Figure 14. Chromatin association of ORC. A, Chromatin association of ORC was studied using cellular fractionation method as illustrated in Figure 13A. Cells were lysed, nuclei were either treated or untreated with MNase. Different cellular fractions were run on SDS-PAGE gel. Coomassie staining shows histones. ORC subunits were studied by western blot. B, Chromatin association of ORC was studied using native cellular fractionation method as illustrated in Figure 13B. Cells were lysed, and nuclei were treated with Benzonase. Different cellular fractions were run on SDS-PAGE gel. C: cytoplasm, N: nucleoplasm, Chr: chromatin, P: insoluble pellet. Coomassie staining shows core histones. ORC subunits were studied by western blot. Asterisk indicates non-specific band in Orc2 blots.

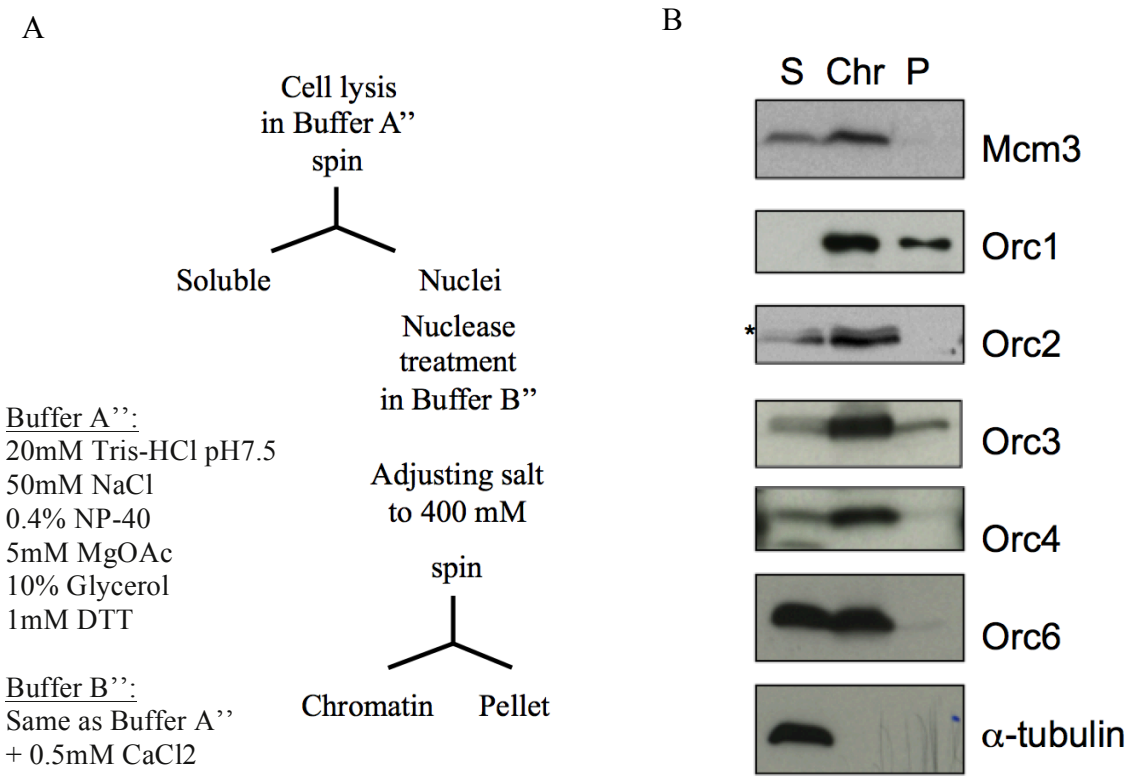

Figure 15. Efficient extraction of ORC by nuclease and high salt cellular fractionation method. A, Overview of the cellular extraction method. Cells were lysed, nuclei were treated with nuclease cocktail (DNase I and Benzonase), salt concentration was adjusted to 400 mM to release chromatin-associated proteins. Buffer compositions are listed. B, Extraction profiles of ORC and MCM as investigated by western blots. Asterisk shows the band in Orc2 blot as verified in an earlier study [5]. S: Soluble fraction Chr: Chromatin bound fraction P: Pellet

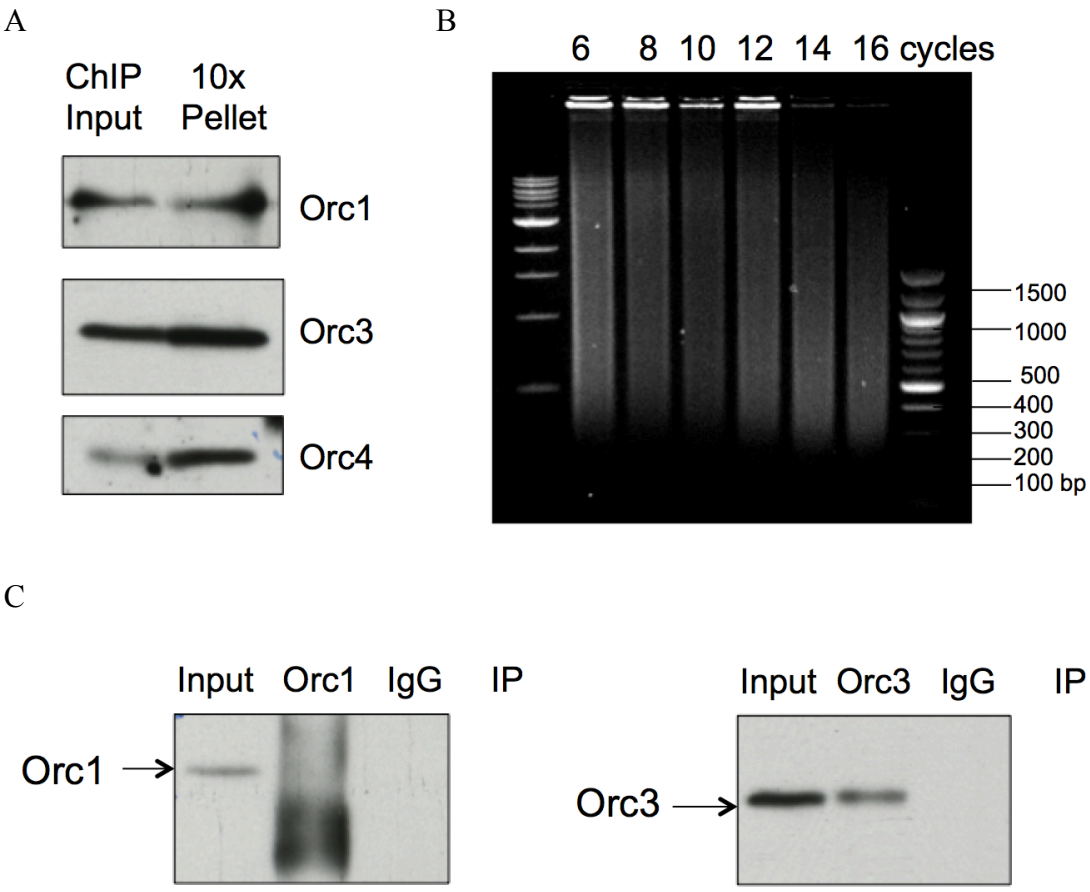

Figure 16. Conventional ChIP method fails to immunoprecipitate ORC efficiently. A, The presence of ORC proteins in the extract was tested by western blot using input extract and 10 fold concentrated insoluble pellet. B, The fragmentation profiles of DNA after indicated successive sonication cycles were analyzed by agarose gel electrophoresis. C, Orc1 and Orc3 chromatin immunoprecipitation and western blot after reversing the crosslinking.

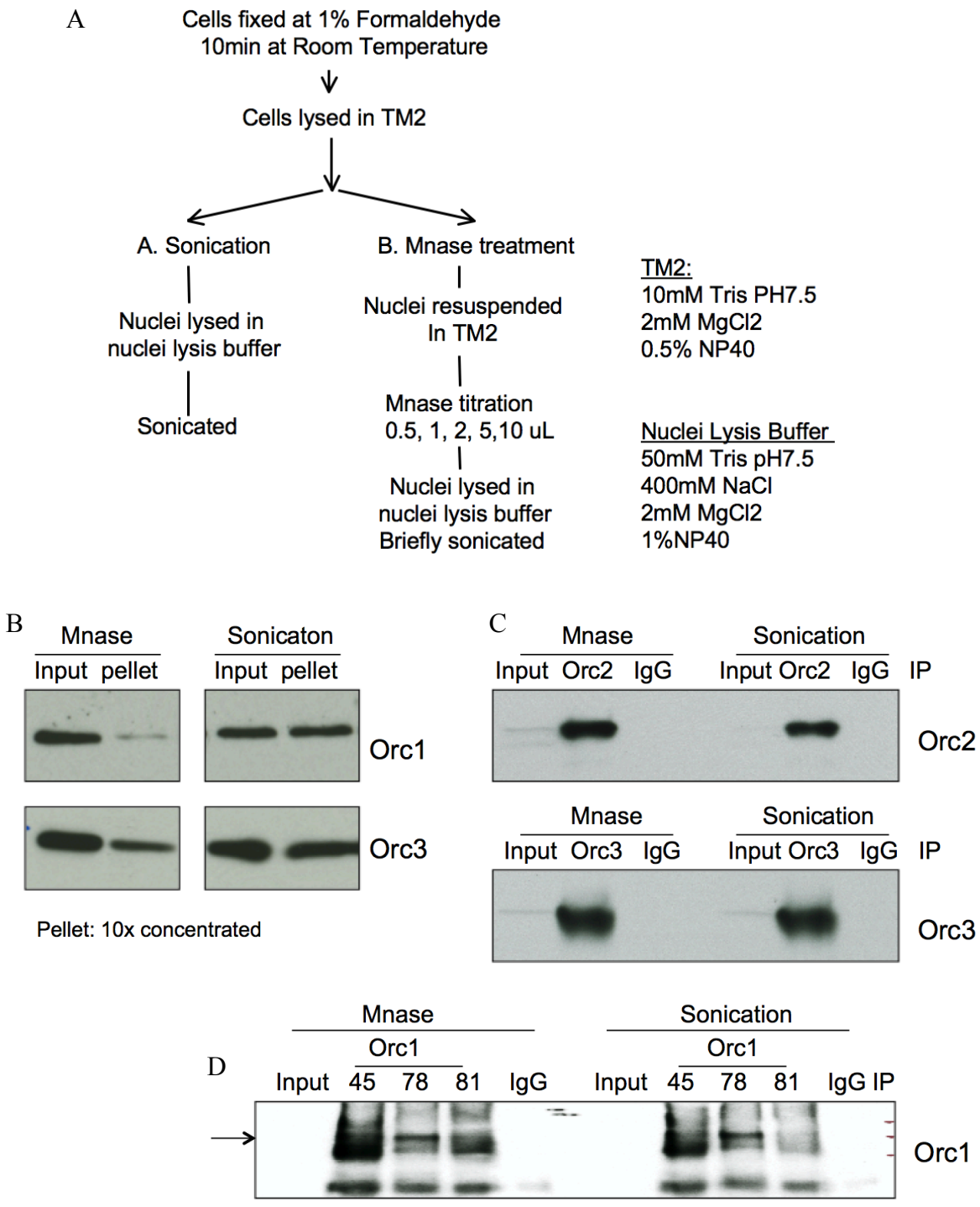

Figure 17. Non-denaturing conditions can be used to chromatin immunoprecipitate ORC.

(Continued on next page)

Figure 17. Non-denaturing conditions can be used to chromatin immunoprecipitate ORC. A, Diagram of non-denaturing ChIP method. Cells were fixed and lysed. Nuclei were either sonicated or digested with micrococcal nuclease (Mnase) treated to fragment the DNA. The salt concentration of the final extract after sonication or Mnase treatment was adjusted to 200mM. B, Levels of Orc1 and Orc3 were measured in the extract to compare solubilization of ORC in sonicated and Mnase treated extracts. C, Orc2 and Orc3 IP efficiency was tested by western blots after reversing the crosslink to protein. D, Orc1 IPs performed using 3 different monoclonal antibodies (45-1-139, 78-1-188, 81-1-172 respectively) and efficiency was tested by western blot after reversal of the crosslinking. Arrow indicates the molecular weight where Orc1 normally runs.

A

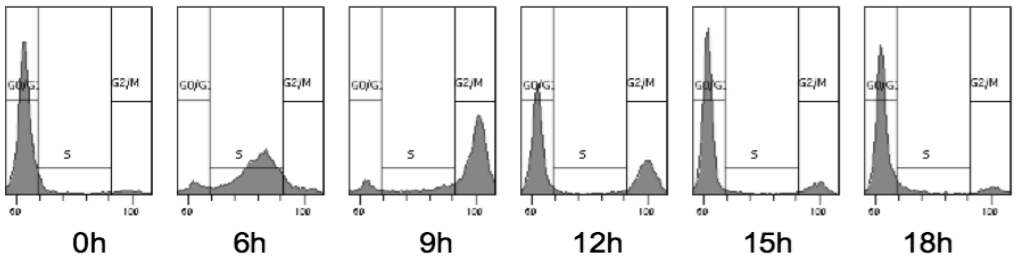

B

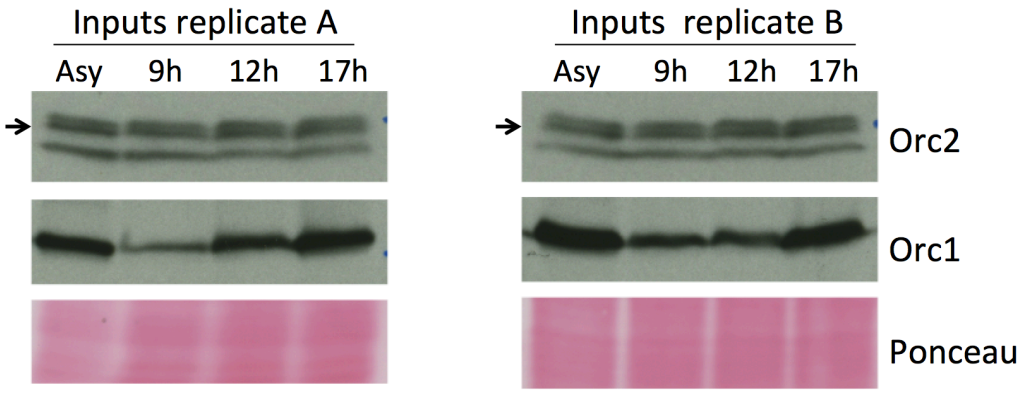

Figure 18. Non-denaturing extracts for ChIP from synchronized HeLa cells. A, HeLa suspension (spinner) cells were synchronized by double thymidine block and release. Cell cycle profile was monitored by flow cytometry using propidium iodide (PI) stained cells. X-axis shows DNA content, Y-axis shows cell count. B, Extracts from each replicate were tested for Orc1 and Orc2. Arrow indicates specific Orc2 band, other bands shown are cross-reacting bands as verified in an earlier study [5].

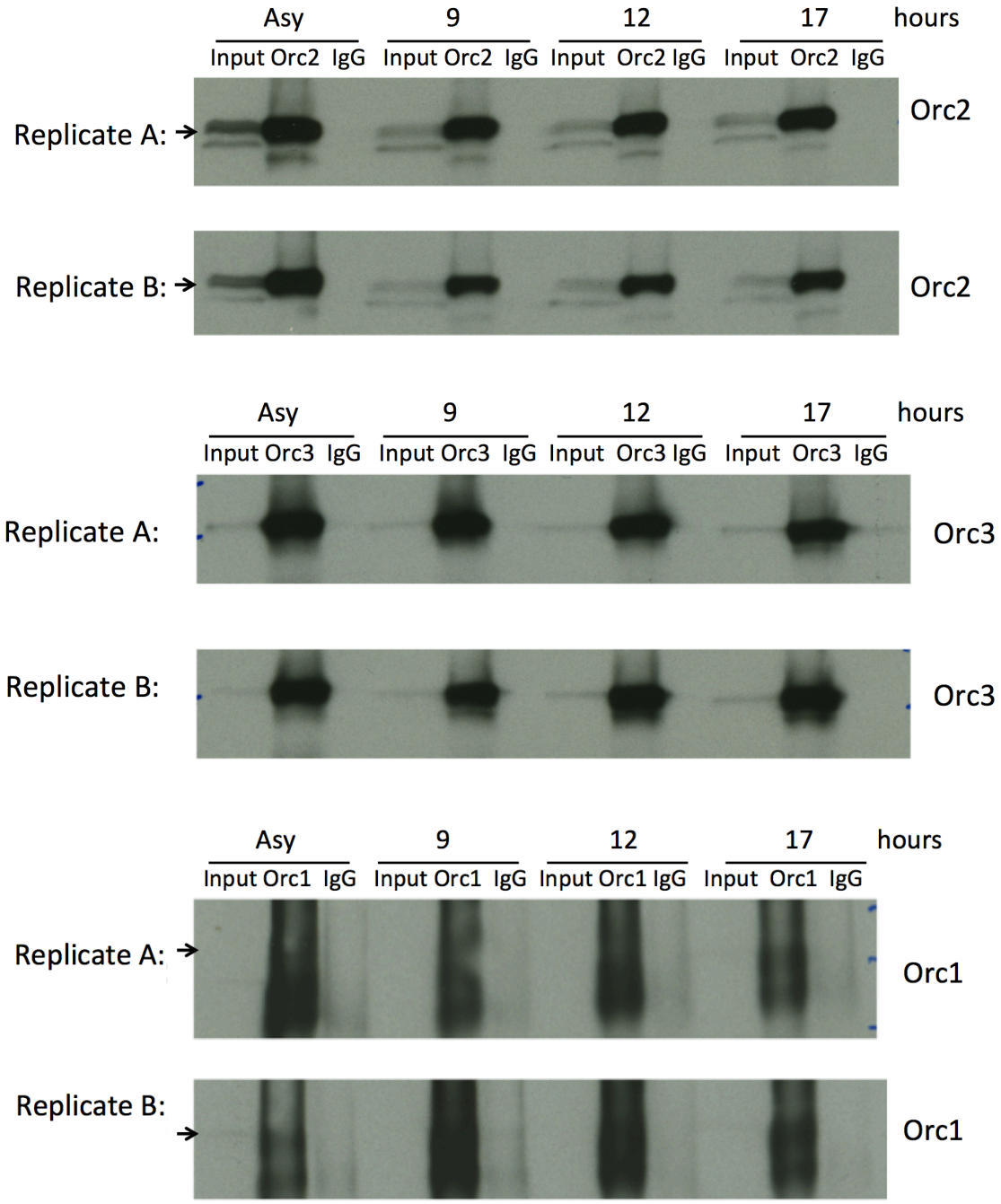

Figure 19. Crosslinked ORC is immunoprecipitated from synchronized HeLa cells. **(Continued on next page).**

Figure 19. Crosslinked ORC is immunoprecipitated from synchronized HeLa cells. HeLa suspension (spinner) cells were grown asynchronously or synchronized by double thymidine block and released for indicated hours and crosslinked. Chromatin extracts were prepared in non-denaturing conditions as described. A, Orc2 immunoprecipitations were performed using asynchronous (Asy) or synchronized (release time points in hours) ChIP extracts. B, Orc3 immunoprecipitations were performed using asynchronous or synchronized ChIP extracts. C, Orc1 immunoprecipitations were performed using asynchronous or synchronized ChIP extracts. Arrows show the molecular weight band where Orc1 normally runs.

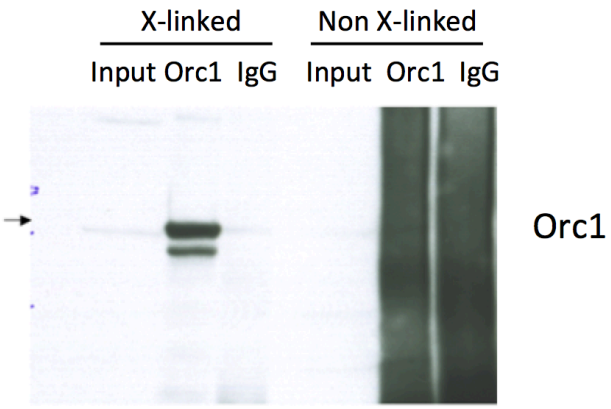

Figure 20. Native ChIP method used for Orc1 immunoprecipitation. Orc1 was immunoprecipitated from non-crosslinked extracts and also from crosslinked extracts. Arrow indicates the molecular weight where Orc1 protein normally runs.

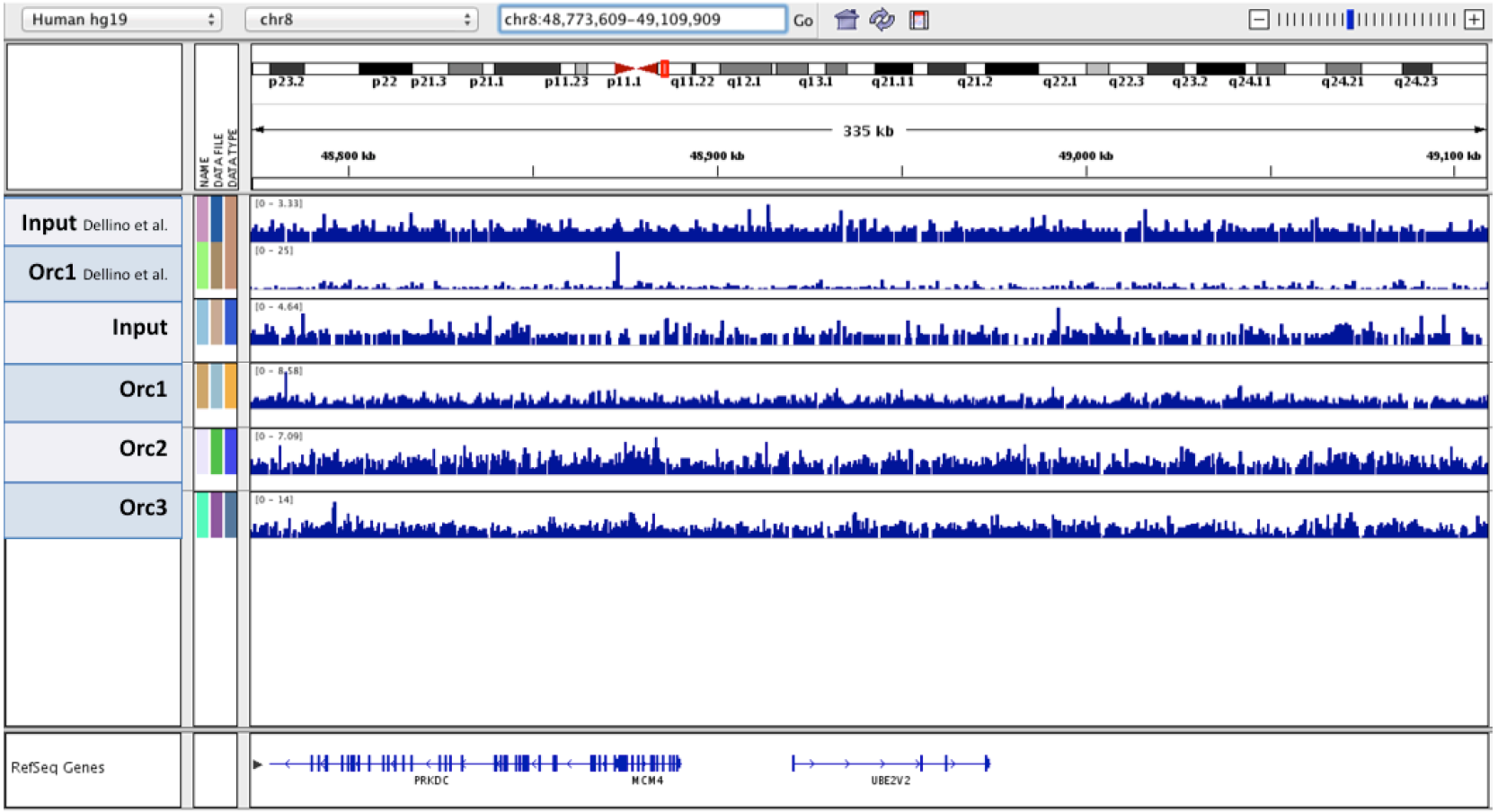

Figure 21. ChIP-Seq profile of ORC on PRKDC Locus. Orc1, Orc2 and Orc3 ChIP-seq tracks from this study are shown (as well as input as a control) using IGV browser. The published data on Orc1 ChIP-seq tracks (indicated as Dellino et al.) is also shown as a reference (input control is shown as well) [2].

Chapter 4

Dynamics of the Origin Recognition Complex during cell cycle

4.1 Synchronization of HeLa cells to study cell division cycle profile

Despite a general knowledge of ORC assembly and disassembly dynamics in vitro, I wanted to study ORC complex dynamics in deeper detail in vivo throughout the cell division cycle. For example, it is not known exactly when all of the ORC subunits form a six-subunit complex in human cells, although it is assumed to be in G1 phase because Orc1 is degraded during the G1 to S phase transition. Monoclonal antibodies that recognize native ORC subunits, including Orc1, Orc2 and Orc3, were used to immunoprecipitate ORC complex at different time-points during cell cycle.

I used human HeLa suspension (spinner) cells to study ORC and pre-RC dynamics in vivo because the amount of cells could be easily scaled up for biochemical analysis. In order to synchronize cells I used a double-thymidine block and release method to arrest them at the G1/S border and then release the block so that cells can progress through S phase and subsequent mitosis. I adapted the protocol from an earlier study with some modifications [3] **(Figure 22)**. Asynchronously growing, early passage HeLa cells were blocked with addition of thymidine to

the culture medium, which creates an imbalance in nucleotide pools causing feedback inhibition of nucleotide synthesis and inhibition of DNA synthesis [120]. After two consecutive thymidine blocks, cells were released into warm medium without additional thymidine to allow cells to progress through cell division cycle **(Figure 22A)**. Samples were collected at various time-points and cell cycle progression was monitored by propidium iodide (PI) staining of DNA and analyzed by flow cytometry **(Figure 22B)**.

Analysis of the cell cycle profile show that cells were successfully blocked at the G1/S border at right before the release (0 hour time-point), cells progressed through S phase and by 6 hours they were in mid-S to late –S phase. A sharp G2/M peak appeared at the 9 hour time-point and persisted during the 10 hour time-point. The cells were also studied under microscope to monitor the presence of mitotic cells by viewing chromatin condensation and the presence of a metaphase chromosome plate and this also peaked at the 9-10 hour samples (results not shown). At 12 hours cells were already in G1 phase and they continued to progress through G1 for up to the 18 hour time point. By 21 hours a fraction of cells entered S phase and 24 hours marked a greater fraction of cells in S phase, however cell synchrony was partially lost at and after this time point.

4.2 Dynamics of pre-RC components monitored during the cell cycle

Unlike yeast cells, human cells are proposed to have a dynamic ORC assembly and disassembly cycle throughout the cell division cycle. Formation of ORC begins with binding of

Orc1 to chromatin, which is followed by recruitment of other ORC subunits during early G1 phase, and as the cells enter S phase the Orc1 subunit is ubiquitinated and targeted for degradation and ORC becomes dispensable [3, 88, 89, 124]. I studied the dynamics ORC along with other pre-RC components in the double thymidine blocked and released HeLa cells **(Figure 23).**

Since ORC is bound to chromatin tightly, especially Orc1, I used the cellular fractionation method described in Chapter 3 that effectively solubilizes ORC from nuclei to study pre-RC levels during cell division cycle **(Figure 15)**. HeLa cells were synchronized at the G1/S border by double thymidine block and release and extracts from each time points were used to study levels of pre-RC components during the cell division cycle. The dynamics of cell division cycle progression was monitored by several cell cycle markers **(Figure 23)**. The results showed that cells started entering S phase as they were released from the block, as seen by the Cyclin E blot which shows that levels were very high at 0-hour time-point but then immediately disappeared. Progression through S phase was monitored by Cyclin A blot, because levels of Cyclin A gradually increased as the cells progressed through S phase and entered into G2 phase. After 9 hours mitotic cells accumulated as seen from the metaphase specific phospho-serine-10 histone H3 blot and by 10 hours the vast majority of the cells were in mitosis.

The levels of Cdc6 in nuclei fluctuate during cell cycle and it has been shown that Cdc6 is targeted for degradation by the Anaphase Promoting Complex E3-ubiquitin ligase (APC-CDH1) that mediates Cdc6 proteolysis during early G1 [125]. In addition, Cdc6 phosphorylation by Cyclin A/CDK2 leads to its re-localization to the cytoplasm during S phase [126]. My results

show that Cdc6 levels were low during S and early G1 phase in nuclei consistent with previous observations. The anti-Cdt1 blot showed that the levels of Cdt1 increased as the cells progressed through G1 phase of the cell division cycle and then it was degraded as cells progressed into S phase. It is known that in human cells, Cdt1 levels accumulate in G1 phase and it is degraded at the onset of S phase to prevent re-licensing of the origins [127-129].

The results show that levels of Orc1 dramatically decreased as the cells entered S-phase while the levels of the other ORC subunits, including Orc2, Orc3 and Orc4, remained fairly constant during the cell division cycle. Orc1 levels started to increase as the cells entered the mitotic phase and accumulated over the course of G1 phase. As mentioned earlier, it is known that Orc1 is ubiquitinated and targeted for degradation on the onset of S phase [88]. Mcm2-7 exists as a chromatin bound complex and in an un-bound form in human cells and chromatin bound form is known to be dissociated as cells progress through S phase [130], whereas chromatin bound Mcm2-7 levels increase in G1 [1]. My results indicate that there was a decrease in chromatin bound Mcm3 during S phase and the levels increased as the cells progressed through G1, concurrent with the increase in Cdt1 levels which is involved in loading of Mcm2-7 onto chromatin [131].

4.3 ORC Complex dynamics during the cell division cycle

I then investigated ORC complex assembly and disassembly dynamics during the cell division cycle in vivo. For this purpose, I performed immunoprecipitations (IP) with ORC antibodies. I needed to optimize the conditions to perform immunoprecipitations to reduce background and increase IP efficiency. For this purpose I developed a protocol to crosslink the antibody to magnetic beads and optimized the conditions to maximize the amount of antibody cross-linked without affecting the efficiency of epitope recognition by the antibody. I found that the ratio of antibody to beads was a crucial factor (results not shown). I also optimized the IP conditions to reduce background and increase efficiency and found several factors including initial concentration of the extract used, incubation time, IP washing conditions, concentration of ATP affect immunoprecipitation efficiency (results not shown). The final method I used is described in the Materials and Methods chapter (Chapter 7).

I performed immunoprecipitations using double thymidine synchronized HeLa cell nuclear extracts with monoclonal antibodies raised against Orc1, Orc2 and Orc3 subunits of the ORC complex **(Figure 24)**. The results show that the amount of Orc1 immunoprecipitated with Orc1 antibody decreased in S phase cells, concomitant with a decrease in the levels of Orc1 during that time. Similarly when Orc2 or Orc3 antibody was used for immunoprecipitation, the amount of Orc1 that co-immunoprecipitated was significantly lower in S phase cells, but the interactions between Orc1 and Orc2, Orc1 and Orc3 and orc1 with Orc4 were detectable by the

beginning of G1, which corresponded to the 12 hour time point in the synchronized HeLa cells. Interestingly, even though Orc1 was present at earlier time-points during mitosis, the interaction between Orc1 with Orc2 or Orc3 or Orc4 occurred only in G1 phase.

On the contrary, the interaction between Orc2 and Orc3 was found to be present throughout the cell division cycle with a slight increase during G1 phase when Orc1 was also present **(Figure 24)**. Earlier reports indicate that in vitro Orc2 and Orc3 interacted regardless of presence of other ORC subunits [132]. Furthermore, Orc2 and Orc3 are known to be associated with chromatin throughout the cell division cycle [1]. The increase in interaction levels in the presence of Orc1 may suggest that Orc1 might stabilize this interaction and/or it might facilitate extra interaction opportunities by recruiting them into ORC in addition to the interactions that were already present in the cell.

The results demonstrated that Orc4 associated with Orc2 and Orc3 only when Orc1 was also present in the complex and the interaction was lost upon degradation of Orc1 during S phase (**Figure 24**). These results suggest that recruitment of Orc4 to ORC is stabilized and/or promoted in the presence of Orc1, which is consistent with an earlier report on assembly of ORC complex both in vitro and in vivo [3]. Unfortunately I was not able to study the association of Orc5 due to lack antibodies that were suitable for this study. I tried raising an antibody against Orc5 protein however the monoclonal hybridoma cell lines that reacted strongly against Orc5 did not proliferate and died.

Overall, our results indicate that ORC is dynamic throughout the cell division cycle. Levels of Orc1 decreased in S phase and gradually increased during mitosis and were highest during G1 phase, while the levels of Orc2, Orc3 and Orc4 were fairly constant. Interaction between Orc1 and the other ORC subunits studied occurred only during G1 phase, while the interaction between Orc2 and Orc3 occurred throughout the cell cycle. Orc4 interaction with ORC only occurred during G1 when Orc1 was present in the complex, suggesting it might be facilitated and/or stabilized by Orc1.

A

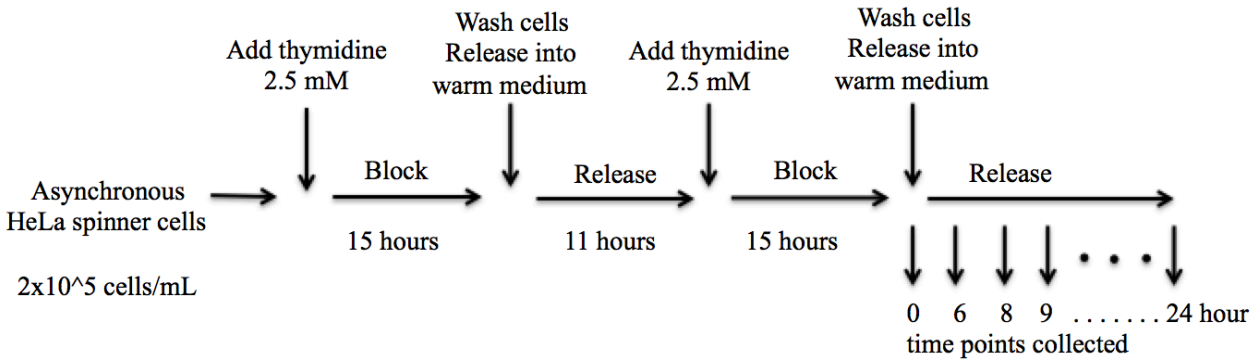

B

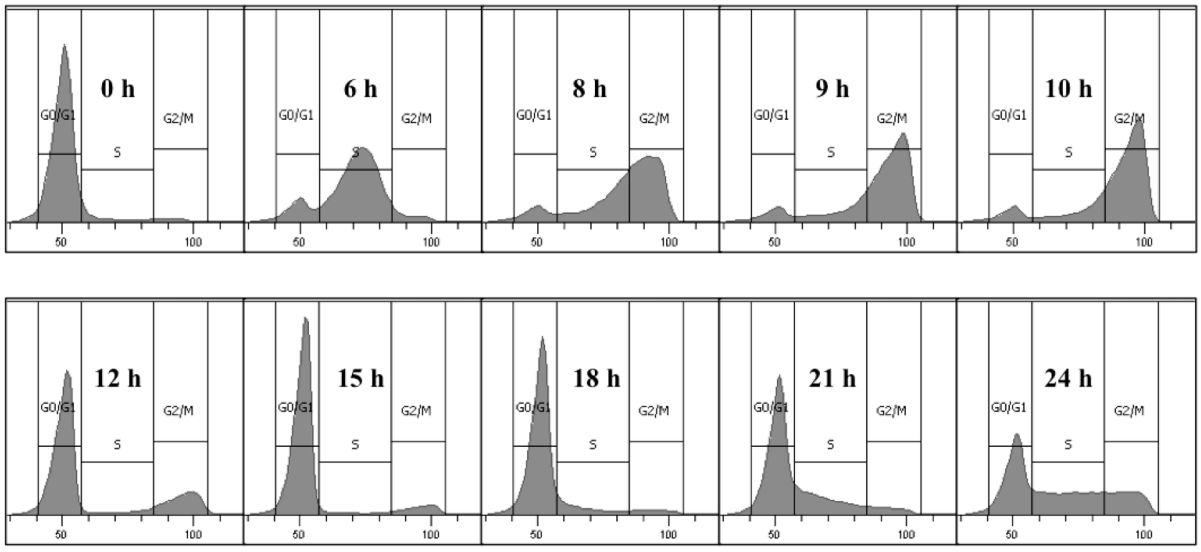

Figure 22. Synchronization of HeLa cells at G1/S border by double thymidine block and release. A, Experimental outline for double thymidine block and release. Cells were blocked in excess thymidine containing medium to arrest them at G1/S border. B, Samples from each time point were collected and DNA content (propidium iodide stained) was monitored using flow cytometry. X-axis shows DNA content (PI-area), Y-axis shows percentage of cells.

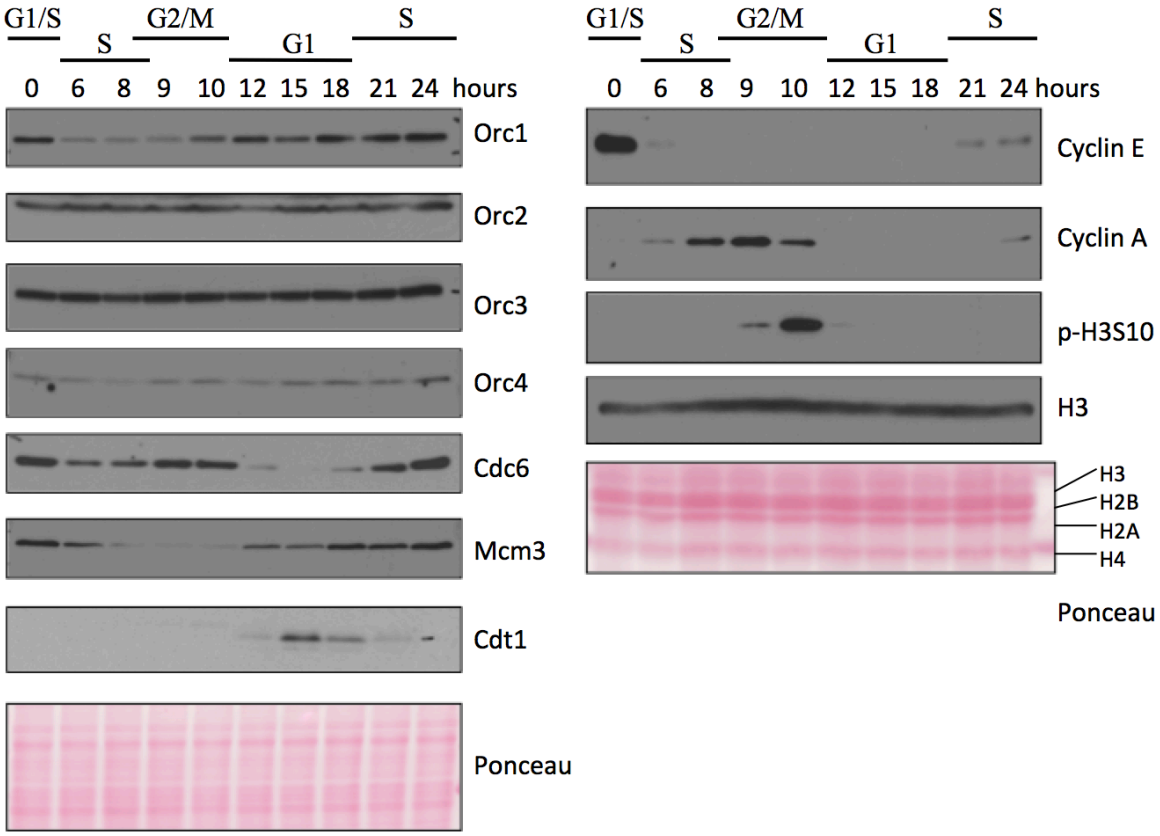

Figure 23. Levels of pre-RC components during the cell division cycle in HeLa nuclear extracts. Levels of pre-RC proteins and cell cycle markers in synchronized HeLa nuclear extracts at indicated time points and cell cycle phase were studied by western blot. p-H3S10 denotes phospho-serine 10 histone H3 blot. Ponceau stained blots are shown as loading controls.

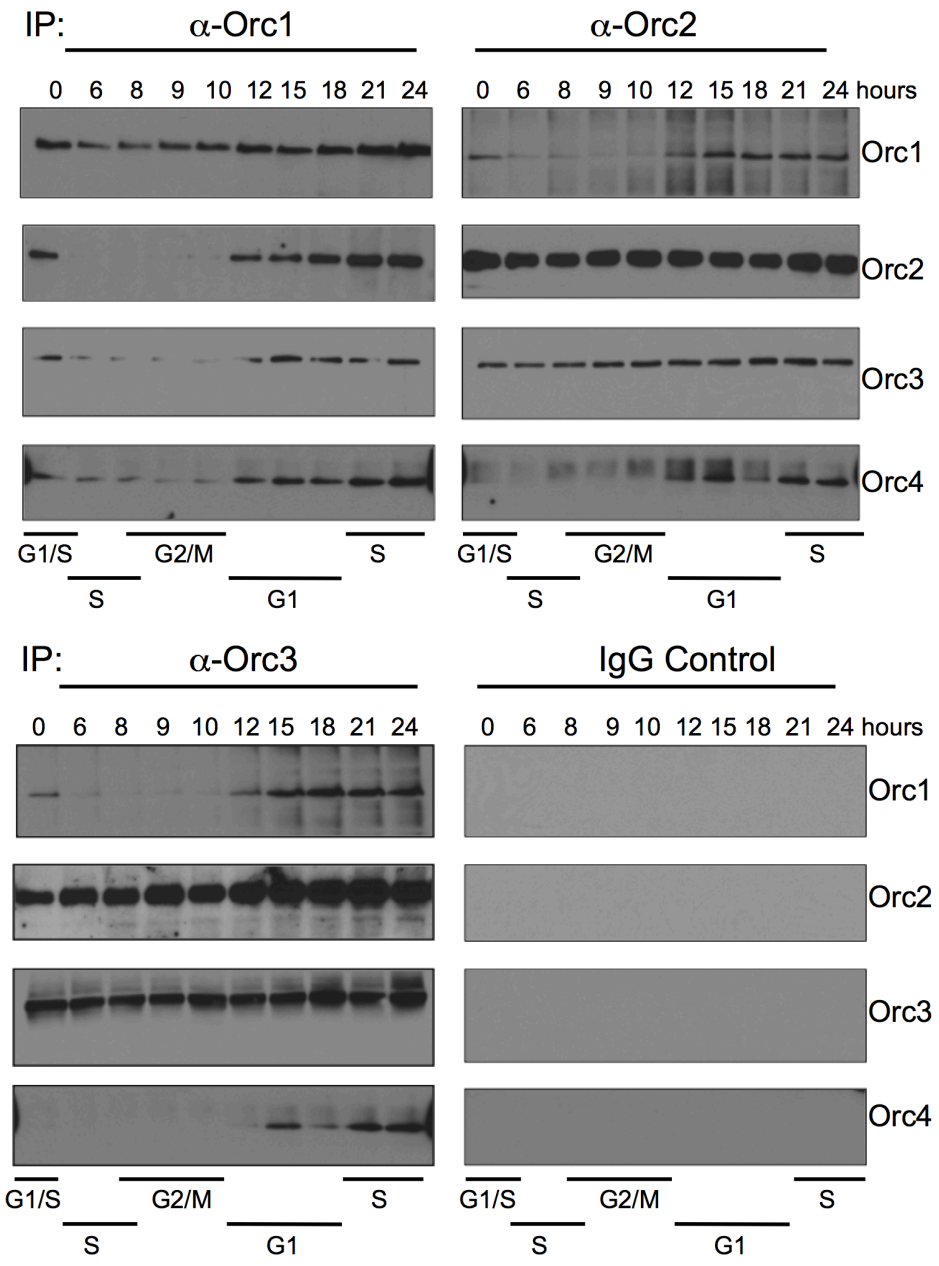

Figure 24. Dynamics of origin recognition complex during cell cycle. Immunoprecipitation (IP) of Orc1, Orc2 and Orc3 were performed from double-thymidine synchronized HeLa suspension cell nuclear extracts at the indicated time-points after release and cell cycle phases. Co-immunoprecipitation of Orc1, Orc2, Orc3 and Orc4 were investigated by western blots as indicated.

Chapter 5

Organized Orc1 spatio-temporal dynamics

5.1 Orc1 is localized to chromatin during mitosis

The observation that levels of Orc1 gradually increase as the cells goes through mitosis **(Figure 17)** led me to investigate when exactly new synthesized Orc1 becomes localized to chromatin.

In collaboration with Drs. Supriya Prasanth and Manzar Hossain, a former and current postdoctoral fellow, respectively, in the Stillman laboratory, I investigated Orc1 chromatin localization dynamics using a YFP-Orc1 U2OS stable cell line **(Figure 25)**. This cell line expresses YFP-Orc1 in levels similar to endogenous Orc1 (result not shown). Live cell imaging showed that in G2 cells, Orc1 levels were low **(Figure 25, a)**. Interestingly, as the cells entered prophase and chromatin condensation began; Orc1 levels increased in cells and became visible exclusively on the condensed chromatin **(Figure 25, d-h)**. Orc1 levels continued to increase on chromatin during metaphase and anaphase, and persisted on chromatin throughout the process of cell division **(Figure 25, e-l**).

In collaboration with Dr. Manzar Hossain, I then investigated Orc1 chromatin localization with live cell imaging during mitosis using a U2OS stable cell line that expressed a teratrcycline (tet)-inducible GFP-Orc1. Levels of GFP-Orc1 expressed in these cells were comparable to endogenous Orc1 levels [100]. Similar to results shown in Figure 23, we observed that Orc1 levels build up in early mitotic cells and Orc1 was loaded onto chromatin during prophase with simultaneous chromatin condensation **(Figure 26, a-s)**. Orc1 was observed on chromatin throughout the extent of mitosis and after the cells underwent telophase, the Orc1 signal became diffuse as the nuclear membrane formed in the daughter cells and chromatin decondensation began **(Figure 26, t-x).**

Orc1 was found to be associated with chromatin earlier than other ORC subunits such as Orc2. During mitosis, Orc2 appeared diffusely distributed in the cell while Orc1 was observed on chromatin in telophase (Figure 27A, a). After mitosis both proteins appeared on nucleus during G1 (Figure 27A, b). Therefore, Orc1 appeared in the daughter nuclei prior to Orc2, suggesting that Orc1 chromatin association was one of the first events in pre-RC assembly. It is known that depletion of Orc1 results in reduced chromatin association of Orc2 [89]. These results indicate that Orc1 is the first ORC subunit to bind to chromatin extensively during mitosis that facilitates recruitment of other ORC subunits to chromatin.

To further support this hypothesis, Orc1 was depleted by siRNA treatment in the YFP-Orc1 U2OS stable cell line and Mcm3 chromatin loading was assessed **(Figure 27, B)**. siRNA oligos targeted against either the coding region of Orc1 or 3'UTR of endogenous Orc1 were used in addition to a control non-targeting siRNA against luciferase. In cells treated with control

siRNA, Orc1 and Mcm3 chromatin loading was normal **(Figure 27B, a)**. However, in cells treated with siRNA against coding region of Orc1, depletion of both endogenous Orc1 and YFP-Orc1 resulted in loss of Mcm3 protein from the chromatin **(Figure 27B, b)**, suggesting loading of Mcm3 protein on chromatin requires Orc1, consistent with earlier findings [89]. To address whether the YFP-Orc1 can functionally complement endogenous Orc1, cells were treated with siRNA targeted against 3'UTR of endogenous Orc1. In these cells only depletion of endogenous Orc1 but not YFP-Orc1 was observed (data not shown). Mcm3 loading was normal in these cells suggesting YFP-Orc1 could functionally complement endogenous Orc1 and rescue MCM3 loading defect **(Figure 27B, c)**.

Together these results suggest that the Orc1 subunit of ORC acts as pioneer factor that binds to chromosomes extensively during mitosis and recruits other pre-RC components to facilitate origin licensing on those sites.

5.2 Dynamic spatio-temporal patterning of Orc1 during G1

The results showed that Orc1 appeared first on chromatin during mitosis, previous studies showed that the binding of Orc1 protein to chromatin was lost during the G1/S transition and Orc1 was degraded as cells enter S phase [87-89]. To study the dynamics of Orc1 in human cells during G1, YFP tagged human Orc1 was used for transient transfection experiments in mammary epithelial MCF7 cells and diploid human fibroblasts IMR-90. In addition to these cells, YFP-Orc1 stable U2OS osteosarcoma cells were also used **(Figure 28)**. YFP-Orc1 in IMR-90 **(Figure**

28A), U2OS cells **(Figure 28B)**, MCF7 cells **(Figure 28C)** all showed variable Orc1 nuclear localization.

Interestingly, Orc1 showed homogenous punctate nuclear staining in a population of cells **(Figure 28A, a; 28B, a-b; 28C, a-c)** while other cells showed that Orc1 was restricted to large and discrete foci **(Figure 28A, b-c; 28B, c-d; 28C, d-i)**. Time-lapse live cell imaging of YFP-Orc1 expressing human MCF7 cells **(Figure 28C)** revealed cell cycle regulated distribution of Orc1. First, Orc1 showed a homogenous punctate distribution **(Figure 28C, a-c)**, later however it was found at larger foci around the nucleoli **(Figure 28C, d-j)** and the nuclear periphery. These patterns formed by Orc1 were striking since they were reminiscent of the pattern of DNA replication in S-phase. By 10-14 hours, Orc1 almost disappeared from the nucleus in MCF7 cells marking the beginning of S phase **(Figure 28C, l)**. Therefore, the results suggest that Orc1 shows dynamic spatiotemporal patterns, after which it is degraded in human cell lines studied.

Spatio-temporal patterns of other pre-RC constituents including Mcm3 and PCNA were also studied during cell cycle **(Figure 29)**. Association of the hexameric MCM complex is the final step in assembly of pre-RC. Earlier reports show that MCM proteins do not co-localize with DNA replication forks during S-phase [133, 134]. S-phase replication patterning is usually monitored by DNA replication fork protein Proliferating Cell Nuclear Antigen (PCNA) staining or BrdU pulse incorporation to mark replication foci in the nuclei [49, 135-137].

Dual immuno-fluorescence labeling of Mcm3 (green) and PCNA (red) after pre-extraction of soluble proteins in MCF7 cells revealed homogenous punctate distribution of

Mcm3 and absence of PCNA in G1 cells **(Figure 29A, a-a'')**. As the cells progress through S phase Mcm3 distribution changed, initially it was localized as punctate foci **(Figure 29A, b-b'')**, later it was found at nuclear and nucleolar periphery **(Figure 29A, c-f)**. Interestingly, spatio-temporal patterning of Mcm3 mimics the PCNA staining during S phase. However, MCM patterns preceded PCNA patterns by about 1-2 hours during cell cycle **(Figure 29A, c-g)**. As the cells entered G2 neither Mcm3 nor PCNA was detectable. These observations are consistent with earlier findings that MCM spatio-temporal dynamics might anticipate replication fork temporal dynamics in S phase [134]. These results suggest that temporal pattern of Mcm3 distribution during G1 precedes S-phase PCNA patterns and temporal dynamics of MCM proteins could anticipate the replication patterns.

Dual immunolabeling of Mcm3 and PCNA in YFP-Orc1 expressing MCF7 cells showed that Orc1 was present only in cells that were PCNA negative and had homogenous punctate Mcm3 distribution **(Figure 29B, a-a''')**. In cells where very faint PCNA staining was observed, indicating very early S-phase, Orc1 staining was also very weak **(Figure 29B, b-b''')**. These results suggest that temporal patterns formed by Orc1 are restricted to G1 nuclei only. However it is sill possible that a small fraction of Orc1 remains bound to chromatin beyond S-phase, similar to Orc2 subunit of ORC, which remains associated with centromeres after S phase [5]. These observations support the earlier findings that Orc1 levels are cell cycle regulated and it is degraded at G1/S boundary [88, 124].

5.3 Orc1 localization in G1 phase anticipates temporal patterning of DNA replication

The finding that spatio-temporal dynamics of Orc1 during G1 phase was similar to some of the global DNA replication patterns, particularly the late replication patterns seen in S phase raised the question whether Orc1 temporal dynamics might reflect temporal replication patterns. The spatio-temporal patterns of DNA replication are known to be inherited from mother nuclei to daughter nuclei [52-54]. Therefore, it is possible to investigate whether the Orc1 replication-like patterns in G1 phase in daughter nuclei coincide with the S-phase pattern of DNA replication of the previous cell cycle. In order to investigate this possibility, YFP-Orc1 U2OS stable cells were pulse labeled with Alexa dUTP 594 in S phase of generation 1. Following three washes to remove nucleotides, cells were allowed to go through mitosis and enter G1 of the next generation and were monitored by live cell imaging **(Figure 30A)**. Imaging for both Alexa dUTP 594 (red) and YFP-Orc1 (green) patterns revealed a significant degree of overlap of the patterns in 6% of the G1 phase cells. **(Figure 30B, a-b)**. In other words, DNA replication patterns from previous generation showed overlap with Orc1 patterns in G1 phase of next generation. Similar results were obtained when cells were labeled with BrdU in S phase, allowed to go through mitosis and YFP-Orc1 pattern was investigated by fixed cell analysis **(Figure 30C)**.

The overlap of YFP-Orc1 and replication pattern was most evident in late S phase patterns. In some cells the YFP-Oc1 pattern did not overlap with Alexa dUTP pattern instead the patterns were adjacent to each other **(Figure 30B, c-c'')**. In most of the cells, no co-localization

between YFP-Orc1 and DNA replication pattern was observed; however, this result was expected since matching of a snapshot of 15 minute S phase pattern to a snapshot of YFP-Orc1 pattern in G1 that changes over the course of 14 hours, was highly unlikely.

These findings strongly suggest that spatio-temporal patterns of Orc1 during late G1 phase reflects the pattern of DNA replication found in late S phase. In addition, successive nuclear patterning profiles seen by Mcm3 also reflect similarity with global DNA replication patterns as seen by PCNA. These results indicate that a similar spatio-temporal patterning dynamics in nucleus is followed by Orc1, Mcm3 and PCNA, sequentially. Orc1 is gradually degraded during late G1 phase and the last remaining Orc1 is associated with chromatin that is late replicating in S phase. It is possible that a common feature that persists through G1, S and subsequent G1, S in next generation causes this phenomenon.

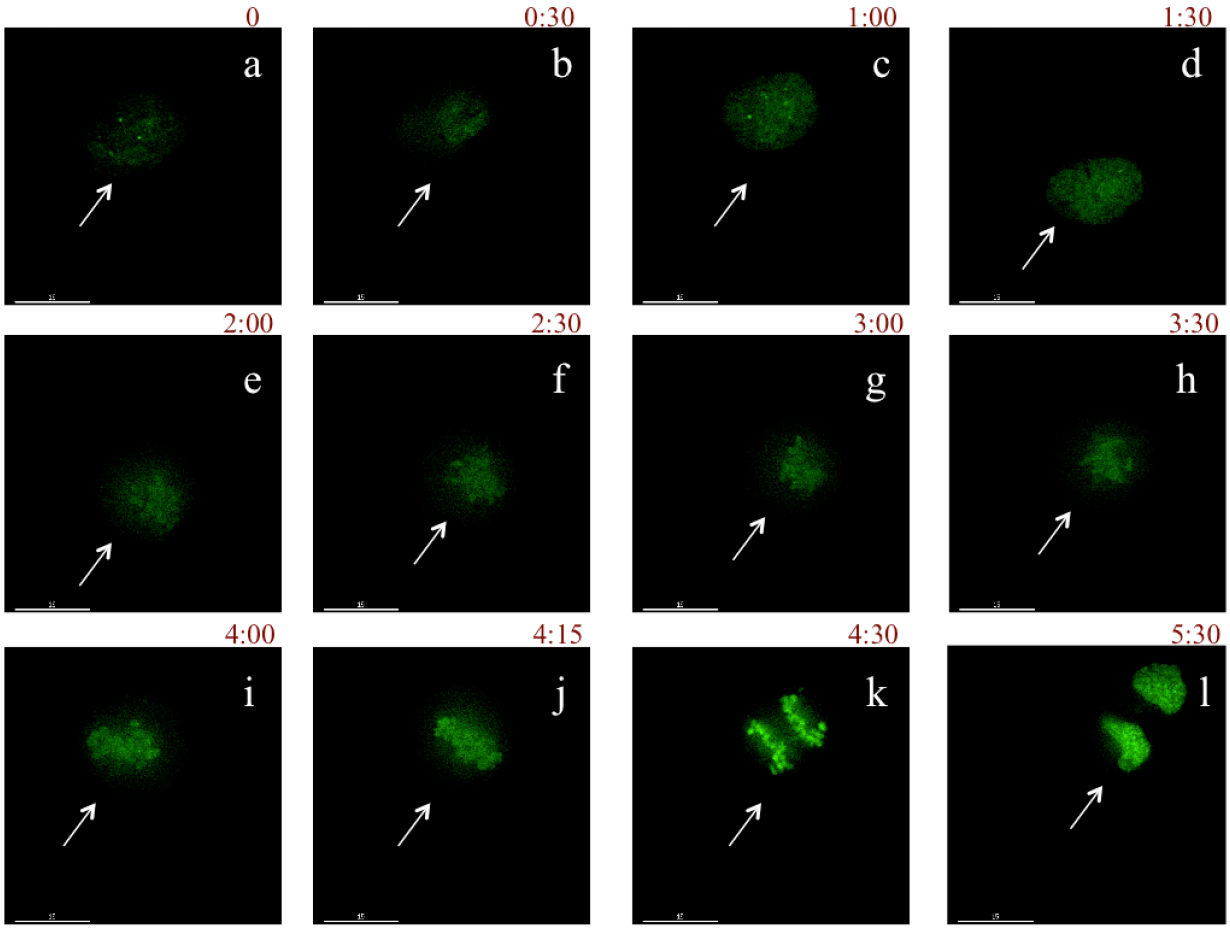

Figure 25. Orc1 localization during mitosis in YFP-Orc1 stable U2OS cells. Cells were monitored by live cell imaging as described in methods section. Frames were selected from live cell imaging movie to show the dynamics of Orc1 localization (a-l) at indicated time points (in hours). Arrow points the cell that was moving along the frame once it became rounded. Scale bar represents 5μm.

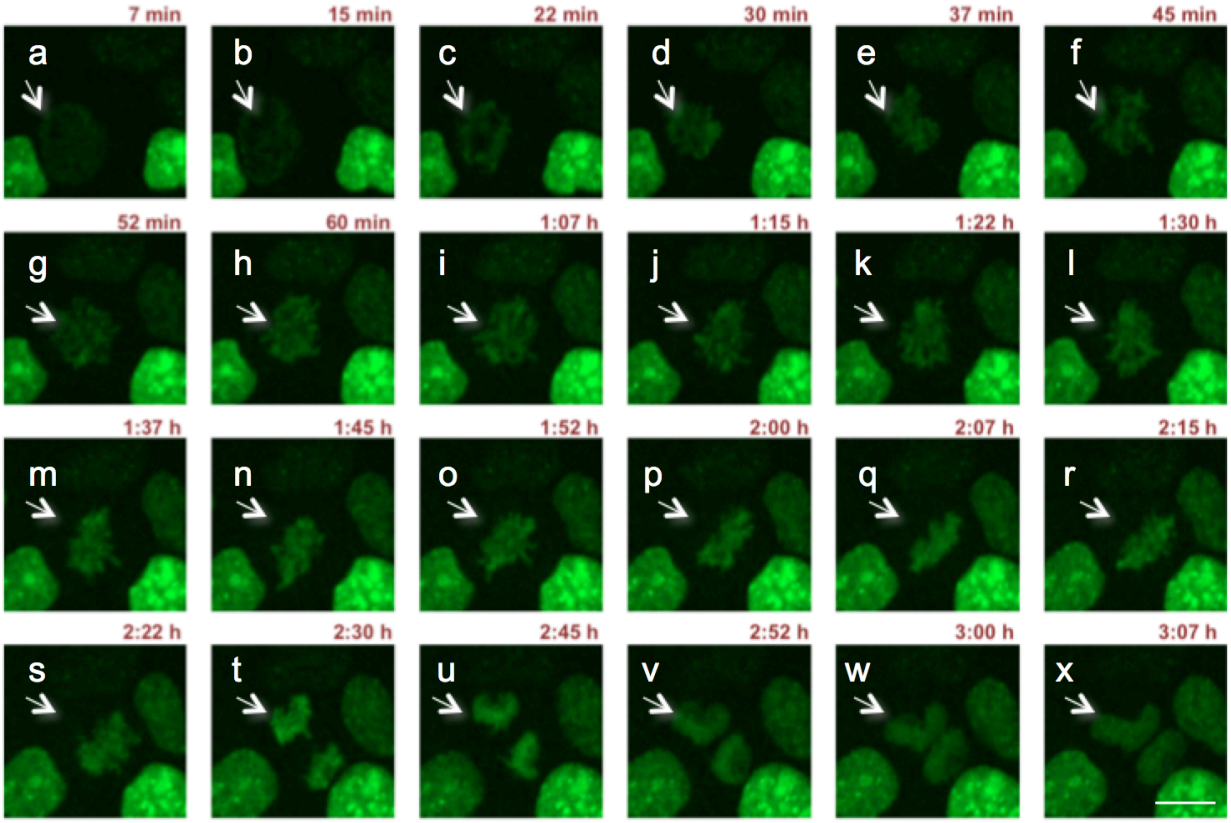

Figure 26. Orc1 is loaded onto chromatin during early prophase in mitosis. Tet-inducible GFP-Orc1 U2OS cell line was followed by live cell imaging through mitosis. Arrow highlights the cell followed through mitosis (a-x) at indicated time points. Orc1 is loaded onto chromatin during prophase and stays on chromatin throughout mitosis. Scale bar represents 5 μm. Data obtained in collaboration with Dr. Manzar Hossain.

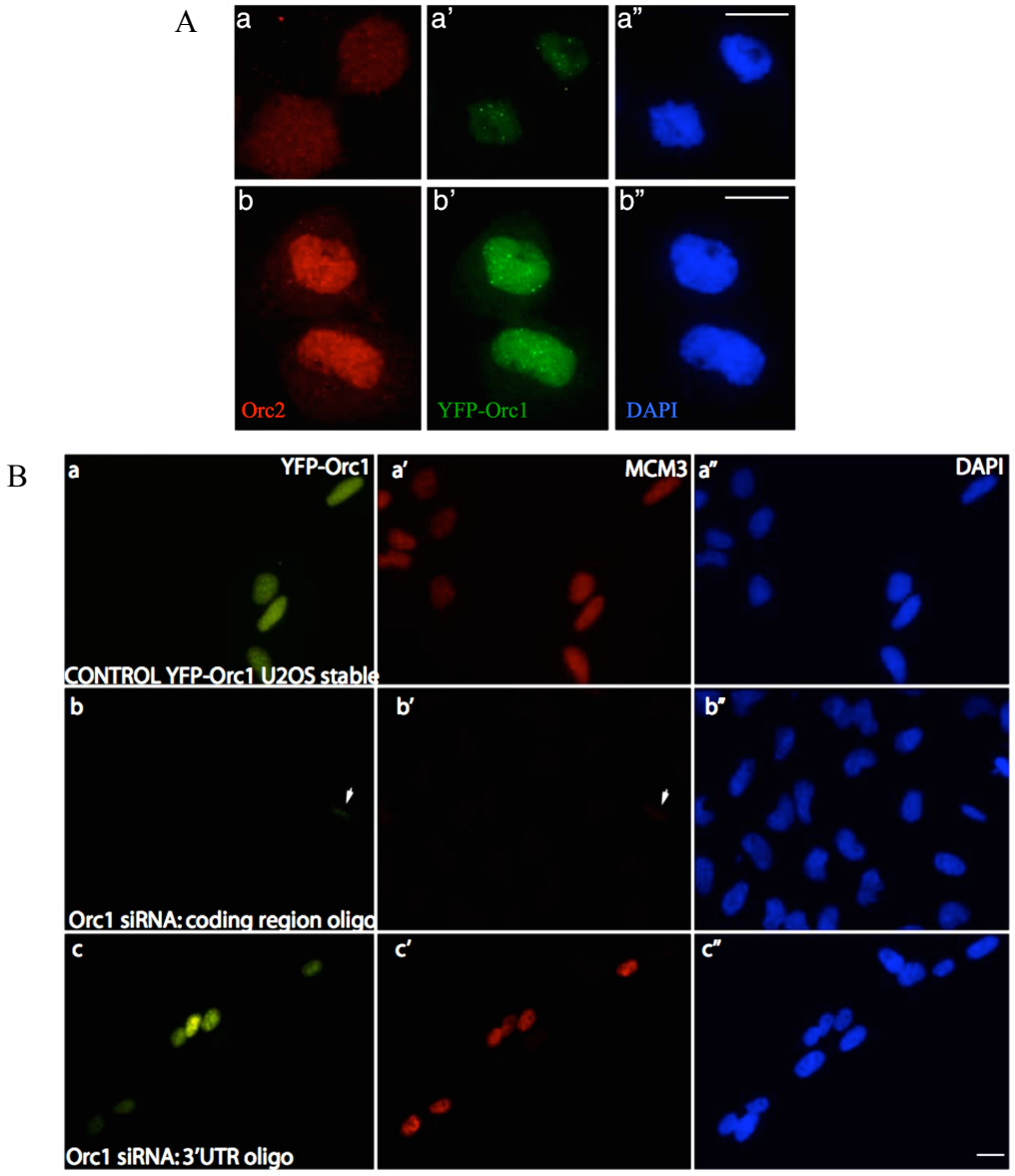

Figure 27. Orc1 loading is the first event in pre-RC formation during cell cycle. A, YFP-Orc1 U2OS stable cell line was studied by Orc2 IF. In mitosis Orc1 appears in the daughter nuclei prior to Orc2, which remain in the cytoplasm (a-a'') and then Orc2 localizes to nuclei (b-b''). B, YFP-Orc1 U2OS cells were treated with siRNA against luciferase (control), coding region of Orc1 or 3' UTR region of Orc1. Depletion of Orc1 causes loss of Mcm3 from chromatin (b-b''). YFP-Orc1 can rescue loss of Mcm3 from chromatin phenotype by functionally complementing endogenous Orc1 (c-c''). Scale bar represents 5 μM. Data obtained by Dr. Supriya Prasanth.

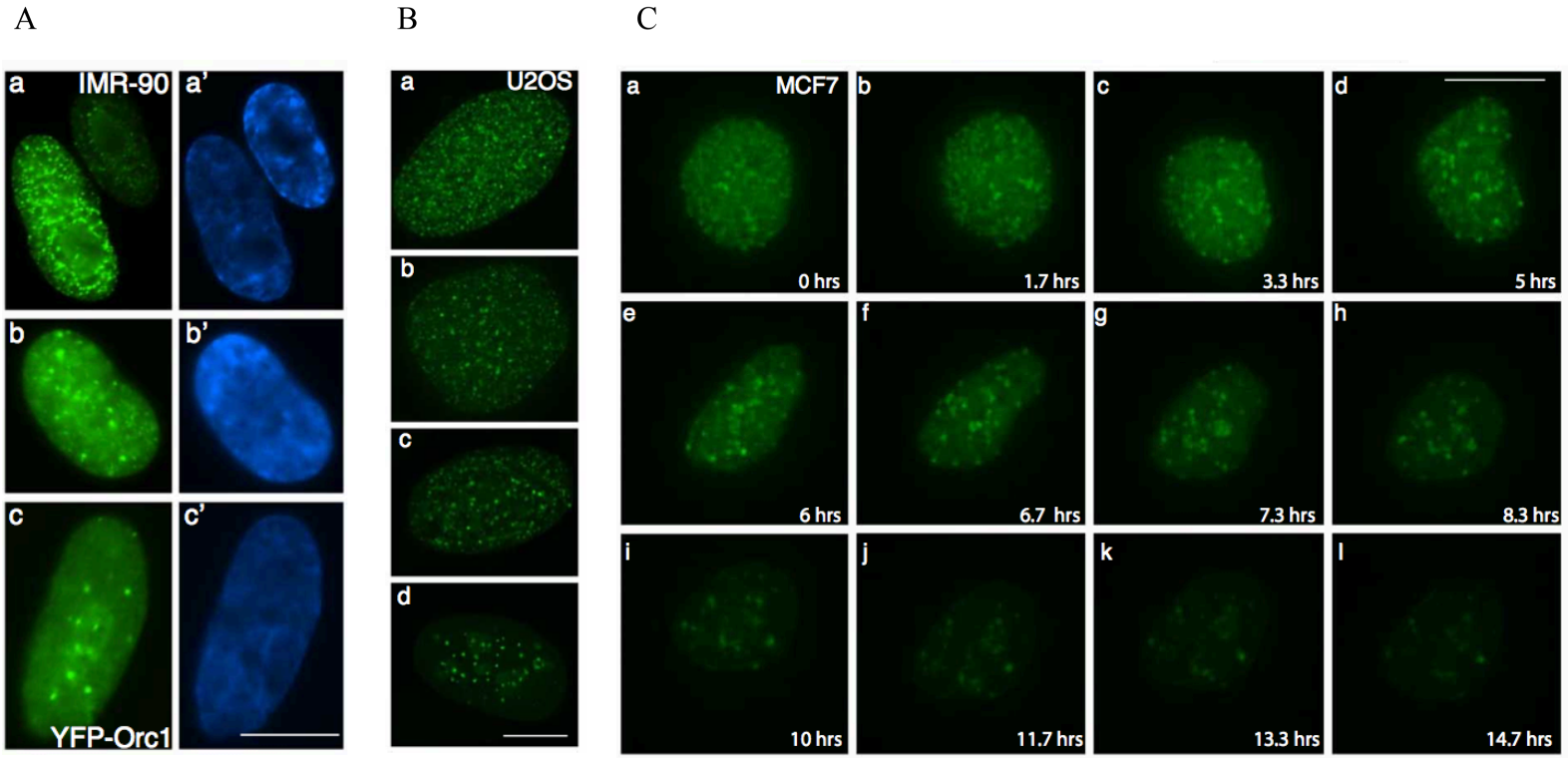

Figure 28. Orc1 shows differential patterning in human cells. A, YFP-Orc1 localization in human diploid fibroblasts IMR-90. Cells were transiently transfected with YFP-Orc1 (green) and chromatin was stained with DAPI. in blue. B, YFP-Orc1 localization pattern in human U2OS cells. Scale bar denotes 5 μm. C, YFP-Orc1 in MCF7 cells monitored by live cell imaging. Frames from movie at indicated time-points are shown. Scale bar is equal to 10 μm. Orc1 initially appears as small punctate loci (a-c) and later relocalizing to larger foci around nucleoli and nuclear periphery. Data obtained by Dr. Supriya Prasanth.

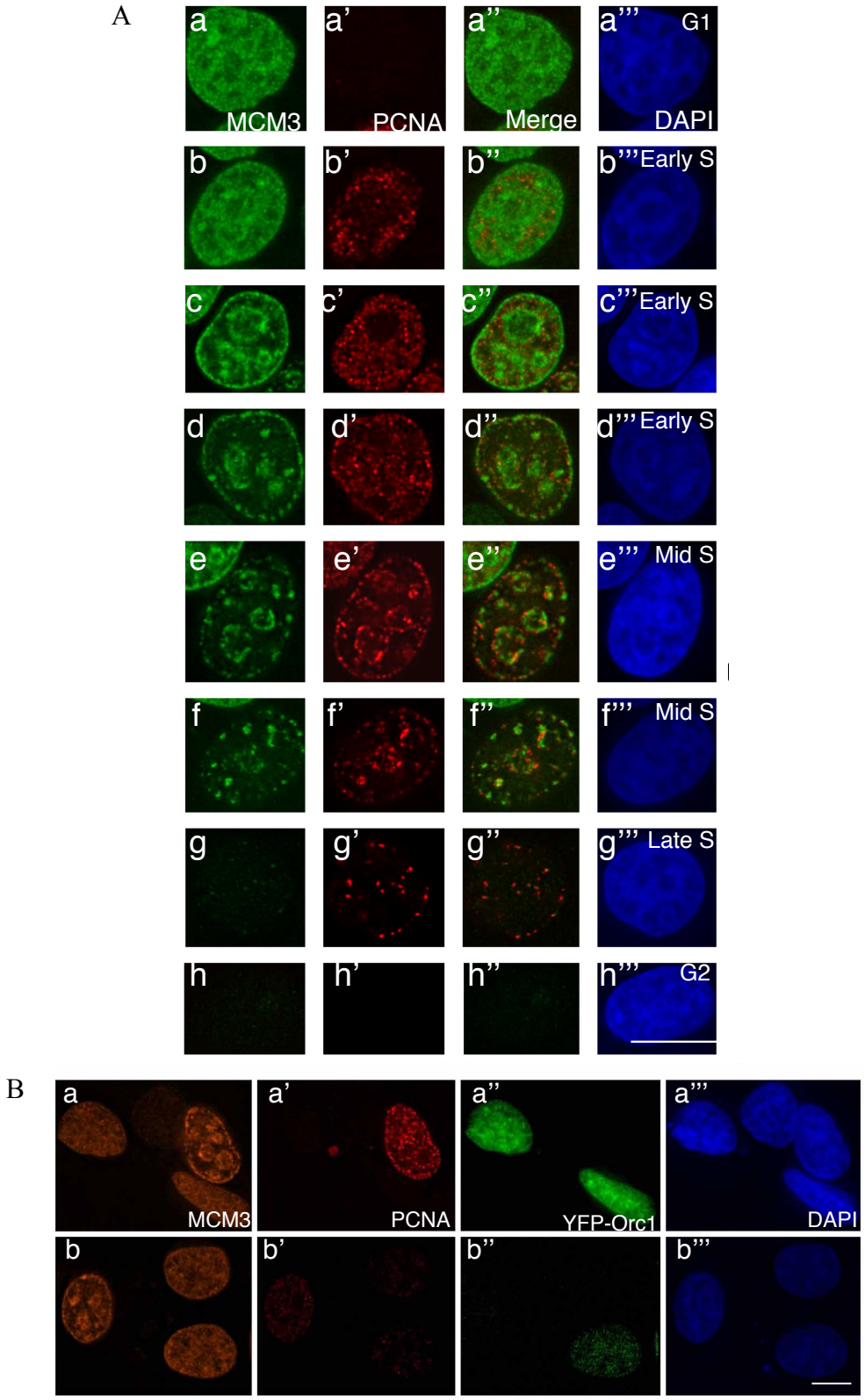

Figure 29. Patterning of replication proteins occurs during G1 and S phase.

(Continued in next page)

Figure 29. Patterning of replication proteins occurs during G1 and S phase. A, Dual color immunofluorescence assay was performed on MCF7 cells. Chromatin bound MCM3 (green) and PCNA (red) in MCF7 cells revealed punctate Mcm3 staining in PCNA negative G1 nuclei (a-a'''). As the cells entered S-phase both Mcm3 and PCNA showed a uniform punctate nuclear labeling (b-b'''). During early S-phase, MCM3 was observed at pericentric heterochromatin while PCNA showed a homogenous nuclear staining (c-d). In mid-S phase, while PCNA showed heterochromatic association, MCM3 staining decreased significantly being restricted to large foci (e-f). By late S most of MCM3 was lost from the chromatin while PCNA labeling was still present as large foci (g-g'''). By G2 both PCNA and MCM3 were absent from the chromatin (h-h'''). Chromatin was stained with DAPI (blue). B, Orc1 distribution is observed only during G1. Immunostaining of MCM3 (orange) and PCNA (red) in YFP-Orc1 (green) expressing MCF7 cells revealed the presence of Orc1 only in PCNA negative G1 cells (a-a'''). Weak signal intensity of YFP-Orc1 was also observed in cells weakly positive for PCNA representing the cells just entering S phase (b-b'''). Scale bar represents 5 μm. Data obtained by Dr. Supriya Prasanth.

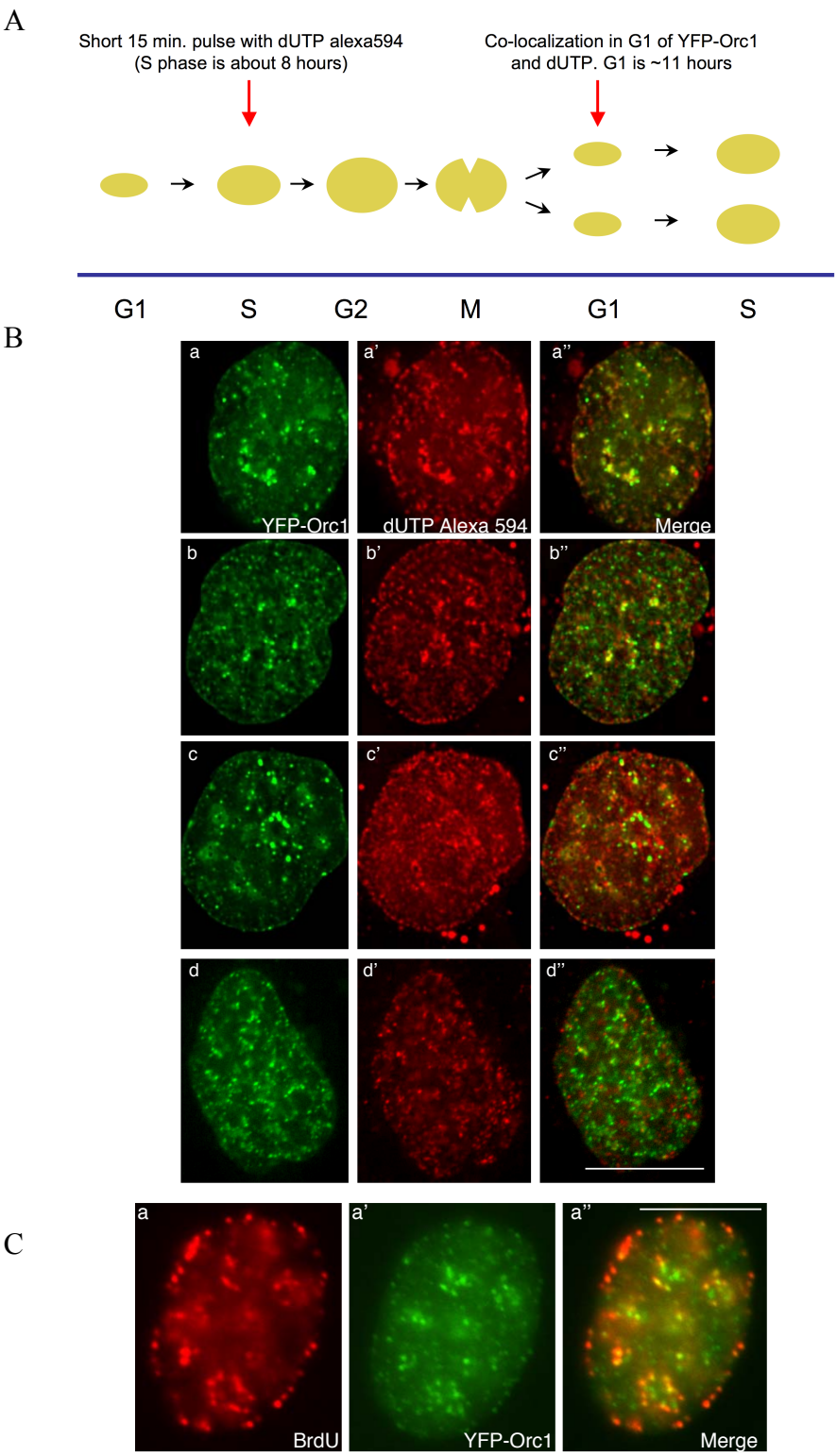

Figure 30. Orc1 localization in G1 phase overlaps with inherited spatiotemporal pattern of DNA replication. (Continued in next page)

Figure 30. Orc1 localization in G1 phase overlaps with inherited spatiotemporal pattern of DNA replication. A, Overview of the experimental outline illustrated. Human U2OS cells expressing YFP-Orc1 (green) were transfected for 15 minutes with dUTP Alexa 594 (red). Following washing out the label and incubation for ~12-14 hrs (ensuring the cells progress from S phase of generation 1 to G1 phase of generation 2), live cell imaging was performed. B, Top two panels represent significant overlap of YFP-Orc1 (green) with the dUTP Alexa 594 (red), both in nuclear and nucleolar periphery (merge; a-b). YFP-Orc1 and dUTP Alexa 594 do not show any overlap, but are immediately adjacent to each other (c-c'') and the lowermost panel show the expected most common situation of no overlap between YFP-Orc1 and dUTP Alexa 594 (d-d''). Scale bar denotes 5 μm. Overlap was seen in 6% of all YFP-Orc1 positive cells. C, Cells expressing YFP-Orc1 were incubated for 10 mins with BrdU, and then extensively washed out. Following ~12-14 hrs incubation (ensuring the cells enter from S phase of generation 1 to G1 phase of generation 2), cells were fixed in 2% formaldehyde. BrdU was detected using anti-BrdU mouse mAb (red) in YFP-Orc1 (green) positive cells. Orc1 was observed both in the nuclear and nucleolar periphery. In a population of cells Orc1 showed significant overlap with BrdU positive regions. Scale bar denotes 5 μm. Data obtained by Dr. Supriya Prasanth.

Chapter 6

Discussion and Perspectives

The initiation of DNA replication involves the ordered and highly regulated assembly of a pre-replicative complex (pre-RC), which requires ORC, Cdc6, Cdt1 to load the hexameric Mcm2-7 complex at all replication origins on chromatin [138-142]. ORC chromatin association dynamics was studied by a successive salt fractionation method which is a valuable tool for profiling proteins and DNA based on their biochemical properties [105, 106]. It has been shown that successive salt-extraction of intact nuclei treated with MNase results in fractions with dramatically different genome-wide DNA profiles [105]. Analysis of ORC by successive salt fractionation showed that ORC was associated with chromatin tightly and among the subunits, Orc1 had significantly higher salt resistance. Two other cellular fractionation methods also showed that Orc1 had the highest degree of salt and nuclease resistance indicating its tighter and less dynamic association with chromatin. The distinct Orc1 chromatin binding dynamics was also observed by a FRAP study in which Orc1 failed to recover completely after photo-bleaching [93]. The overall salt resistance of ORC subunits in salt fractionation might be due to strong binding of ORC complex to chromatin that is facilitated by Orc1. In *Drosophila*, low salt soluble chromatin is enriched for transcriptionally active regions, depleted of histone H3.3 and correlated with histone H2A.Z and RNA polymerase II profiles (Pol II) [105]. Interestingly, high salt insoluble chromatin was also enriched for transcribed regions, and overall it showed a similar

profile to low salt soluble chromatin, but was broader and contained additional sites possibly representing other regions with chromatin bound complexes. I found that a fraction of Orc1 remained insoluble in the pellet fraction. It has been reported that large molecular weight complexes, or nuclear matrix associated proteins are highly insoluble. It is known that the large Pol II elongator complex is nuclease resistant and insoluble [143, 144], similarly ISWI chromatin remodeler is also highly salt resistant [105]. It is also known that in human cells Rif1, which regulates chromatin loop size and is a critical determinant for replication timing control, is associated with insoluble matrix-associated nuclear structures in late M/early G1[145]. Similar results were also observed in mouse cells and deficiency of Rif1 altered the global replication timing program [146]. My results with Orc1 might indicate that a significant fraction of Orc1 is associated with these nuclease resistant insoluble structures. Future studies will determine which regions of Orc1 mediate the tight interaction between Orc1 and these structures, and potentially elicit any mechanisms that involve Orc1 in replication timing.

In human cells, Orc2-5 forms the core ORC and Orc1 is known to be transiently associated with this complex [3, 88, 139, 147, 148]. The results show that Orc1 associates with chromatin beginning in early mitosis, and is the first one among pre-RC components to bind to chromatin. Orc1 levels gradually increased as the cells progress through mitosis and in G1 phase the highest levels of Orc1 on chromatin were present. Levels of other ORC subunits including Orc2, Orc3 and Orc4 were fairly constant throughout the cell division cycle. Interactions between Orc1 and Orc2, Orc1 and Orc3, Orc1 and Orc4, Orc2 and Orc4, and Orc3 with Orc4 were detectable by the beginning of G1. Association of Orc4 with the complex occurred only when Orc1 was also present suggesting that recruitment of Orc4 to ORC is facilitated or

stabilized by Orc1. Interestingly, even though Orc1 was present at earlier time-points during mitosis, the interaction between Orc1 with Orc2 or Orc3 or Orc4 occurred only in G1 phase. The results indicated that Orc2 and Orc3 interaction on chromatin persisted throughout the cell cycle and slightly more interaction was seen in G1. It has been shown that in vitro Orc2 and Orc3 interacted regardless of the presence of other ORC subunits [132]. The increase in interaction levels between Orc2 and Orc3 in the presence of Orc1 may suggest that Orc1 might stabilize this interaction or facilitate extra interaction by recruiting them into ORC in addition to interactions that were already present. In addition to these observations, depletion of Orc1 prevented formation of the pre-RC as measured by reduced Mcm3 recruitment to chromatin. Together, these results suggest that Orc1 is the initial and crucial factor that binds to chromatin and enables other proteins involved in DNA replication initiation to bind to chromatin.

Pioneer factors are transcription factors that can bind to silent chromatin and enable other factors to bind. FoxA factors are examples of such pioneer factors [149]. FoxA proteins have the ability to bind compacted chromatin, which is mediated through a high affinity DNA binding site, and interaction with histones H3 and H4 [150]. FoxA1 is a member of the FoxA subfamily of proteins, and it has been recently shown that FoxA1 shows extensive mitotic binding, and slow recovery kinetics in interphase nuclei by FRAP compared to mitotic, cells and has more extensive background chromatin binding in mitotic chromosomes than interphase by ChIP-seq [151]. Interestingly, some of these characteristics are similar to Orc1, which also shows extensive mitotic chromosome binding and slow recovery kinetics in interphase nuclei. Another important feature of FoxA pioneer factors is the resemblance of their DNA binding domain (DBD) to the linker histone DBD. There is structural similarity between the wing helix motif

DBDs of FoxA and the linker histone 5 [152]. FoxA and linker histone bind along the minor grooves of DNA through their wing helix motifs [152, 153]. Interestingly the bacterial initiator protein DnaA and archaeal Cdc6/Orc1 both have a wing helix motif linked to their AAA+ domain [154, 155]. Alignment of amino acid sequences of FOXA1 and Orc1 also revealed similarity between mammalian Orc1 proteins and FoxA1 wing helix motifs **(Figure 31)**. Orc1 localizes to chromatin before Orc2 early in mitosis, thus it might be the primary determinant for origin recognition. This finding is consistent with the evolutionary perspective that in archaea there is only an Orc1 like protein for origin recognition and other ORC subunits do not exist [156, 157]. These findings suggest that Orc1 might act as a pioneer factor that binds to compact chromatin during mitosis and later recruits other factors that are necessary for initiation of DNA replication. I am currently determining whether the Orc1 winged-helix domain is required for binding of Orc1 to mitotic chromosomes.

DNA replication shows a global level of spatio-temporal patterning throughout S phase which could be categorized into early, mid and late S phase patterns based on the distribution of DNA replication foci **(Figure 1)**. These patterns can be visualized by fluorescent tagged nucleotide analogs or proteins localized to the replication fork such as PCNA. The spatiotemporal regulation of these patterns suggests that certain clusters of replication origins are activated at the same time during a specific time point in S phase.

Several factors are involved in governing spatial-temporal regulation of DNA replication including chromatin structure and modifications, rate limiting DNA replication factors and chromosomal position and organization [reviewed in [6, 158]]. Selection of new replication sites

occurs at each cycle at a specific time point in G1 called the origin decision point (ODP) [46]. At a later timing decision point (TDP) during G1, the global temporal order of DNA replication program is predetermined during G1 [47, 48]. G2 nuclei lack these determinants suggesting that they need to be established every cell cycle for proper spatio-temporal regulation of DNA replication [159]. The results showed that, in human cells Orc1 is localized to chromatin during mitosis and stays on chromatin as the cells go through telophase and shows dynamic nuclear patterning in G1 daughter nuclei. Among the ORC subunits studied, only Orc1 shows dynamic patterns during G1 and Orc1 is the first protein to localize to chromatin in mitosis among other ORC subunits. Orc1 is a member of AAA+ ATPase family proteins with a Walker A and Walker B motif and binding of ATP is essential for its ATPase, DNA binding and replication initiation ability [157, 160-162]. Unpublished results from Dr. Supriya Prasanth showed that intact ATP binding domain of Orc1 is important for dynamic patterning in G1, but is not essential for its degradation during G1/S boundary (personal communication). Thus the dynamic G1 patterns displayed by Orc1 might be forming as the Orc1 is selectively degraded from chromatin.

Histone acetylation plays an important role in temporal regulation of DNA replication. It has been suggested that there is a strong correlation between histone acetylation and temporal firing of origins in several organisms including, budding yeast, *Drosophila, Xenopus* and human cells [45, 67, 163]. In human cells, Orc1 interacts with HBO1 (Histone acetyltransferase binding to ORC) [71].Studies in *Xenopus* and human cells showed that depletion of HBO1 causes defects in MCM chromatin loading [72, 164]. In human cells, HBO1 associates with origins during G1 and this association was stabilized by Cdt1 through direct interaction with HBO1 [165]. In addition, HBO1 enhances Cdt1 replication licensing activity, which might explain the MCM

loading defect in HBO1 depleted cells [165]. Geminin binds to Cdt1 and inhibits the acetylase activity of the HBO1-Cdt1 complex, which is essential for MCM loading and inhibits licensing activity [166, 167]. It is possible that Orc1 promotes chromatin modifications through interactions with HBO1 during mitosis and G1 that in turn establish the temporal dynamics of DNA replication during S phase. Another possibility is Orc1 might be reading a chromatin mark that is inherited from the mother nuclei to daughter nuclei and specifying the spatial-temporal pattern of DNA replication. The spatial overlap of Orc1 patterns with inherited DNA replication patterns suggests these two possibilities. Future studies will demonstrate whether there is such a heritable mark that is promoted or read by Orc1. Another possibility is Orc1 binding to chromatin is dependent on accessibility of chromatin, its 3-D chromosomal organization and epigenetic marks. In early G1, Orc1 is localized to regions with higher accessibility and recruits ORC to those sites, later as the pre-RC forms, Orc1 dissociates from those sites. Later during G1, Orc1 starts to accumulate in sites with less accessible heterochromatin features and is followed by formation of pre-RC at those sites. Accessibility of a particular region on chromosome can be governed by several factors including, primary DNA sequence, epigenetic and histone modifications, presence of other DNA binding elements including, transcription factors or machinery, chromatin remodeling factors, and insulating elements. Orc1 localizes to chromatin in mitotic cells and during G1 it shows dynamic patterning. The earlier the Orc1 is bound to a particular site, the earlier pre-RC can form at those sites. This is consistent with the finding that in fission yeast timing of ORC binding determines the timing of pre-RC formation and timing of replication [81]. ORC dynamics during the M/G1 period of the cell division cycle pre-determine DNA replication origin usage and efficiency in S phase, and is also related to the timing of pre-RC assembly in G1. Timing of ORC binding to an origin is correlated to the time of firing of the

origin in S phase in the sense that during late G1 phase, Orc1 remains bound to late firing origins while removed from all other chromatin. Delaying Orp1 binding, the *S. pombe* Orc1 homolog, to an early origin by mutating it resulted in a delay in Mcm4 recruitment and Cdc45 binding and this was also reflected as a delay in DNA replication timing. Lengthening the M phase using a microtubule-depolymerizing agent caused redistribution of Orp1 at origins such that a more homogenous loading of Orp1 occurred at origins and the consequent DNA replication pattern of these origins changed, with efficient and early origins firing later while inefficient and late origins firing earlier in S phase. Furthermore over-expression of Cdc45, Hsk1 (Cdc7 homolog) and Dfp1 (Hsk1 activator) caused increased firing in efficient and inefficient origins [81]. In *Drosophila*, high density ORC binding to chromosomal sites is correlated with early replication of those sites [82], and ORC preferentially binds to sites with open chromatin features [84]. Recently, it has been reported that human Orc1 is associated with transcriptional start sites (TSSs), and transcription rate from those sites is correlated with replication timing [2], although as discussed earlier in Chapter 3, the peak heights of the Orc1 binding sites are not high compared to conventional DNA binding proteins.

The results presented here suggest that a similar spatial-temporal patterning dynamics in the nucleus is followed by Orc1, Mcm3 and PCNA, sequentially. It is possible that a common feature persisting through G1, S and subsequent G1, S in the next generation is sensed and read by these replication factors. Patterning of MCM proteins occurs from G1 to the S phase of the cell cycle [134]. The DNA replication fork protein PCNA can be used to follow the movement of the replication fork during S phase of the cell cycle [135-137]. Dual immunofluorescence study of Mcm3 and PCNS shows tah the temporal pattern of Mcm3 precedes the temporal patterns

displayed by PCNA suggesting MCM might be orchestrating the coordination of multiple DNA replication forks during S phase.

To conclude, the results indicate that Orc1 acts as a pioneer factor by binding chromatin during mitosis first among other ORC subunits. ORC associates with chromatin strongly and particularly Orc1 shows tight association. Formation of ORC complex occurs during G1 phase; even though Orc4 is present throughout cell cycle it only associates with ORC on chromatin only when Orc1 is present, suggesting that Orc1 might stabilize or facilitate recruitment of Orc4. The dynamic patterns formed by Orc1 during G1 are also followed by MCM and eventually PCNA as multiple waves of similar patterns formed by different DNA replication proteins at successive time points during the cell division cycle. It still needs to be determined how the dynamic Orc1 patterns predict the spatiotemporal dynamics of DNA replication. The spatial organization of the genome, nuclear architecture and epigenetic marks might all play a role in dynamic Orc1 binding and spatiotemporal regulation of DNA replication. It is possible that either Orc1 is contributing or reading some inherited pattern present in the chromatin.

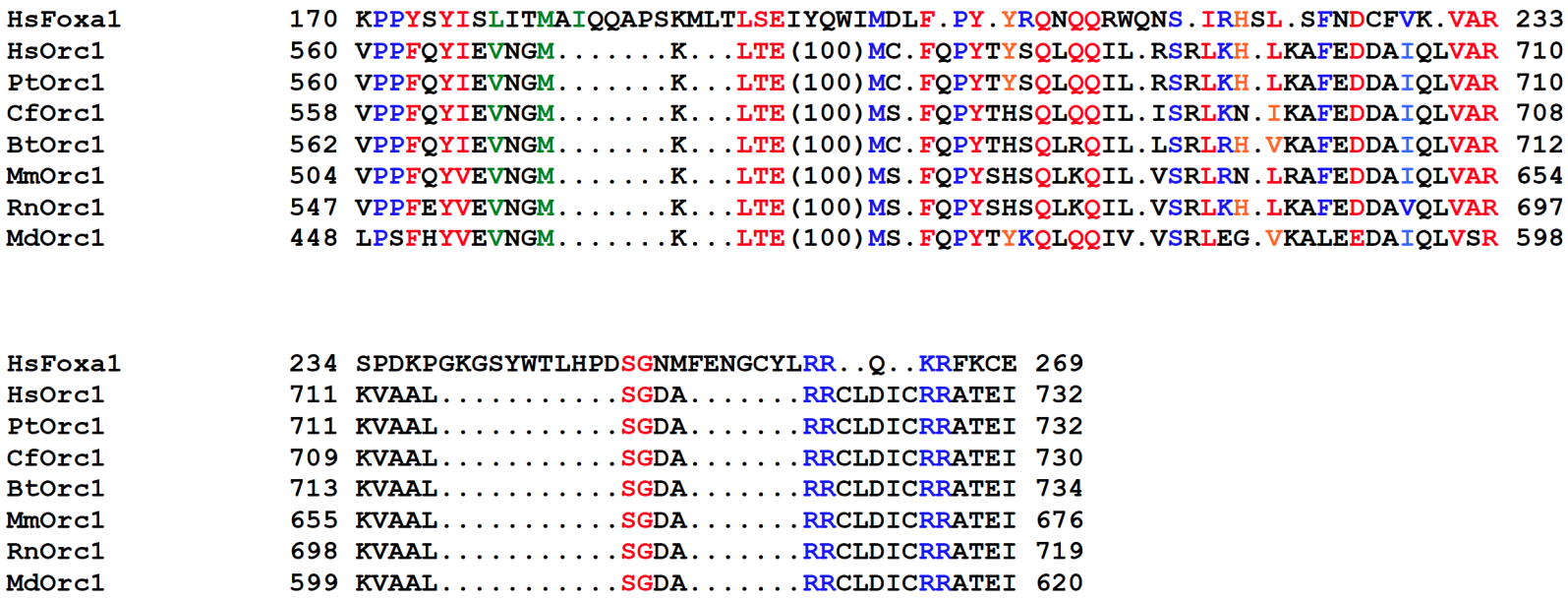

Figure 31. Alignment of human FOXA1 protein with mammalian Orc1 proteins. Hs: *Homo sapiens* (human), Pt: *Pan troglodytes* (chimpanzee), Cf: *Canis familiaris* (dog), Bt: *Bos taurus* (bovine), Mm: *Mus musculus* (mouse), Rt: *Rattus norvegicus* (rat), Md: *Monodelphis domestica* (opossum). 100 means Orc1 protein sequences have 100 amino acid intervening residues. It suggests that Orc1 contains two motifs separated by 100 amino acid residues.

Chapter 7

Materials and Methods

Cell culture and synchronization HeLa suspension cells were grown in suspension (spinner) flasks at 37^{o}C in JMEM supplemented with 5% CS. Cells were synchronized as described previously [3] with some modifications. Early passage (up to passage 10) cells were grown until cell density reached 2x10^{5} cell/mL, then the culture was supplemented with 2.5 mM thymidine and incubated for 14-16 hours. It is important to use early passage cells as higher passage cells gave inconsistent cell cycle profiles by flow cytometry. The cells were then washed with fresh warm medium thrice and resuspended into fresh warm medium, and incubated for 10-12 hours to let the cells release from initial block. The medium was supplemented with 2.5 mM thymidine once again and incubated for 14-16 hours to synchronize them at G1/S transition. For time point 0 h, aliquots of cells were removed, washed with PBS thrice and processed immediately. For time points beyond, cells were washed with warm fresh medium thrice and released into fresh warm medium and incubated at 37 ^{o}C. At successive time points aliquots of cells were removed, washed with PBS thrice and processed accordingly. HeLa, U2OS and MCF7 human cells were grown in DMEM supplemented with penicillin-streptomycin and 10% FBS.

For stable cell lines a U2OS stable cell line containing the pEYFP-C1-Orc1, to express YFP-tagged-Orc1, was generated and maintained in DMEM (high glucose) with 10% fetal

bovine serum (FBS) and 0.5 mg/ml G418 (Invitrogen, Carlsbad, CA). Also previously described tet inducible GFP-Orc1 cell line was used [100].

Human Orc1 cDNA that was cloned into pEYFP-C1 or pEYFP-N1 and expressed from a CMV promoter (CLONTECH Laboratories) were used for transient transfections with lipofectamine and stable cell line generation using antibiotic selection.

Cell cycle analysis For flow cytometry analysis pelleted cells were fixed in 100% cold ethanol overnight. Then cells were washed thrice in PBS and treated with RNase. Next, they were incubated with propidium iodide (PI) solution to stain nucleic acids. Acquisitions were done in BD LSR II flow cytometry instrument. Analysis was done using FACS DIVA and FlowJo software.

Fractionation and cellular extracts Successive salt fractionation was done as described previously [106]. Nuclear extracts were prepared by resuspending the cells in Buffer A (20mM Tris-HCl pH7.5, 50mM NaCl, 0.4% NP-40, 5mM MgOAc, 10% Glycerol, 1mM DTT, 20uM MG132, 1mM ATP) the suspension was homogenized in a Dounce B pestle. The pelleted nuclei were washed, resuspended in Buffer A +0.5mM $CaCl_2$ and treated with DNase I (Invitrogen) and Benzonase ultra (Sigma) for 1 hour. The salt concentration was then brought up to 400mM NaCl and incubated for 30 min, the salt was then adjusted to 200mM. The nuclear extracts were cleared by high-speed spin at a table top centrifuge at 4 ^{o}C.

Immunoprecipitations Immunoprecipitations were carried out using antibody crosslinked Protein G Dynabeads (Invitrogen). The antibody was cross-linked to beads in the presence of 20mM dimethyl pimelimidate (Sigma) in 0.2M triethanolamine, pH 8.2 (Sigma) for 30 min at 20^{o}C. The beads were then resuspended in 50mM Tris pH 7.5, washed with wash buffer (20 mM TrisCl pH 7.5, 200 mM NaCl, 0.4% NP40) and kept at 4 ^{o}C until use. Immunoprecipitations were carried out for 2-8h at 4 ^{o}C on rocker. The samples were washed thrice with cold wash buffer, eluted with 2xSDS sample buffer (0.12 M Tris pH 6.8, 20% glycerol, 4% SDS, 0.2 M DTT) at 30 ^{o}C for 20 mins. Eluates were then boiled for 5min prior to loading onto SDS- Polyacrylamide Gel Electrophoresis (SDS-PAGE) gel.

Antibodies For immunoprecipitations the following mouse monoclonal antibodies were used: Orc1 78-1-172, Orc2 920-2-44, Orc3 PKS1-16. For western blots rabbit polyclonal anti-Orc1 (Bethyl Labs), rabbit polyclonal anti-Orc2 CS205-5, rabbit polyclonal anti-Orc3 CS1890, goat polyclonal anti-Orc4 (Abcam) were used.

Western blot. Cells or extracts that are in 2X SDS sample buffer (0.12 M Tris pH 6.8, 20% glycerol, 4% SDS, 0.2 M DTT) were boiled for 5 min. Samples were than loaded to SDS-PAGE gel and typically run at 100V. The gel were transferred to Whatman® nitrocellulose membranes. Transferred membranes were then blocked in 5% nonfat milk in TBST (Tris buffered saline +0.05% Tween-20) for 1 hour at room temperature, and then incubated with primary antibody solution in 5% nonfat milk in TBST for 2 hours at room temperature or overnight at 4 °C. The membranes were washed in TBST solution thrice for 10 min each, and

incubated appropriate HRP-conjugated secondary antibodies in 5% nonfat milk in TBST for 1 hour at room temperature. The membranes were developed using Supersignal West Dura or Pico substrate (Thermo Scientific) and Kodak Biomax Light films were used.

Raising antibody against human Orc1 protein GST-Orc1 ΔN400 was expressed and purified from *E.coli* BL21 (DE3) cells as described previously with some modifications (HN300 +0.1 %Triton X-100 buffer was used) [3], the GST tag was cleaved by prescission protease (GE Healthcare). The monoclonal antibody was raised according to protocols as described previously [103]. The hybridomas were screened by enzyme-linked immunosorbent assay and positive ones were screened further for ability to immunoprecipitate GST and MBP tagged Orc1. Positive clones were screened further to test ability of immunoprecipitating endogenous Orc1 from HeLa whole cell extracts. The clone used in this study is Orc1 78-1-172. MBP tagged Orc1 was purified as described previously [100].

Live cell microscopy Tet-inducible GFP-Orc1 U2OS stable cells were used to make the movie after 16 hours of tetratcycline treatment (1ug/ml). The images were obtained using a Perkin Elmer Spinning Disk Confocal microscope with a 40x objective. The images were further processed using ImageJ 1.46r software. Human cells stably expressing YFP-Orc1 or transiently transfected with 2 μg EYFP-Orc1 and/or ECFP-PCNA were also used for live-cell imaging. The cells were transferred to a live-cell chamber mounted onto the stage of a Delta Vision optical sectioning deconvolution instrument (Applied Precision) on a Olympus microscope and kept at 37^{o}C in L-15 medium (minus phenol red) containing 30% FBS. Time-lapse images acquired

with a 63X 1.4 N.A. objective lens were captured with a Coolsnap CCD camera.

Immunofluorescence For PCNA and MCM dual immunofluorescence, cells were first pre-extracted in cytoskeletal buffer (CSK buffer) (10mM PIPES, pH 7; 100mM NaCl, 300mM Sucrose, 3mM MgCl2) supplemented with 0.5% Triton-X for 5 min on ice to remove soluble proteins. Cells were then fixed in 1.7% paraformaldehyde at room temperature, then extracted with chilled methanol. Immunofluorescence was done using standard protocols. Slides were examined using a Zeiss Axioplan 2i fluorescence microscope (Carl Zeiss Inc., Thornwood, NY) which has Chroma filters (Chroma Technology, Brattleboro, VT), to collect digital images OpenLab software (Improvision, Boston, MA) was used with a Hamamatsu ORCA cooled CCD camera. Antibodies used were: anti-PCNA PC10 monoclonal, anti-Mcm3 738 polyclonal, anti-Orc2 CS205 polyclonal. Anti-GFP monoclonal antibody was from Roche and Anti-BrdU monoclonal antibody from Molecular Probes.

Conventional chromatin immunoprecipitation Hela suspension (spinner) cells were washed with 1xPBS three times and fixed with 1% formaldehyde in PBS for 10 min at room temperature and quenched by 0.125M glycine as described previously [119]. Cells were lysed in a hypotonic buffer (10mM Tris-Cl pH 8.0, 10mM NaCl, 0.2% NP-40) and then nuclei were lysed in 1x volume of nuclear lysis buffer (50 mM Tris-Cl pH 8.0, 1%SDS, 10mM EDTA). Next, 1x volume IP dilution buffer (20 mM Tris pH 8.1, 2 mM EDTA, 150 mM NaCl, 1% Triton X-100, 0.01% SDS) was added to lysed nuclear extracts and the mixture was sonicated. After removal of insoluble debris by high-speed spinning, the lysates were further diluted by addition of 3x volume IP dilution buffer. The immunoprecipitations were performed using crosslinked antibody

magnetic beads overnight at 4 ^{o}C. The next day, beads were washed once with IP wash buffer 1 (20 mM Tris-Cl pH 8.0, 2 mM EDTA, 50 mM NaCl, 1% Triton X-100, 0.1% SDS), then washed twice with high salt wash buffer (20 mM Tris-Cl pH 8.0, 2 mM EDTA, 500 mM NaCl, 1% Triton X-100, 0.01% SDS), once with IP wash buffer 2 (10 mM Tris-Cl pH 8.0, 1 mM EDTA, 0.25M LiCl, 1% NP-40, 1% deoxycholic acid), and twice with TE (Tris-EDTA buffer) as final washes. Chromatin was eluted with 100 ul elution buffer (100 mM sodium bicarbonate, 1% SDS) twice at room temperature. To reverse crosslinks and digest RNA, 2 ug of RNase A and 12 ul of 5 M NaCl were added and incubated overnight at 65 ^{o}C. Eluates were then treated with 60 micrograms of Proteinase K at 42 ^{o}C for 2 hours. Samples were then diluted 2x with TE. Samples were then phenol chloroform extracted and ethanol precipitated. The pellets were dissolved in nuclease free water.

Non-denaturing chromatin immunoprecipitation Hela suspension (spinner) cells were washed with 1xPBS three times and fixed with 1% formaldehyde in PBS for 10 min at room temperature and quenched by 0.125M glycine. Cells were lysed in TM2 buffer (10mM Tris-Cl pH 7.5, 2mM $MgCl_2$, 0.5% NP-40) and then nuclei were resuspended in TM2 buffer and treated with micrococcal nuclease (5000 units per 1 million cells). The amount of Mnase should be optimized for each batch of the enzyme such that only mono and dinucleosome sized fragments are present along with small amount of trinucleosome sized DNA fragments after treatment. Next, nuclei were lysed in nuclei lysis buffer (50mM Tris pH 7.5, 400mM NaCl, 2mM $MgCl_2$, 1% NP40) and sonicated briefly (2 -3 cycles 30 sec on/30 sec off) to enable complete lysis. After removal of insoluble debris by high-speed spinning, the lysates were adjusted to 200mM salt. The immunoprecipitations were performed using crosslinked antibody magnetic beads overnight

at 4 ^{o}C. The next day, beads were washed once with IP wash buffer 1 (20 mM Tris-Cl pH 7.5, 2 mM EDTA, 50 mM NaCl, 1% Triton X-10), then washed twice with high salt wash buffer (20 mM Tris-Cl pH 8.0, 2 mM EDTA, 500 mM NaCl, 1% Triton X-100), once with IP wash buffer 2 (10 mM Tris-Cl pH 8.0, 1 mM EDTA, 0.25M LiCl, 1% NP-40, 1% deoxycholic acid), and twice with TE (Tris-EDTA buffer) as final washes. Chromatin was eluted with 100 ul elution buffer (100 mM sodium bicarbonate, 1% SDS) twice at room temperature. To reverse crosslinks and digest RNA, 2 ug of RNase A and 12 ul of 5 M NaCl were added and incubated overnight at 65 ^{o}C. Eluates were then treated with 60 micrograms of Proteinase K at 42 ^{o}C for 2 hours. Samples were then diluted 2x with TE. Samples were then phenol chloroform extracted and ethanol precipitated. The pellets were dissolved in nuclease free water. Libraries for next generation sequencing were prepared using Illumina Tru-seq DNA sample preparation kit according to manufacturers instructions. 18 or 11 rounds of PCR were performed to amplify the libraries. Quantification and quality control of libraries were performed using Agilent Bioanalyzer.

References:

1. Mendez, J. and B. Stillman, *Chromatin association of human origin recognition complex, cdc6, and minichromosome maintenance proteins during the cell cycle: assembly of prereplication complexes in late mitosis.* Mol Cell Biol, 2000. **20**(22): p. 8602-12.
2. Dellino, G.I., et al., *Genome-wide mapping of human DNA-replication origins: levels of transcription at ORC1 sites regulate origin selection and replication timing.* Genome Res, 2013. **23**(1): p. 1-11.
3. Siddiqui, K. and B. Stillman, *ATP dependent assembly of the human origin recognition complex.* J Biol Chem, 2007.
4. Aygün, O., J. Svejstrup, and Y. Liu, *A RECQ5-RNA polymerase II association identified by targeted proteomic analysis of human chromatin*, in *Proc Natl Acad Sci USA*. 2008. p. 8580-8584.
5. Prasanth, S.G., et al., *Human Orc2 localizes to centrosomes, centromeres and heterochromatin during chromosome inheritance.* Embo J, 2004. **23**(13): p. 2651-63.
6. Aladjem, M.I., *Replication in context: dynamic regulation of DNA replication patterns in metazoans.* Nat Rev Genet, 2007. **8**(8): p. 588-600.
7. Casas-Delucchi, C.S. and M.C. Cardoso, *Epigenetic control of DNA replication dynamics in mammals*, in *Nucleus*. 2011. p. 370-382.

8. Diffley, J.F.X., *Quality control in the initiation of eukaryotic DNA replication*, in *Philosophical Transactions of the Royal Society B: Biological Sciences*. 2011. p. 3545-3553.

9. Masai, H., et al., *Eukaryotic chromosome DNA replication: where, when, and how?*, in *Annu Rev Biochem*. 2010. p. 89-130.

10. Diffley, J.F. and J.H. Cocker, *Protein-DNA interactions at a yeast replication origin.* Nature, 1992. **357**(6374): p. 169-72.

11. Randell, J.C., et al., *Sequential ATP hydrolysis by Cdc6 and ORC directs loading of the Mcm2-7 helicase.* Mol Cell, 2006. **21**(1): p. 29-39.

12. Seki, T. and J.F. Diffley, *Stepwise assembly of initiation proteins at budding yeast replication origins in vitro.* Proc Natl Acad Sci U S A, 2000. **97**(26): p. 14115-20.

13. Hua, X.H. and J. Newport, *Identification of a preinitiation step in DNA replication that is independent of origin recognition complex and cdc6, but dependent on cdk2.* J Cell Biol, 1998. **140**(2): p. 271-81.

14. Rowles, A., S. Tada, and J.J. Blow, *Changes in association of the Xenopus origin recognition complex with chromatin on licensing of replication origins.* J Cell Sci, 1999. **112 (Pt 12)**: p. 2011-8.

15. Shimada, K., P. Pasero, and S.M. Gasser, *ORC and the intra-S-phase checkpoint: a threshold regulates Rad53p activation in S phase.* Genes Dev, 2002. **16**(24): p. 3236-52.

16. Moreno, S. and P. Nurse, *Regulation of progression through the G1 phase of the cell cycle by the rum1+ gene.* Nature, 1994. **367**(6460): p. 236-42.

17. Hardy, C.F., et al., *mcm5/cdc46-bob1 bypasses the requirement for the S phase activator Cdc7p.* Proc Natl Acad Sci U S A, 1997. **94**(7): p. 3151-5.

18. Hardy, C.F. and A. Pautz, *A novel role for Cdc5p in DNA replication.* Mol Cell Biol, 1996. **16**(12): p. 6775-82.

19. Dutta, A. and B. Stillman, *cdc2 family kinases phosphorylate a human cell DNA replication factor, RPA, and activate DNA replication.* EMBO J, 1992. **11**(6): p. 2189-99.

20. Moyer, S.E., P.W. Lewis, and M.R. Botchan, *Isolation of the Cdc45/Mcm2-7/GINS (CMG) complex, a candidate for the eukaryotic DNA replication fork helicase*, in *Proc Natl Acad Sci USA*. 2006. p. 10236-10241.

21. Pacek, M., et al., *Localization of MCM2-7, Cdc45, and GINS to the site of DNA unwinding during eukaryotic DNA replication.* Mol Cell, 2006. **21**(4): p. 581-7.

22. Zou, L. and B. Stillman, *Formation of a preinitiation complex by S-phase cyclin CDK-dependent loading of Cdc45p onto chromatin.* Science, 1998. **280**(5363): p. 593-6.

23. Zou, L. and B. Stillman, *Assembly of a complex containing Cdc45p, replication protein A, and Mcm2p at replication origins controlled by S-phase cyclin-dependent kinases and Cdc7p-Dbf4p kinase.* Mol Cell Biol, 2000. **20**(9): p. 3086-96.

24. Sheu, Y.-J. and B. Stillman, *The Dbf4-Cdc7 kinase promotes S phase by alleviating an inhibitory activity in Mcm4.*, in *Nature*. 2010. p. 113-117.

25. Sheu, Y.J. and B. Stillman, *Cdc7-Dbf4 phosphorylates MCM proteins via a docking site-mediated mechanism to promote S phase progression.* Mol Cell, 2006. **24**(1): p. 101-13.

26. Masumoto, H., et al., *S-Cdk-dependent phosphorylation of Sld2 essential for chromosomal DNA replication in budding yeast.* Nature, 2002. **415**(6872): p. 651-5.

27. Tanaka, S., et al., *CDK-dependent phosphorylation of Sld2 and Sld3 initiates DNA replication in budding yeast.* Nature, 2007. **445**(7125): p. 328-32.

28. Zegerman, P. and J.F. Diffley, *Phosphorylation of Sld2 and Sld3 by cyclin-dependent kinases promotes DNA replication in budding yeast.* Nature, 2007. **445**(7125): p. 281-5.

29. Mimura, S., et al., *Central role for cdc45 in establishing an initiation complex of DNA replication in Xenopus egg extracts.* Genes Cells, 2000. **5**(6): p. 439-52.

30. Tanaka, T. and K. Nasmyth, *Association of RPA with chromosomal replication origins requires an Mcm protein, and is regulated by Rad53, and cyclin- and Dbf4-dependent kinases.* EMBO J, 1998. **17**(17): p. 5182-91.

31. Walter, J. and J. Newport, *Initiation of eukaryotic DNA replication: origin unwinding and sequential chromatin association of Cdc45, RPA, and DNA polymerase alpha.* Mol Cell, 2000. **5**(4): p. 617-27.

32. Collins, K.L. and T.J. Kelly, *Effects of T antigen and replication protein A on the initiation of DNA synthesis by DNA polymerase alpha-primase.* Mol Cell Biol, 1991. **11**(4): p. 2108-15.

33. Melendy, T. and B. Stillman, *An interaction between replication protein A and SV40 T antigen appears essential for primosome assembly during SV40 DNA replication.* J Biol Chem, 1993. **268**(5): p. 3389-95.

34. Murakami, Y., T. Eki, and J. Hurwitz, *Studies on the initiation of simian virus 40 replication in vitro: RNA primer synthesis and its elongation.* Proc Natl Acad Sci U S A, 1992. **89**(3): p. 952-6.

35. Tsurimoto, T. and B. Stillman, *Replication factors required for SV40 DNA replication in vitro. II. Switching of DNA polymerase alpha and delta during initiation of leading and lagging strand synthesis.* J Biol Chem, 1991. **266**(3): p. 1961-8.

36. Tsurimoto, T. and B. Stillman, *Replication factors required for SV40 DNA replication in vitro. I. DNA structure-specific recognition of a primer-template junction by eukaryotic DNA polymerases and their accessory proteins.* J Biol Chem, 1991. **266**(3): p. 1950-60.

37. Saha, P., et al., *The human homolog of Saccharomyces cerevisiae CDC45.* J Biol Chem, 1998. **273**(29): p. 18205-9.

38. Hopwood, B. and S. Dalton, *Cdc45p assembles into a complex with Cdc46p/Mcm5p, is required for minichromosome maintenance, and is essential for chromosomal DNA replication.* Proc Natl Acad Sci U S A, 1996. **93**(22): p. 12309-14.

39. Mimura, S. and H. Takisawa, *Xenopus Cdc45-dependent loading of DNA polymerase alpha onto chromatin under the control of S-phase Cdk.* EMBO J, 1998. **17**(19): p. 5699-707.

40. Krysan, P.J., S.B. Haase, and M.P. Calos, *Isolation of human sequences that replicate autonomously in human cells.* Mol Cell Biol, 1989. **9**(3): p. 1026-33.

41. Masukata, H., et al., *Autonomous replication of human chromosomal DNA fragments in human cells.* Mol Biol Cell, 1993. **4**(11): p. 1121-32.

42. Vashee, S., et al., *Sequence-independent DNA binding and replication initiation by the human origin recognition complex*, in *Genes Dev*. 2003. p. 1894-1908.

43. Raghuraman, M.K., et al., *Replication dynamics of the yeast genome.* Science, 2001. **294**(5540): p. 115-21.

44. Tanaka, S., et al., *Origin association of Sld3, Sld7, and Cdc45 proteins is a key step for determination of origin-firing timing.* Curr Biol, 2011. **21**(24): p. 2055-63.

45. Vogelauer, M., et al., *Histone acetylation regulates the time of replication origin firing.* Mol Cell, 2002. **10**(5): p. 1223-33.

46. Wu, J.R. and D.M. Gilbert, *The replication origin decision point is a mitogen-independent, 2-aminopurine-sensitive, G1-phase event that precedes restriction point control*, in *Mol Cell Biol*. 1997. p. 4312-4321.

47. Dimitrova, D.S. and D.M. Gilbert, *The spatial position and replication timing of chromosomal domains are both established in early G1 phase.* Mol Cell, 1999. **4**(6): p. 983-93.

48. Li, F., et al., *The replication timing program of the Chinese hamster beta-globin locus is established coincident with its repositioning near peripheral heterochromatin in early G1 phase.* J Cell Biol, 2001. **154**(2): p. 283-92.

49. O'Keefe, R.T., S.C. Henderson, and D.L. Spector, *Dynamic organization of DNA replication in mammalian cell nuclei: spatially and temporally defined replication of chromosome-specific alpha-satellite DNA sequences.* J Cell Biol, 1992. **116**(5): p. 1095-110.

50. Baddeley, D., et al., *Measurement of replication structures at the nanometer scale using super-resolution light microscopy.* Nucleic Acids Res, 2010. **38**(2): p. e8.

51. Jackson, D.A. and A. Pombo, *Replicon clusters are stable units of chromosome structure: evidence that nuclear organization contributes to the efficient activation and propagation of S phase in human cells*, in *J Cell Biol*. 1998. p. 1285-1295.

52. Li, F., et al., *Spatial distribution and specification of mammalian replication origins during G1 phase.* J Cell Biol, 2003. **161**(2): p. 257-66.

53. Ma, H., et al., *Spatial and temporal dynamics of DNA replication sites in mammalian cells.* J Cell Biol, 1998. **143**(6): p. 1415-25.

54. Sadoni, N., et al., *Stable chromosomal units determine the spatial and temporal organization of DNA replication.* J Cell Sci, 2004. **117**(Pt 22): p. 5353-65.

55. Moindrot, B., et al., *3D chromatin conformation correlates with replication timing and is conserved in resting cells.*, in *Nucleic Acids Res*. 2012. p. 9470-9481.

56. Ryba, T., et al., *Evolutionarily conserved replication timing profiles predict long-range chromatin interactions and distinguish closely related cell types.* Genome Res, 2010. **20**(6): p. 761-70.

57. Takebayashi, S.-i., et al., *Chromatin-interaction compartment switch at developmentally regulated chromosomal domains reveals an unusual principle of chromatin folding.*, in *Proc Natl Acad Sci USA*. 2012. p. 12574-12579.

58. Yaffe, E., et al., *Comparative Analysis of DNA Replication Timing Reveals Conserved Large-Scale Chromosomal Architecture*, in *PLoS Genet*. 2010. p. e1001011.

59. Goren, A. and H. Cedar, *Replicating by the clock*, in *Nat Rev Mol Cell Biol*. 2003. p. 25-32.

60. Hiratani, I., et al., *Replication timing and transcriptional control: beyond cause and effect--part II.*, in *Curr Opin Genet Dev*. 2009. p. 142-149.

61. Stevenson, J.B. and D.E. Gottschling, *Telomeric chromatin modulates replication timing near chromosome ends.* Genes Dev, 1999. **13**(2): p. 146-51.

62. Rundlett, S.E., et al., *Transcriptional repression by UME6 involves deacetylation of lysine 5 of histone H4 by RPD3.* Nature, 1998. **392**(6678): p. 831-5.

63. Carrozza, M.J., et al., *Histone H3 methylation by Set2 directs deacetylation of coding regions by Rpd3S to suppress spurious intragenic transcription.* Cell, 2005. **123**(4): p. 581-92.

64. Aparicio, J., et al., *The Rpd3-Sin3 histone deacetylase regulates replication timing and enables intra-S origin control in Saccharomyces cerevisiae*, in *Mol Cell Biol*. 2004. p. 4769.

65. Knott, S.R.V., et al., *Genome-wide replication profiles indicate an expansive role for Rpd3L in regulating replication initiation timing or efficiency, and reveal genomic loci of Rpd3 function in Saccharomyces cerevisiae.*, in *Genes Dev*. 2009. p. 1077-1090.

66. Unnikrishnan, A., P.R. Gafken, and T. Tsukiyama, *Dynamic changes in histone acetylation regulate origins of DNA replication*, in *Nat Struct Mol Biol*. 2010. p. 430-437.

67. Lucas, I., et al., *High-throughput mapping of origins of replication in human cells.* EMBO Rep, 2007. **8**(8): p. 770-7.

68. Kemp, M.G., et al., *The histone deacetylase inhibitor trichostatin A alters the pattern of DNA replication origin activity in human cells*, in *Nucleic Acids Res*. 2005. p. 325-336.

69. Goren, A., et al., *DNA replication timing of the human beta-globin domain is controlled by histone modification at the origin*, in *Genes Dev*. 2008. p. 1319-1324.

70. Perry, P., et al., *A dynamic switch in the replication timing of key regulator genes in embryonic stem cells upon neural induction*, in *Cell Cycle*. 2004. p. 1645-1650.

71. Iizuka, M. and B. Stillman, *Histone acetyltransferase HBO1 interacts with the ORC1 subunit of the human initiator protein.* J Biol Chem, 1999. **274**(33): p. 23027-34.

72. Iizuka, M., et al., *Regulation of replication licensing by acetyltransferase Hbo1.*, in *Mol Cell Biol*. 2006. p. 1098-1108.

73. Hyrien, O., K. Marheineke, and A. Goldar, *Paradoxes of eukaryotic DNA replication: MCM proteins and the random completion problem.* Bioessays, 2003. **25**(2): p. 116-25.

74. Rhind, N., *DNA replication timing: random thoughts about origin firing.* Nat Cell Biol, 2006. **8**(12): p. 1313-6.

75. Hyrien, O., C. Maric, and M. Mechali, *Transition in specification of embryonic metazoan DNA replication origins.* Science, 1995. **270**(5238): p. 994-7.

76. Hyrien, O. and M. Mechali, *Chromosomal replication initiates and terminates at random sequences but at regular intervals in the ribosomal DNA of Xenopus early embryos.* EMBO J, 1993. **12**(12): p. 4511-20.

77. Hiratani, I., et al., *Global reorganization of replication domains during embryonic stem cell differentiation.* PLoS Biol, 2008. **6**(10): p. e245.

78. Hakim, O. and T. Misteli, *SnapShot: Chromosome Confirmation Capture*, in *Cell*. 2012.

79. Hiratani, I., et al., *Genome-wide dynamics of replication timing revealed by in vitro models of mouse embryogenesis.*, in *Genome Res*. 2010. p. 155-169.

80. Ryba, T., et al., *Replication timing: a fingerprint for cell identity and pluripotency.*, in *PLoS Comput. Biol.* 2011. p. e1002225.

81. Wu, P.Y. and P. Nurse, *Establishing the program of origin firing during S phase in fission Yeast.* Cell, 2009. **136**(5): p. 852-64.

82. MacAlpine, H.K., et al., *Drosophila ORC localizes to open chromatin and marks sites of cohesin complex loading.* Genome Res, 2010. **20**(2): p. 201-11.

83. Deal, R.B., J.G. Henikoff, and S. Henikoff, *Genome-wide kinetics of nucleosome turnover determined by metabolic labeling of histones*, in *Science*. 2010. p. 1161-1164.

84. Eaton, M.L., et al., *Chromatin signatures of the Drosophila replication program.* Genome Res, 2011. **21**(2): p. 164-74.

85. Duncker, B.P., I.N. Chesnokov, and B.J. McConkey, *The origin recognition complex protein family*, in *Genome Biol*. 2009. p. 214.

86. Bell, S.P., *The origin recognition complex: from simple origins to complex functions.* Genes Dev, 2002. **16**(6): p. 659-72.

87. Kreitz, S., et al., *The human origin recognition complex protein 1 dissociates from chromatin during S phase in HeLa cells.* J Biol Chem, 2001. **276**(9): p. 6337-42.

88. Mendez, J., et al., *Human origin recognition complex large subunit is degraded by ubiquitin-mediated proteolysis after initiation of DNA replication.* Mol Cell, 2002. **9**(3): p. 481-91.

89. Ohta, S., et al., *The ORC1 cycle in human cells: II. Dynamic changes in the human ORC complex during the cell cycle.* J Biol Chem, 2003. **278**(42): p. 41535-40.

90. Chesnokov, I.N., O.N. Chesnokova, and M. Botchan, *A cytokinetic function of Drosophila ORC6 protein resides in a domain distinct from its replication activity*, in *Proc Natl Acad Sci USA*. 2003. p. 9150-9155.

91. Prasanth, S.G., K.V. Prasanth, and B. Stillman, *Orc6 involved in DNA replication, chromosome segregation, and cytokinesis*, in *Science*. 2002. p. 1026-1031.

92. Huijbregts, R.P.H., et al., *Drosophila Orc6 facilitates GTPase activity and filament formation of the septin complex*, in *Mol Biol Cell*. 2009. p. 270-281.

93. Prasanth, S.G., et al., *Human origin recognition complex is essential for HP1 binding to chromatin and heterochromatin organization.* Proc Natl Acad Sci U S A, 2010. **107**(34): p. 15093-8.

94. Bartke, T., et al., *Nucleosome-interacting proteins regulated by DNA and histone methylation*, in *Cell*. 2010. p. 470-484.

95. Vermeulen, M., et al., *Quantitative interaction proteomics and genome-wide profiling of epigenetic histone marks and their readers*, in *Cell*. 2010. p. 967-980.

96. Hemerly, A.S., et al., *Orc1 controls centriole and centrosome copy number in human cells.* Science, 2009. **323**(5915): p. 789-93.

97. Bicknell, L.S., et al., *Mutations in the pre-replication complex cause Meier-Gorlin syndrome*, in *Nat Genet*. 2011.

98. Bicknell, L.S., et al., *Mutations in ORC1, encoding the largest subunit of the origin recognition complex, cause microcephalic primordial dwarfism resembling Meier-Gorlin syndrome*, in *Nat Genet*. 2011.

99. Guernsey, D.L., et al., *Mutations in origin recognition complex gene ORC4 cause Meier-Gorlin syndrome*, in *Nat Genet*. 2011.

100. Hossain, M. and B. Stillman, *Meier-Gorlin syndrome mutations disrupt an Orc1 CDK inhibitory domain and cause centrosome reduplication.* Genes Dev, 2012. **26**(16): p. 1797-810.

101. Kuo, A.J., et al., *The BAH domain of ORC1 links H4K20me2 to DNA replication licensing and Meier-Gorlin syndrome.*, in *Nature*. 2012.

102. Lim, C., et al., *Functional dissection of latency-associated nuclear antigen 1 of Kaposi's sarcoma-associated herpesvirus involved in latent DNA replication and transcription of terminal repeats of the viral genome.* J Virol, 2002. **76**(20): p. 10320-31.

103. Harlow, E. and D. Lane, *Antibodies : a laboratory manual*. 1988, Cold Spring Harbor, NY: Cold Spring Harbor Laboratory. xiii, 726 p.

104. Gilden, R.V., T.G. Beddow, and R.J. Huebner, *Production of high-titer antibody in serum and ascitic fluid of hamsters for a variety of virus-induced tumor antigens.* Appl Microbiol, 1967. **15**(3): p. 657-60.

105. Henikoff, S., et al., *Genome-wide profiling of salt fractions maps physical properties of chromatin.* Genome Res, 2009. **19**(3): p. 460-9.

106. Sanders, M.M., *Fractionation of nucleosomes by salt elution from micrococcal nuclease-digested nuclei.* J Cell Biol, 1978. **79**(1): p. 97-109.

107. Tatsumi, Y., et al., *Association of human origin recognition complex 1 with chromatin DNA and nuclease-resistant nuclear structures.* J Biol Chem, 2000. **275**(8): p. 5904-10.

108. Fujita, M., et al., *Cell cycle regulation of human CDC6 protein. Intracellular localization, interaction with the human mcm complex, and CDC2 kinase-mediated hyperphosphorylation.* J Biol Chem, 1999. **274**(36): p. 25927-32.

109. Abdurashidova, G., et al., *Localization of proteins bound to a replication origin of human DNA along the cell cycle.* Embo J, 2003. **22**(16): p. 4294-303.

110. ElShamy, W. and D. Livingston, *Identification of BRCA1-IRIS, a BRCA1 locus product*, in *Nat Cell Biol*. 2004. p. 954-967.

111. Keller, C., et al., *The origin recognition complex marks a replication origin in the human TOP1 gene promoter*, in *J Biol Chem*. 2002. p. 31430-31440.

112. Ladenburger, E.-M., C. Keller, and R. Knippers, *Identification of a binding region for human origin recognition complex proteins 1 and 2 that coincides with an origin of DNA replication*, in *Mol Cell Biol*. 2002. p. 1036-1048.

113. Lidonnici, M.R., et al., *Subnuclear distribution of the largest subunit of the human origin recognition complex during the cell cycle.* J Cell Sci, 2004. **117**(Pt 22): p. 5221-31.

114. Rowntree, R.K. and J.T. Lee, *Mapping of DNA replication origins to noncoding genes of the X-inactivation center*, in *Mol Cell Biol*. 2006. p. 3707-3717.

115. Schaarschmidt, D., et al., *Human Mcm proteins at a replication origin during the G1 to S phase transition*, in *Nucleic Acids Res*. 2002. p. 4176-4185.

116. Sibani, S., G.B. Price, and M. Zannis-Hadjopoulos, *Ku80 binds to human replication origins prior to the assembly of the ORC complex*, in *Biochemistry*. 2005. p. 7885-7896.

117. Mendoza-Maldonado, R., et al., *Interaction of the retinoblastoma protein with Orc1 and its recruitment to human origins of DNA replication*, in *PLoS ONE*. 2010. p. e13720.

118. Todorovic, V., et al., *Human origins of DNA replication selected from a library of nascent DNA*, in *Mol Cell*. 2005. p. 567-575.

119. Steger, D.J., et al., *DOT1L/KMT4 recruitment and H3K79 methylation are ubiquitously coupled with gene transcription in mammalian cells.* Mol Cell Biol, 2008. **28**(8): p. 2825-39.

120. Harper, J.V., *Synchronization of cell populations in G1/S and G2/M phases of the cell cycle*, in *Methods Mol Biol*. 2005. p. 157-166.

121. Turner, B., *ChIP with Native Chromatin: Advantages and Problems Relative to Methods Using Cross-Linked Material*, in *Mapping Protein/DNA Interactions by Cross-Linking*. 2001: Paris.

122. Kaguni, J.M., *Replication initiation at the Escherichia coli chromosomal origin*, in *Curr Opin Chem Biol*. 2011. p. 606-613.

123. Kulartz, M. and R. Knippers, *The replicative regulator protein geminin on chromatin in the HeLa cell cycle*, in *J Biol Chem*. 2004. p. 41686-41694.

124. Tatsumi, Y., et al., *The ORC1 cycle in human cells: I. cell cycle-regulated oscillation of human ORC1*. J Biol Chem, 2003. **278**(42): p. 41528-34.

125. Petersen, B.O., et al., *Cell cycle- and cell growth-regulated proteolysis of mammalian CDC6 is dependent on APC-CDH1*. Genes Dev, 2000. **14**(18): p. 2330-43.

126. Petersen, B.O., et al., *Phosphorylation of mammalian CDC6 by cyclin A/CDK2 regulates its subcellular localization.* EMBO J, 1999. **18**(2): p. 396-410.

127. Nishitani, H., Z. Lygerou, and T. Nishimoto, *Proteolysis of DNA replication licensing factor Cdt1 in S-phase is performed independently of geminin through its N-terminal region.*, in *J Biol Chem*. 2004. p. 30807-30816.

128. Nishitani, H., et al., *The human licensing factor for DNA replication Cdt1 accumulates in G1 and is destabilized after initiation of S-phase*, in *J Biol Chem*. 2001. p. 44905-44911.

129. Sugimoto, N., et al., *Cdt1 phosphorylation by cyclin A-dependent kinases negatively regulates its function without affecting geminin binding.*, in *J Biol Chem*. 2004. p. 19691-19697.

130. Fujita, M., et al., *Cell cycle- and chromatin binding state-dependent phosphorylation of human MCM heterohexameric complexes. A role for cdc2 kinase.* J Biol Chem, 1998. **273**(27): p. 17095-101.

131. You, Z. and H. Masai, *Cdt1 forms a complex with the minichromosome maintenance protein (MCM) and activates its helicase activity.* J Biol Chem, 2008. **283**(36): p. 24469-77.

132. Ranjan, A. and M. Gossen, *A structural role for ATP in the formation and stability of the human origin recognition complex.* Proc Natl Acad Sci U S A, 2006. **103**(13): p. 4864-9.

133. Laskey, R.A. and M.A. Madine, *A rotary pumping model for helicase function of MCM proteins at a distance from replication forks.* EMBO Rep, 2003. **4**(1): p. 26-30.

134. Prasanth, S.G., et al., *Dynamics of pre-replication complex proteins during the cell division cycle.* Philos Trans R Soc Lond B Biol Sci, 2004. **359**(1441): p. 7-16.

135. Bravo, R. and H. Macdonald-Bravo, *Existence of two populations of cyclin/proliferating cell nuclear antigen during the cell cycle: association with DNA replication sites.* J Cell Biol, 1987. **105**(4): p. 1549-54.

136. Celis, J.E. and A. Celis, *Cell cycle-dependent variations in the distribution of the nuclear protein cyclin proliferating cell nuclear antigen in cultured cells: subdivision of S phase.* Proc Natl Acad Sci U S A, 1985. **82**(10): p. 3262-6.

137. Leonhardt, H., et al., *Dynamics of DNA replication factories in living cells.* J Cell Biol, 2000. **149**(2): p. 271-80.

138. Bell, S.P. and A. Dutta, *DNA replication in eukaryotic cells.* Annu Rev Biochem, 2002. **71**: p. 333-74.

139. DePamphilis, M.L., *The 'ORC cycle': a novel pathway for regulating eukaryotic DNA replication.* Gene, 2003. **310**: p. 1-15.

140. Kelly, T.J. and G.W. Brown, *Regulation of chromosome replication.* Annu Rev Biochem, 2000. **69**: p. 829-80.

141. Mendez, J. and B. Stillman, *Perpetuating the double helix: molecular machines at eukaryotic DNA replication origins.* Bioessays, 2003. **25**(12): p. 1158-67.

142. Aparicio, O.M., D.M. Weinstein, and S.P. Bell, *Components and dynamics of DNA replication complexes in S. cerevisiae: redistribution of MCM proteins and Cdc45p during S phase.* Cell, 1997. **91**(1): p. 59-69.

143. Kimura, H., et al., *Quantitation of RNA polymerase II and its transcription factors in an HeLa cell: little soluble holoenzyme but significant amounts of polymerases attached to the nuclear substructure.* Mol Cell Biol, 1999. **19**(8): p. 5383-92.

144. Otero, G., et al., *Elongator, a multisubunit component of a novel RNA polymerase II holoenzyme for transcriptional elongation.* Mol Cell, 1999. **3**(1): p. 109-18.

145. Yamazaki, S., et al., *Rif1 regulates the replication timing domains on the human genome.* EMBO J, 2012. **31**(18): p. 3667-77.

146. Cornacchia, D., et al., *Mouse Rif1 is a key regulator of the replication-timing programme in mammalian cells.* EMBO J, 2012. **31**(18): p. 3678-90.

147. Dhar, S.K., L. Delmolino, and A. Dutta, *Architecture of the human origin recognition complex.* J Biol Chem, 2001. **276**(31): p. 29067-71.

148. Vashee, S., et al., *Assembly of the human origin recognition complex.* J Biol Chem, 2001. **276**(28): p. 26666-73.

149. Zaret, K.S. and J.S. Carroll, *Pioneer transcription factors: establishing competence for gene expression.* Genes Dev, 2011. **25**(21): p. 2227-41.

150. Cirillo, L.A., et al., *Opening of compacted chromatin by early developmental transcription factors HNF3 (FoxA) and GATA-4.* Mol Cell, 2002. **9**(2): p. 279-89.

151. Caravaca, J.M., et al., *Bookmarking by specific and nonspecific binding of FoxA1 pioneer factor to mitotic chromosomes.* Genes Dev, 2013. **27**(3): p. 251-60.

152. Clark, K.L., et al., *Co-crystal structure of the HNF-3/fork head DNA-recognition motif resembles histone H5.* Nature, 1993. **364**(6436): p. 412-20.

153. Ramakrishnan, V., et al., *Crystal structure of globular domain of histone H5 and its implications for nucleosome binding.* Nature, 1993. **362**(6417): p. 219-23.

154. Erzberger, J.P., M.M. Pirruccello, and J.M. Berger, *The structure of bacterial DnaA: implications for general mechanisms underlying DNA replication initiation.* EMBO J, 2002. **21**(18): p. 4763-73.

155. Liu, J., et al., *Structure and function of Cdc6/Cdc18: implications for origin recognition and checkpoint control.* Mol Cell, 2000. **6**(3): p. 637-48.

156. Dueber, E.L., et al., *Replication origin recognition and deformation by a heterodimeric archaeal Orc1 complex.* Science, 2007. **317**(5842): p. 1210-3.

157. Gaudier, M., et al., *Structural basis of DNA replication origin recognition by an ORC protein.* Science, 2007. **317**(5842): p. 1213-6.

158. Aparicio, O.M., *Location, location, location: it's all in the timing for replication origins.* Genes Dev, 2013. **27**(2): p. 117-28.

159. Lu, J., et al., *G2 phase chromatin lacks determinants of replication timing.* J Cell Biol, 2010. **189**(6): p. 967-80.

160. Chesnokov, I., D. Remus, and M. Botchan, *Functional analysis of mutant and wild-type Drosophila origin recognition complex.* Proc Natl Acad Sci U S A, 2001. **98**(21): p. 11997-2002.

161. Giordano-Coltart, J., et al., *Studies of the properties of human origin recognition complex and its Walker A motif mutants.* Proc Natl Acad Sci U S A, 2005. **102**(1): p. 69-74.

162. Klemm, R.D., R.J. Austin, and S.P. Bell, *Coordinate binding of ATP and origin DNA regulates the ATPase activity of the origin recognition complex.* Cell, 1997. **88**(4): p. 493-502.

163. Bell, O., et al., *Accessibility of the Drosophila genome discriminates PcG repression, H4K16 acetylation and replication timing.* Nat Struct Mol Biol, 2010. **17**(7): p. 894-900.

164. Wu, Z. and X. Liu, *Role for Plk1 phosphorylation of Hbo1 in regulation of replication licensing*, in *Proceedings of the National Academy of Sciences*. 2008. p. 1919.

165. Miotto, B. and K. Struhl, *HBO1 histone acetylase is a coactivator of the replication licensing factor Cdt1*, in *Genes Dev*. 2008. p. 2633-2638.

166. Miotto, B. and K. Struhl, *HBO1 histone acetylase activity is essential for DNA replication licensing and inhibited by Geminin*, in *Mol Cell*. 2010. p. 57-66.

167. Miotto, B. and K. Struhl, *JNK1 Phosphorylation of Cdt1 Inhibits Recruitment of HBO1 Histone Acetylase and Blocks Replication Licensing in Response to Stress*, in *Mol Cell*. 2011. p. 62-71.